Università degli Studi di Padova

Department of Medicine

---

**Ph.D. course in Clinical and Experimental Sciences**

Curriculum: Rheumatological and Laboratory Sciences

XXXV Series

# STUDY OF EXTRACELLULAR VESICLES IN PATIENTS WITH IDIOPATHIC INFLAMMATORY MYOPATHIES: DEVELOPMENT OF A NOVEL ISOLATION METHOD, CHARACTERIZATION, miRNA PROFILING AND EVALUATION OF CLINICAL CORRELATES. A CROSS-SECTIONAL COMPARATIVE ANALYSIS FROM A MONOCENTRIC COHORT

**Coordinator:** Ch.mo Prof. Alberto Ferlin

**Supervisor**: Ch.mo Prof. Andrea Doria

**Co-Supervisor**: Dr. Mariele Gatto

**Ph.D. candidate**: Chiara Franco

# Index

# ABSTRACT

**Background.** Idiopathic inflammatory myopathies (IIM) are a heterogeneous group of autoimmune disorders whose pathogenesis has not yet been completely elucidated and for which biomarkers for early diagnosis have not yet been identified. Extracellular vesicles (EVs) are cell-derived nanoparticles involved in intercellular signaling convoying their cargo of proteins, lipids, and nucleic acids that act in autoimmune diseases. They also carry microRNAs (miRNAs), short non-coding RNA sequences that regulate post-transcriptional gene expression and whose dysregulation has been associated with the development and progression of several autoimmune diseases.

**Aim.** This study aims to investigate the potential role of circulating EVs as biomarkers in IIM by validating a methodological approach for EVs isolation from blood samples, characterizing the isolated EVs, evaluating their cellular origin, exploring their miRNA cargo, and correlating clinical characteristics of IIM with EVs features.

**Methods.** EVs were isolated from platelet-free plasma of adult (≥18 years old) IIM patients followed at the Unit of Rheumatology of Padua University Hospital and sex- and age- matched healthy donors (HDs) through size-exclusion chromatography and ultrafiltration. EVs were observed through transmission electron microscopy (TEM), immuno-characterized by imaging-flow cytometry (IFC), quantified by nanoparticles tracking analysis (NTA), and EV-miRNAs cargo was investigated through Next-Generation Sequencing (NGS). Clinical data concerning IIM patients were assessed by a specialized clinician.

**Results.** Sixty-five consecutive IIM patients and 65 HDs were included in the study. The patient cohort was composed as follows: dermatomyositis (DM) n=19; polymyositis (PM) n=8; inclusion body myositis (IBM) n=2; anti-synthetase syndrome (ASyS) n=17; cancer-associated myositis (CAM) n=16; unspecified n=3.

TEM images (n=10) showed intact small particles with the typical “cup-shape” morphology of EVs.

IFC showed EVs to be positive for constitutive surface tetraspanins CD63, CD81, CD9, and integrin CD11c, with a prevalence of CD63+ EVs ($p<0.0001$) in both IIM (n=30) and HDs (n=30) (mean [EVs/mL] ± SD $2.91x10^8 \pm 2.07x10^8$ vs. $2.40x10^8 \pm 1.85x10^8$, respectively). Moreover, IFC analysis highlighted a prevalence of CD3-CD19+ EVs compared to CD3+ EVs in both IIM (n=26) and HDs (n=25) groups ($p<0.0001$ for both).

NTA measurements of nanoparticles concentration and size reported a significantly higher mean concentration of circulating EVs in IIM patients (n=65) than in HDs (n=65) (mean [EVs/mL] ± SD $1.71x10^{10} \pm 1.29x10^{10}$ vs. $1.31x10^{10} \pm 7.17x10^9$, p=0.0306). Across IIM subsets, the highest EVs levels were found in CAM vs. HDs ($2.35x10^{10} \pm 2.20x10^{10}$ vs. $1.31x10^{10} \pm 7.17x10^9$, p=0.0026) and

no CAM patients ($2.35x10^{10} \pm 2.20x10^{10}$ vs. $1.51x10^{10} \pm 7.51x10^{9}$, p=0.0206). Patients in clinical remission displayed higher EVs levels than active patients ($2.13x10^{10} \pm 1.60x10^{10}$ vs. $1.46x10^{10} \pm 1.02x10^{10}$, p=0.0452). Patients on glucocorticoids (GC) alone displayed higher EVs levels than patients receiving GC and immunosuppressants (IS) ($2.23x10^{10} \pm 1.99x10^{10}$ vs. $1.49x10^{10} \pm 7.25x10^{9}$, p=0.0482). EVs concentration was significantly decreased in patients receiving rituximab (RTX) vs. other therapies ($9.63x10^{9} \pm 3.26x10^{9}$ vs. $1.96x10^{10} \pm 1.46x10^{10}$, p=0.0228).

NGS analysis detected 10 EV-miRNAs with different expression profiles between IIM (n=21) and HDs (n=21): hsa-miR-451a (p=0.0010), hsa-miR-15a-5p (p=0.0086), hsa-miR-486-5p (p=0.0012), hsa-miR-222-3p (p=0.0098), hsa-miR-32-5p (p=0.0038), hsa-miR-185-5p (p=0.0217) were up-regulated in IIM, while hsa-let-7b-5p (p=0.0046), hsa-let-7a-5p (p=0.0032), hsa-let-7e-5p (p=0.014), hsa-let-7f-5p (p=0.0123) were down-regulated in IIM patients vs. HD. Other EVs-miRNAs expression varied across IIM subsets: CAM patients displayed down-regulated expression of hsa-miR-23b-3p (p=0.0303), hsa-miR-361-5p (p=0.0468), hsa-miR-143-3p (p=0.0312) and up-regulated expression of hsa-miR-374a-5p (p=0.0068) and hsa-miR-26b-5p (p=0.0468). PM + ASyS showed up-regulated expression of hsa-miR-30c-5p (p=0.0333) and hsa-miR-186-5p (p=0.0241). DM displayed up-regulated expression of hsa-miR-125b-5p (p=0.0215), hsa-miR-29c-3p (p=0.0275), hsa-miR-361-5p (p=0.0394). Hsa-miR-122-5p was down-regulated in IIM patients with a concurrent diagnosis of interstitial-lung disease (ILD) (p=0.0482). Hsa-miR-155-5p resulted up-regulated (p=0.0259) and hsa-miR-347a-5p down-regulated (p=0.0420) in patients characterized by active disease compared to clinical remission.

**Conclusions.** We propose a novel EVs isolation method consisting of size-exclusion chromatography combined with ultrafiltration as a reliable approach to obtain intact EVs with preserved morphology and good purity from blood, as confirmed by the different characterization techniques. The prevalence of B lymphocytes markers on circulating EVs surface might indicate their cell origin. Peculiar differences in EVs concentrations and EV-miRNAs expression profile tell apart IIM from healthy and may provide an early distinction among specific IIM subtypes, thus submitting EVs as potential biomarkers of disease, differential diagnosis, and treatment response.

# RIASSUNTO

**Stato dell'arte.** Le miopatie infiammatorie idiopatiche (MII) sono un gruppo eterogeneo di malattie autoimmuni la cui patogenesi non è stata ancora completamente chiarita e per le quali non sono stati ancora identificati biomarcatori per la diagnosi precoce. Le vescicole extracellulari (EV) sono nanoparticelle di origine cellulare coinvolte nella comunicazione intercellulare che trasportano il loro carico di proteine, lipidi e acidi nucleici ed hanno un ruolo nelle malattie autoimmuni. Le EV trasportano anche microRNA (miRNA), brevi sequenze di RNA non codificanti che regolano l'espressione genica post-trascrizionale e la cui deregolazione è stata associata allo sviluppo e alla progressione di diverse malattie autoimmuni.

**Scopo.** Questo studio ha l'obiettivo di indagare il potenziale ruolo delle EV circolanti come biomarcatori di MII validando un approccio metodologico per l'isolamento delle EV dai campioni di sangue, caratterizzando le EV isolate, valutando la loro origine cellulare, esplorando il loro carico di miRNA e correlando le caratteristiche cliniche con le peculiarità delle EV.

**Metodi.** Le EV sono state isolate dal plasma privo di piastrine di pazienti MII adulti (≥18 anni) seguiti presso l'Unità di Reumatologia dell'Azienda Ospedaliera-Università di Padova e da donatori sani (DS) appaiati per sesso ed età mediante cromatografia ad esclusione dimensionale ed ultrafiltrazione. Le EV sono state osservate mediante microscopia elettronica a trasmissione (MET), immuno-caratterizzate mediante citofluorimetria per immagini (*imaging flow cytometry*: IFC), quantificate mediante *nanoparticles tracking analysis* (NTA) e il cargo di EV-miRNA è stato studiato attraverso *Next-Generation Sequencing* (NGS). I dati clinici relativi ai pazienti MII sono stati valutati da un medico specializzato.

**Risultati.** Nello studio sono stati inclusi 65 pazienti consecutivi MII e 65 DS. La coorte di pazienti era composta come segue: dermatomiosite (DM) n=19; polimiosite (PM) n=8; miosite a corpi inclusi (IBM) n=2; sindrome anti-sintetasica (ASyS) n=17; miosite associata al cancro (CAM) n=16; non specificato n=3.

Le immagini MET (n=10) mostrano piccole particelle intatte con la tipica morfologia a "forma di coppa" delle EV.

L'analisi IFC ha riportato che le EV sono positive per le tetraspanine costitutive di superficie CD63, CD81, CD9 e l'integrina CD11c, con una prevalenza di EV CD63+ ($p<0,0001$) sia nelle MII (n=30) che nei DS (n=30) (media [EV/mL] ± SD $2,91x10^8$ ± $2,07x10^8$ rispetto a $2,40x10^8$ ± $1,85x10^8$, rispettivamente). Inoltre, l'analisi IFC ha evidenziato una prevalenza di EV CD3-CD19+ rispetto a EV CD3+ in entrambi i gruppi MII (n=26) e DS (n=25) ($p<0,0001$ per entrambi).

Le misurazioni NTA della concentrazione e delle dimensioni delle nanoparticelle hanno riportato una concentrazione media significativamente più alta di EV circolanti nei pazienti con MII (n=65) rispetto ai DS (n=65) (media [EV/mL] ± SD $1{,}71x10^{10} \pm 1{,}29x10^{10}$ vs. $1{,}31x10^{10} \pm 7{,}17x10^{9}$, p=0,0306). Tra i sottogruppi di MII, i livelli più elevati di EV sono stati trovati nei pazienti CAM rispetto ai DS ($2{,}35x10^{10} \pm 2{,}20x10^{10}$ rispetto a $1{,}31x10^{10} \pm 7{,}17x10^{9}$, p=0,0026) e in confronto ai pazienti senza CAM ($2{,}35x10^{10} \pm 2{,}20x10^{10}$ rispetto a $1{,}51x10^{10} \pm 7{,}51\ x10^{9}$, p=0,0206). I pazienti in remissione clinica hanno mostrato livelli di EV più elevati rispetto ai pazienti attivi ($2{,}13x10^{10} \pm 1{,}60x10^{10}$ vs. $1{,}46x10^{10} \pm 1{,}02x10^{10}$, p=0,0452). I pazienti trattati solo con glucocorticoidi (GC) hanno mostrato livelli di EV più elevati rispetto ai pazienti trattati con GC e immunosoppressori (IS) ($2{,}23x10^{10} \pm 1{,}99x10^{10}$ vs. $1{,}49x10^{10} \pm 7{,}25x10^{9}$, p=0,0482). La concentrazione di EV è risultata significativamente ridotta nei pazienti trattati con rituximab (RTX) rispetto ad altre terapie ($9{,}63x10^{9} \pm 3{,}26x10^{9}$ vs. $1{,}96x10^{10} \pm 1{,}46x10^{10}$, p=0,0228).

L'analisi NGS ha rilevato 10 EV-miRNA con profili di espressione differenti tra MII (n=21) e DS (n=21): hsa-miR-451a (p=0,0010), hsa-miR-15a-5p (p=0,0086), hsa-miR-486-5p (p=0,0012), hsa-miR-222-3p (p=0,0098), hsa-miR-32-5p (p=0,0038), hsa-miR-185-5p (p=0,0217) erano sovra-espressi nei pazienti MII, mentre hsa-let-7b-5p (p=0,0046), hsa-let-7a-5p (p=0,0032), hsa-let-7e-5p (p=0,014), hsa-let-7f-5p (p=0,0123) erano sotto-espressi nei pazienti MII rispetto ai DS. L'espressione di altri EV-miRNA variava tra i sottogruppi di MII: i pazienti CAM mostravano un'espressione sotto-regolata di hsa-miR-23b-3p (p=0,0303), hsa-miR-361-5p (p=0,0468), hsa-miR-143-3p (p=0,0312) ed una sovra-espressione di hsa-miR-374a-5p (p=0,0068) e hsa-miR-26b-5p (p=0,0468). PM + ASyS dimostrava una sovra-espressione di hsa-miR-30c-5p (p=0,0333) e hsa-miR-186-5p (p=0,0241). DM riportava una sovra-regolazione di hsa-miR-125b-5p (p=0,0215), hsa-miR-29c-3p (p=0,0275), hsa-miR-361-5p (p=0,0394). Hsa-miR-122-5p era sotto-espresso nei pazienti MII con una diagnosi concomitante di malattia polmonare interstiziale (*interstitial-lung disease*: ILD). Hsa-miR-155-5p è risultato sovra-espresso (p=0,0259) e hsa-miR-347a-5p sotto-espresso (p=0,0420) in pazienti caratterizzati da malattia attiva rispetto a quelli in remissione clinica.

**Conclusioni.** Noi proponiamo un nuovo metodo di isolamento delle EV costituito da cromatografia ad esclusione dimensionale combinato con ultrafiltrazione come approccio affidabile per ottenere EV intatte con una morfologia preservata e buona purezza da campioni di sangue, come confermato dalle diverse tecniche di caratterizzazione. La prevalenza dei marcatori dei linfociti B sulla superficie delle EV circolanti potrebbe indicare la loro origine cellulare. Differenze peculiari nelle concentrazioni di EV e nel profilo di espressione di EV-miRNA distinguono i pazienti MII dai soggetti sani e potrebbero fornire una distinzione precoce tra specifici sottotipi di MII, presentando così le EV come potenziali biomarcatori di malattia, diagnosi differenziale e risposta al trattamento.

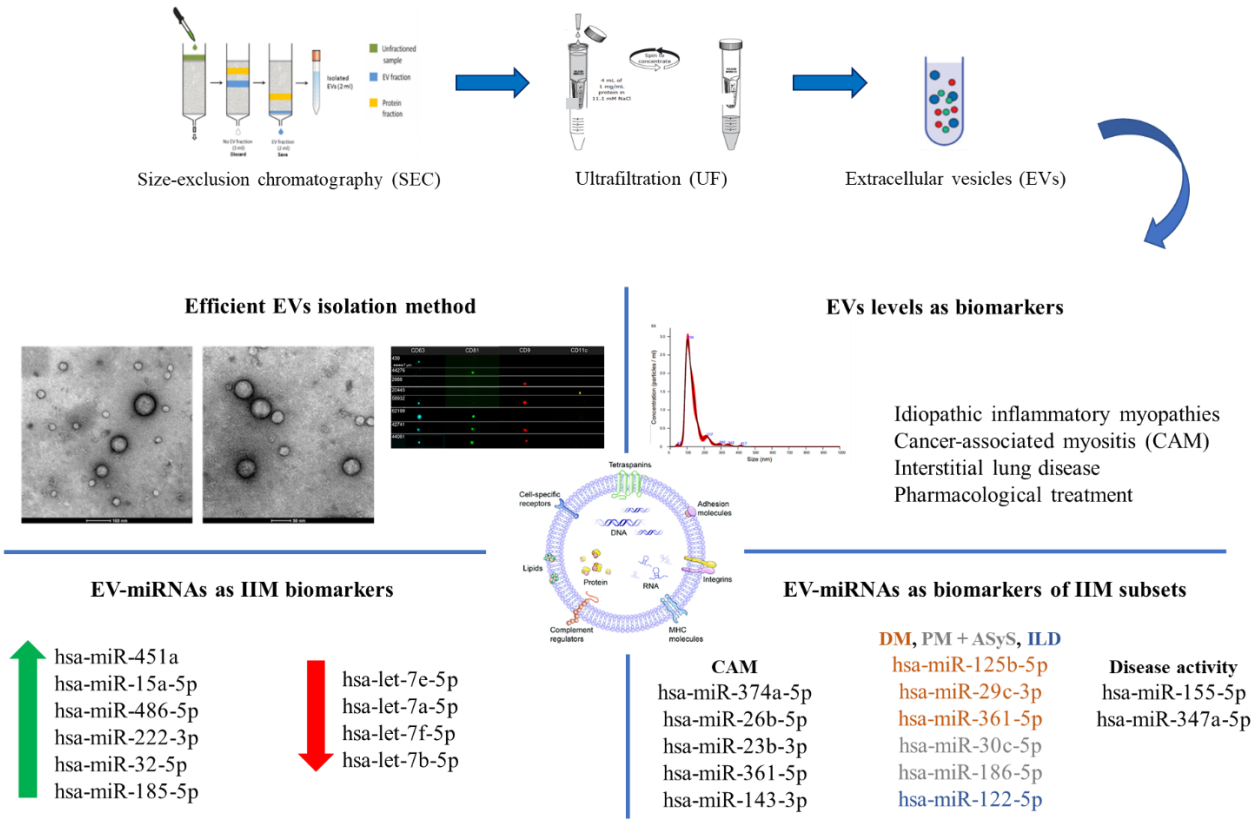


***Graphical abstract.*** *Summary figure representing the method for the isolation of extracellular vesicles from human blood samples and the main results supporting the potential role of EVs and EV-miRNAs as biomarkers in idiopathic inflammatory myopathies. EVs: extracellular vesicles; miRNAs: microRNAs; CAM: cancer-associated myositis; DM: dermatomyositis; PM: polymyositis; ASyS: anti-synthetase syndrome.*

# 1 Introduction

## 1.1 Idiopathic inflammatory myopathies (IIM)

### *1.1.1 Definition*

Idiopathic inflammatory myopathies (IIM) are a heterogeneous group of rare and chronic conditions of autoimmune connective tissue diseases characterized by immune-mediated injury primarily targeting the striated muscles presenting progressive weakness of the proximal muscles in a symmetrical fashion as well as extra-muscular manifestations typically involving the skin, joints and pulmonary interstitium, potentially leading to severe disability and life-threatening complications [1–3]. The presence of several disease phenotypes displays diverse clinical manifestations, as well as histopathologic findings, serologic profiles, and treatment responses.

### *1.1.2 Classification*

The current EULAR/ACR classification criteria for adult and juvenile idiopathic inflammatory myopathies and their major subgroups (**Table 1**) have been developed in 2017 and encompass the following subtypes of IIM: polymyositis (PM), inclusion-body myositis (IBM), dermatomyositis (DM), amyopathic dermatomyositis (ADM), juvenile dermatomyositis (JDM), and non-JDM juvenile myositis [4]. These criteria reach a maximum sensitivity of 93% and a specificity of 88% when providing the histology, otherwise limited to 87% and 82%, respectively. However, due to their extremely low prevalence, the following subtypes of disease could not be acknowledged as independent entities: immune-mediated necrotizing myopathy (IMNM), hypomyopathic DM, juvenile PM (JPM), cancer-associated myositis (CAM), and anti-synthetase syndrome (ASyS) [5]. Likewise, overlap syndromes with myositis (OM) had long been overlooked until 2005 [6].

**Table 2** The European League Against Rheumatism/American College of Rheumatology (EULAR/ACR) classification criteria for adult and juvenile idiopathic inflammatory myopathies (IIMs)

**When no better explanation for the symptoms and signs exists, these classification criteria can be used**

| Variable | Score points | | |
|---|---|---|---|
| | Without muscle biopsy | With muscle biopsy | Definition |
| Age of onset | | | |
| Age of onset of first symptom assumed to be related to the disease ≥18 years and <40 years | 1.3 | 1.5 | 18≤Age (years) at onset of first symptom assumed to be related to the disease <40 |
| Age of onset of first symptom assumed to be related to the disease ≥40 years | 2.1 | 2.2 | Age (years) at onset of first symptom assumed to be related to the disease ≥40 |
| Muscle weakness | | | |
| Objective symmetric weakness, usually progressive, of the proximal upper extremities | 0.7 | 0.7 | Weakness of proximal upper extremities as defined by manual muscle testing or other objective strength testing, which is present on both sides and is usually progressive over time |
| Objective symmetric weakness, usually progressive, of the proximal lower extremities | 0.8 | 0.5 | Weakness of proximal lower extremities as defined by manual muscle testing or other objective strength testing, which is present on both sides and is usually progressive over time |
| Neck flexors are relatively weaker than neck extensors | 1.9 | 1.6 | Muscle grades for neck flexors are relatively lower than neck extensors as defined by manual muscle testing or other objective strength testing |
| In the legs, proximal muscles are relatively weaker than distal muscles | 0.9 | 1.2 | Muscle grades for proximal muscles in the legs are relatively lower than distal muscles in the legs as defined by manual muscle testing or other objective strength testing |
| Skin manifestations | | | |
| Heliotrope rash | 3.1 | 3.2 | Purple, lilac-coloured or erythematous patches over the eyelids or in a periorbital distribution, often associated with periorbital oedema |
| Gottron's papules | 2.1 | 2.7 | Erythematous to violaceous papules over the extensor surfaces of joints, which are sometimes scaly. May occur over the finger joints, elbows, knees, malleoli and toes |
| Gottron's sign | 3.3 | 3.7 | Erythematous to violaceous macules over the extensor surfaces of joints, which are not palpable |
| Other clinical manifestations | | | |
| Dysphagia or oesophageal dysmotility | 0.7 | 0.6 | Difficulty in swallowing or objective evidence of abnormal motility of the oesophagus |
| Laboratory measurements | | | |
| Anti-Jo-1 (anti-histidyl-tRNA synthetase) autoantibody present | 3.9 | 3.8 | Autoantibody testing in serum performed with standardised and validated test, showing positive result |
| Elevated serum levels of creatine kinase (CK)* *or* lactate dehydrogenase (LD)* *or* aspartate aminotransferase (ASAT/AST/SGOT)* *or* alanine aminotransferase (ALAT/ALT/SGPT)* | 1.3 | 1.4 | The most abnormal test values during the disease course (highest absolute level of enzyme) above the relevant upper limit of normal |
| Muscle biopsy features—presence of: | | | |
| Endomysial infiltration of mononuclear cells surrounding, but not invading, myofibres | | 1.7 | Muscle biopsy reveals endomysial mononuclear cells abutting the sarcolemma of otherwise healthy, non-necrotic muscle fibres, but there is no clear invasion of the muscle fibres |
| Perimysial and/or perivascular infiltration of mononuclear cells | | 1.2 | Mononuclear cells are located in the perimysium and/or located around blood vessels (in either perimysial or endomysial vessels) |
| Perifascicular atrophy | | 1.9 | Muscle biopsy reveals several rows of muscle fibres, which are smaller in the perifascicular region than fibres more centrally located |
| Rimmed vacuoles | | 3.1 | Rimmed vacuoles are bluish by H&E staining and reddish by modified Gomori trichrome stains |

*Serum levels above the upper limit of normal.

***Table 1.*** *EULAR/ACR classification criteria for adult and juvenile idiopathic inflammatory myopathies and their major subgroups. Lundberg I. et al., 2017* [7].

The diagnostic algorithm suggested by the EULAR/ACR criteria for IIM classification to identify the main disease phenotypes was shown in **Figure 1** [4,8].

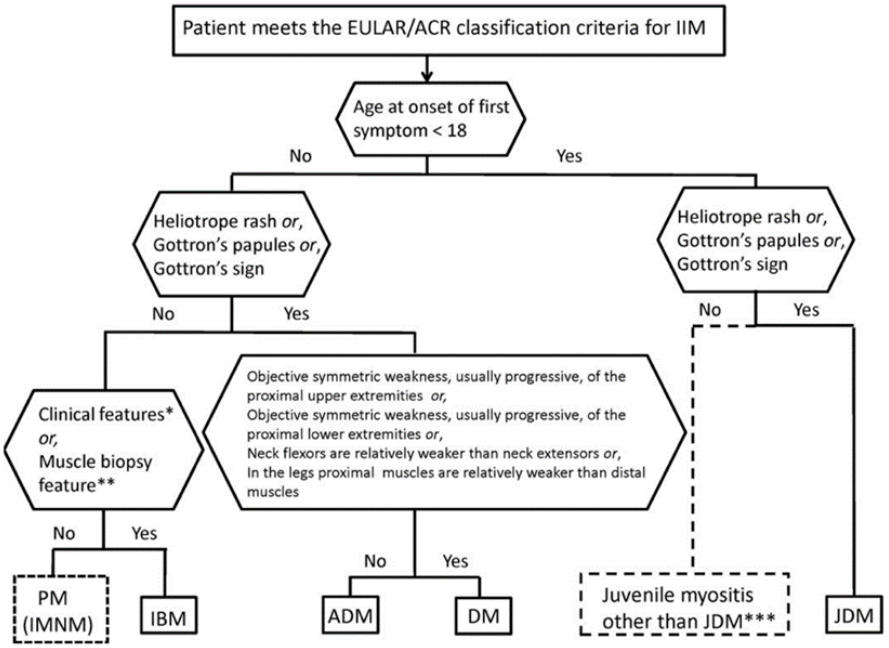


***Figure 1.*** *Diagnostic algorithm of EULAR/ACR classification criteria for adult and juvenile idiopathic inflammatory myopathies and their major subgroups. Lundberg I. et al., 2017* [4].

ASyS appears to be a very heterogeneous condition characterized by a variety of phenotypic features. The literature confirms the lack of adequate data and consensus to develop a validated definition of ASyS [9]. Therefore, the diagnosis and management of ASyS are still difficult due to masked and/or nonspecific symptoms at disease onset. The lack of a data-driven and validated set of classification criteria for ASyS may lead to under-recognition and misclassification of this syndrome [9]. In this regard, two main classifications criteria have been proposed for ASyS subgroup, namely the Connors' [10] and the Solomon's [11] criteria (**Table 2**) [12]. An effort to overcome the need for additional data and consensus-driven classification criteria for ASyS using clinical and/or serological features is led by the ACR/EULAR Classification of ASyS project [9].

| Connors et al. (2010) | Solomon et al (2011) |
|---|---|
| **Required:** Presence of an anti-aminoacyl tRNA synthetase antibody | **Required:** Presence of anti-aminoacyl tRNA synthetase antibody |
| **PLUS** *one or more* of the following clinical features:<br>• Raynaud's phenomenon<br>• Arthritis<br>• Interstitial lung disease<br>• Fever (not attributable to another cause)<br>• Mechanic's hands (thickened and cracked skin on hands, particularly at fingertips) | **PLUS** *two major* or *one major and two minor criteria*:<br>Major:<br>1. Interstitial Lung Disease (not attributable to another cause)<br>2. Polymyositis or dermatomyositis by Bohan and Peter critieria<br>Minor:<br>1. Arthritis<br>2. Raynaud's phenomenon<br>3. Mechanic's hands |

***Table 2.*** *Classification criteria for Anti-synthetase Syndrome. Witt L. et al., 2016* [12].

### *1.1.3 Epidemiology*

IIM have a prevalence ranging from 3 to 34 cases per 100.000 inhabitants and an incidence between 11 and 660 patients per a million person per year [13]. The incidence increases according to age and reaches the peak in the fifth decade [14]. Similarly to other autoimmune diseases, IIM displays a preference for the female gender with an overall female-to-male ratio of about 2:1 with the exceptions of IBM and CAM, characterized by a male-to-female ratios of 3:1 and 2:1, respectively. The gender shift appears to be attenuated in the juvenile forms [15]. The mortality rates range between 20% and 90% and it varies depending on the study design and the population cohorts. The main cause of death is the rapid progression of interstitial lung disease (ILD), followed by cardiovascular complications and malignancies [16].

### *1.1.4 Etiology*

The etiology of IIM is complex and multifactorial, and it varies across the subtypes of disease. It is recognized the interplay of both genetic and environmental factors, although specific pathogenic pathways have not been completely clarified.

The strongest genetic predisposing factor associated with IIM pathogenesis is the human leukocyte antigen (HLA) genes on chromosome 6. In particular, specific HLA-alleles of the ancestral haplotype (8.1AH) are associate with clinical phenotypes, such as HLA-DRB1*03:01 alleles to PM and HLA-B*08:01 alleles to DM [17]. Different HLA associate with subset of IIM defined by myositis-specific antibodies (MSA) [18]. Moreover, also non-HLA genes predispose to an increased risk of IIM. PM has been tied to PTPN22, a tyrosine phosphatase involved in TCR signal transduction, IL18R1 (belonging to the IL1R family), and RGS1, a regulator of G-protein signaling. DM is associated with GSDMB (Gasdermin-B) whose gene family is implicated in cancer and apoptosis regulation in epithelial cells, PLCL1 (phospholipase C-like 1), and BLK (non-receptor tyrosine-kinase of the Src family of proto-oncogenes involved in B-cell receptor signaling and B-cell development). Other mutated genes involved in the IIM pathogenesis are STAT4, fundamental in the TCR signaling transduction, and TRAF6 and UBE2L3 involved in NF-kB pathway of B cells [17,18].

Among the environmental factors as triggers of IIM, are paramount recognized the viral infections, statin use in combination with other drugs, smoke, UV radiation, and exposure organic solvents [18].

The pathogenetic role of viruses in the disease seems to be independent from a direct infection of the muscle tissue proposing these triggers to mediate an autoimmune response [19].

Statins are potent cholesterol-lowering agents that can be associated with myalgias and elevation of muscle enzymes, but not muscle weakness. These effects are often temporary upon discontinuation of the drug. On the other hand, a brief or a chronic use of statins can up-regulate the ectopic expression of 3-Hydroxy-3-Methylglutaryl-CoA Reductase (HMGCR) on the cell membrane leading to the loss of immune tolerance. In fact, IMNM patients with a history of statin exposure can be characterized by long-standing and irreversible damages of the immune response that progresses despite statin discontinuation [19–21]. Furthermore, tumor necrosis factor (TNF)-inhibitors, interferon (IFN)-α and IFN-β, and checkpoint-inhibitors are suspected to be involved in the development of IIM [19,22].

Smoking represents a prominent trigger of ASyS mediated by increased induction of anti-Jo1 antibody positivity.

A higher risk of IIM disease is developed in patients with prior exposure to organic solvents.

UV radiation may be involved in the pathogenesis of DM, particularly characterized by anti-Mi2 antibodies positivity, due to the photo-sensitive induction of Mi2 expression in keratinocytes [23].

Moreover, a proportion of IIM is preceded or followed by the diagnosis of a neoplasm form with higher occurrence in DM phenotype (25%), especially among elderly males.

### *1.1.5 Pathogenetic mechanisms*

The IIM are characterized by both inflammatory mechanisms, innate and adaptive immune abnormalities and non-immune mechanisms sustained by genetic and environmental predisposing factors [3,24]. The disease shares the feature of immune-mediated muscle injury although the precise mechanisms is not completely clear and vary across the phenotypes.

#### *Dermatomyositis (DM)*

DM is mainly characterized by muscle and skin involvement represented with heliotrope rash, Grotton's sign and papules besides cuticular dystrophy, mechanic's hand, and cutaneous ulcers or calcinosis. The histology of DM patients presents perifascicular myofiber atrophy alongside the capillary and perimysial abnormalities [15]. The initial pathogenetic event is an antibody and complement-mediated microangiopathy with deposition of membrane attack complexes (MAC) on endothelial cells that determines ischemia and microinfarctions, resulting in perifascicular myofiber atrophy. The MAC activation induces the release of pro-inflammatory cytokines and the expression

on the endothelial cells of adhesion molecules that trigger the infiltration of macrophages, B and T CD4+ lymphocytes and dendritic cells into the muscle tissue [25]. Moreover, it has been demonstrated that the interferon type 1 (IFN-I), and particularly IFN-β, is a keystone of DM pathogenesis: its abundant production amplifies the inflammatory and immune response implying the lesion of the endothelium, perimysial fiber cells, and vacuolar alterations of basal keratinocytes [26]. Both fibroblasts, myofibers, and keratinocytes are responsible for the massive and sustained production of IFN-I leading to the injury to myofibers and keratinocytes through mechanisms including the endoplasmic reticulum (ER) overload response and the unfolded protein response. The ER stress may cause the oxidative damage through the production of reactive oxygen species (ROS) due to the dysregulated mitochondria in a calcium-rich intracellular environment. Finally, the cells damage amplifies the immune response with the release of pro-inflammatory cytokines to create a cyclical mechanism [27].

***Polymyositis (PM)***

PM is characterized by progressive proximal and symmetrical muscle weakness. The pelvic girdle can be involved as well as neck flexors causing the inability to overhead abduction. The primary mechanism that evolves in PM pathogenesis is the inflammatory processes within the muscle due to CD8+ cytotoxic T cells invasion of myofibers expressing major histocompatibility complex (MHC)-I. Cytotoxic T lymphocytes release metalloproteinases and perforin granules that injure the myofiber to necrosis [13]. PM/IBM group is difficult to diagnose and manage effectively. To date, the diagnosis in these patients required in-depth differential diagnostics that depends on a careful consideration of the combined clinical, electrodiagnostic, and pathologic findings. In fact, it has been demonstrated that focal invasion of non-necrotic fibers by inflammatory cells is not always found in PM. In addition, the 37% of patients with biopsy features of PM had the same clinical features compared to IBM, including lack of response to treatment suggesting that muscle biopsy is a reliable instrument in approximately 85% of patients with PM and IBM, but it is not a canonical finding for either entity [28].

***Inclusion body myositis (IBM)***

IBM presents subtle and progressive painless weakness of finger flexors, femoral quadriceps and can involve also muscle including biceps, triceps, anterior leg compartment, face and swallowing muscles. Patients affected with IBM are refractory to immunosuppressive therapy [29,30]. The degenerative component of IBM is mediated by the ER stress response to rimmed vacuoles and

sarcoplasmic protein aggregates (P62 and TDP43) [30]. The association with HLA molecules is defined for DRB1*03:01 and HLA-B*08:01 haplotypes. The autoimmunity involvement is represented by cytotoxic T cells, myeloid dendritic cells and macrophages surrounding and invading myofibers [31]. In fact, the antigen stimulation hints the clonal expansion of plasma cells and cytotoxic T cells within the muscle tissue leading the patients to a positive serology for anti-CN1A antibodies directed against the 5' cytosolic nucleotidase IA [30]. These CD8+ cytotoxic T cells display a particular markers phenotype consistent with a terminal differentiation in reaction to unidentified specific antigens [30,32] whose marked cytotoxicity is mediated through the release of granzymes and perforins responsible of cells injury. They secrete high levels of IFN-γ determining the over-expression of MHC-I on myocytes, ER stress, and protein aggregates [30].

***Anti-synthetase syndrome (ASyS)***

ASyS displays typical clinical manifestations defined by the presence of mutually exclusive autoantibodies directed against an aminoacyl-tRNA synthetase (ARS), including anti-Jo1, anti-PL7, and anti-PL12 [10,11,33,34]. This phenotype generally initiates with a single manifestation, such as arthritis, ILD, fever and subsequent symptoms appear over time. In a minority of cases, it starts with the classical clinical features characterized by myositis, arthritis, mechanic's hand and ILD [33]. The pulmonary involvement in ASyS often occurs after the exposure to triggers such as smoke and viral infections that can induce to aberrant exposure of self-antigen and loss of tolerance in subjects with a favorable genetic background, then activating the innate and adaptive immunity in abnormal manner [35]. Among ARS, the histidyl-tRNA synthetase appears to act as a chemokine regulating lymphocyte migration and monocyte activation [36]. Moreover, the clonally expanded T CD4+ lymphocytes in both blood and lungs were found to be reactive against histidyl-tRNA synthetase [36]. Furthermore, the natural killer (NK) cells assume a characteristic phenotype in active forms of ASyS with reduced ability to release IFN-γ and increased ability to release proteolytic enzymes and degranulate. These cells infiltrate the perimysium and surround the myofibrils and are detected in the lung tissue of ASyS patients [36]. Of interest, it has been demonstrated that circulating histidyl-tRNA synthetase is undetectable in patients with anti-Jo-1-positive ASyS. On the other hand, higher levels are detected in anti-Jo-1-negative patients, potentially because of the increased expression of histidyl-tRNA synthetase observed in regenerating muscle cells from patients with IIM. This observation suggests a potential role of histidyl-tRNA synthetase in ameliorating inflammatory muscle conditions resulting in a possible pathogenetic significance of the autoantibodies. In addition, the autoantibody generation in ASyS is tied to the activation of the immune system and perpetuates a chronic/acute inflammatory condition [37].

***Immune-mediated necrotizing myopathies (IMNM)***

IMNM presents extensive myofibers necrosis that leads to high serum levels of creatine kinase and intense proximal muscle weakness characterized by limited inflammatory infiltrate. There are three subgroups of IMNM: seronegative, HMGCR-positive and SRP-positive IMNM [38]. In the pathogenesis of seropositive forms, anti-SRP or anti-HMGCR antibodies bind to target autoantigens ectopically expressed on the myocytes surface. This binding triggers the classical complement pathway resulting in the formation of MAC to the sarcolemma that leads to necrosis. Then, the macrophages recruitment involves myophagocytosis and the release of pro-inflammatory cytokines, such as IL-1, IL-6 e TNF-α. More, muscle regeneration is impaired by an altered antibody-mediated myoblast differentiation and low levels of IL-4 and IL-13 [21]. In fact, anti-SRP and anti-HMGCR titers correlates with muscle weakness and increased creatine phosphokinase (CPK) [39]. HMGCR-positive IMNM occurs when in a genetically susceptible individual associated with HLA DRB1*11:01) up-regulates HMGCR, especially after a statin drug exposure [40]. The seronegative IMNM has a pathogenesis still obscure.

***Cancer-associated myositis (CAM)***

CAM phenotype has been extensively reported as the association between cancer and IIM. It can develop before, concurrently, or after the onset of IIM. The higher risk of this paraneoplastic complication concerns DM and PM patients, particularly during the 3 years before or after the diagnosis of IIM, and it is one of the main causes of mortality in this population [41]. CAM pathogenesis is complex and two main hypotheses are proposed. The exposure of neo-antigens on the cell membrane of neoplastic cells or regenerating myofibers may initiate the immune response by molecular mimicry. Besides, the prolonged antigen presentation or the post-translational modification of self-proteins may trigger the loss of self-tolerance in an altered tumor microenvironment [42]. Mutations of ubiquitous antigens involved in the carcinogenesis, such as TIF1-γ, can cause the expression or unmasking of onco-antigens capable of stimulating the production of autoantibodies which could cross-react with muscle and skin antigens [43,44].

### *1.1.6 Diagnosis*

Laboratory findings in IIM patients interest several biochemical abnormalities, some of which are non-specific like as C-reactive protein (CRP) and erythrocyte sedimentation rate (ESR), while others are more specific including the muscle enzymes and serologic markers.

Patients affected with IIM usually show an increase of muscle enzymes, including CPK, myoglobin, aldolase, and lactate dehydrogenase (LDH). Following a muscle damage also aspartate aminotransferase (AST) and alanine aminotransferase (ALT) increased, and γ-glutamyltransferase (GGT) might even be needed in case a liver dysfunction had to be ruled out [13,45].

The serologic markers comprehend myositis specific antibodies (MSAs), among which anti-MDA5 [46], antiTIF1-γ [47], anti-Mi2 and anti-tRNA synthetase, and myositis associated-antibodies (MAAs) that are share with other rheumatic diseases such as anti-Ro/SSA, anti-U1RNP, anti-PM/Scl and anti-Ku [48]. These autoantibodies target ubiquitously expressed intracellular self-antigens involved in numerous cellular processes such as transcription and gene regulation.

***MSAs***

Anti-Mi2 is directed against a helicase with a role in transcriptional activation. It is detected in a relative acute onset of DM with important skin manifestations such as shawl or V-neck sign. Anti-Mi2 implies a lower risk of malignancy, and it is renowned for having a good response to treatment [49].

Anti-tRNA synthase antibodies, with the major representative anti-histidyl t-RNA synthetase (anti-Jo1), determine ASyS. Other autoantibodies belonging to this category are anti-PL12, anti-OJ, anti-PL7, anti-EJ, anti-KS, anti-Zo and anti-Ha. Anti-Jo1 is present in over 20% of patients, while the other ones are rare. Anti-Jo1 and anti-PL12 associates to an ILD form without proper evidence of myositis.

Anti-MDA5 antibodies target the RNA helicase encoded by the melanoma differentiation-associated gene 5. Usually, it determines a peculiar phenotype consisting in a rapidly progressive ILD, arthritis, clinically amyopathic dermatomyositis and, occasionally, ulcerations of papules and Gottron's sign plus non-scarring alopecia [46].

Anti-TIF1-γ antibodies target the transcriptional intermediary factor 1 gamma and entail a higher risk of malignancy as well as characteristic skin findings including hyperkeratotic papules on the palms and soles, psoriasis-like lesions and "red-on-white" patches [47].

Anti-SRP-positive patients mostly develop IMNM. The involved antigen is the signal recognition particle with a role in the translocation of newly synthesized proteins into the ER. Cardiac involvement is expected in this population with a severe prognosis and scarce response to treatment [50].

Anti-HMGCR-positive serology suggests an IMNM phenotype due to exposure to statins which recognize the 3-hydroxy-3-methylglutaryl coenzyme A reductase. The presentation can be similar to anti-SRP-positive cases [40].

Anti-NT5c1A antibodies are present in over 50% of IBM cases targeting the 5'cytosolic nucleotidase IA where they represent a diagnostic biomarker [51].

Anti-SAE are antibodies directed against the small ubiquitin-like modifier activating enzyme which regulates the gene transcription. Neoplasms are more frequent among anti-SAE-positive patients than in the general population. Moreover, commonly features are dysphagia and cutaneous manifestations are common that anticipate the development of myopathy [52].

Anti-NXP2 antibodies recognize nuclear matrix protein 2 which is a transcriptional regulator. It is commonly determined among JDM patients with severe disease, oedema, and calcinosis as well as associates with malignancy [47]. However, a meta-analysis recently conducted on twenty cohorts of IIM patients challenged the latter point, indicating that anti-NXP2 had no relation with malignancy in adult patients [53]. Indeed, recent research confirmed that the risk of developing CAM was similar between anti-NXP2-positive and anti-NXP2-negative IIM patients [54].

***MAAs***

Anti-Ro/SSA antibodies are frequently present in patients with ASyS and correlate with a higher risk of ILD. The immune response is directed against antigens associated with hY-RNAs, poorly understood small RNA molecules. Among anti-Ro/SSA antibodies, anti-Ro52 is the most prevalent in IIM. It has been reported a prognostic value of anti-Ro52 antibodies in anti-Jo-1 positive patients, being associated with a higher risk of severe IIM, ILD, joint involvement, and cancer compared with anti-Jo1-positive patients without anti-Ro52 antibodies [55,56]. Anti-Ro52 adds important information concerning patient management and outcomes in IIM and rapidly progressive-ILD. Ro52 is involved in the host responses to viral infections through IFN signaling. It acts to downregulate IFN transcription factors influencing the proinflammatory cytokine responses. It seems a potential target for autoimmune response by virtue of protein-protein interactions, and it seems to act neutralizing and degrading pathogens that antibodies have carried into the cell. Besides, anti-Ro52 antibodies might play a direct pathogenic role. They may block the regulatory activity of Ro52 protein and directly amplify proinflammatory signals mediated through IFN-I [57].

Anti-Sm antibodies target the common core of small nuclear ribonucleoprotein (snRNP) particles and this positivity may imply an overlap with systemic lupus erythematosus (SLE) disease.

Anti-U1-small nuclear RNP (anti-U1RNP) is encountered in mixed connective tissue disease, generally Sjogren's syndrome (SSc) and SLE.

Anti-PM/Scl antibodies against the human exosome protein complex and anti-Ku against the regulatory subunit of DNA-dependent protein kinase indicate the coexistence of SSc that present myositis accompanied by scleroderma-type cutaneous and pulmonary manifestations [58].

The clinical evaluation of IIM diagnosis comprises several techniques. The electromyography (EMG) for electro-neurophysiological study and nerve conduction studies (NCS) allow to distinguish among causes of motor weakness discriminating muscular or neuropathic causes. The myogenic pattern that IIM share with other muscle damage is the presence of fibrillation potentials.

Magnetic Resonance Imaging (MRI) is the gold standard for muscle imaging evaluation. It permits the differentiation of muscle in acute or chronic structural changes in terms of inflammatory and degenerative alterations. This technique has not been included in the EULAR/ACR classification criteria. Nevertheless, muscle MRI provides a global topographic map of muscle involvement and allow the identification of the appropriate site to perform the biopsy [59,60].

The pulmonary involvement in IIM patients in the major cause of morbidity and mortality. Pulmonary function tests (PFT) should be performed as baseline screening tools in IIM patients. For better investigating a suspected lung involvement or in presence of ILD-associated serological abnormalities (e.g., anti-t-RNA synthetase or anti-MDA5 antibodies), the high-resolution CT scan (HRCT) is a fundamental examination to differentiate a distinctive pattern of ILD according to ATS/ERS consensus for idiopathic interstitial pneumonia [61]. HRCT and PFT are useful to monitoring the disease activity and therapies efficacy. Moreover, to minimize the exposure to radiation, lung ultrasound has been proposed as a screening examination for ILD. The occurrence of pulmonary hypertension (PH) in ASyS, mainly associated with ILD, dramatically worsens the prognosis suggesting a pulmonary vascular involvement [62]. ILD and pericardial effusion may contribute to the development of clinically silent PH in PM [63]. The clinical investigation of early PH screening implies different tools, including physical examination, laboratory indictors, and thoracic HRCT imaging [62]. Right heart catheterisation (RHC) is recognized as the gold standard for diagnosing PH [63]. Echocardiography has a key role in the non-invasive screening of patients with suspected PH, while RHC is required to confirm pre-capillary PH [62,63].

Muscle and skin biopsies should be performed when clinical and laboratory data do not provide a clear diagnosis. In particular, to avoid sampling errors the interested area should be chosen on the grounds of a reduced manual muscle testing (MMT)-8, an EMG and/or MRI appearance that indicate inflammatory activity. Biochemical assays are performed to rule out metabolic myopathies, and immunohistology allows to evaluate mutant proteins responsible for muscle dystrophies. The histologic features shared among IIM include necrosis, degeneration and regeneration of the myofiber, and inflammatory infiltration. However, the muscle tissue affected by different IIM subtype presents distinguishing features as show in **Table 3** [13].

| Myositis subtype | Muscle fibres and tissue | Inflammatory cell infiltrates | MHC I expression | MAC depositions | Other specific findings |
|---|---|---|---|---|---|
| Dermatomyositis | Perifascicular atrophy, reduced number of capillaries | Perivascular, perimysial, T cells, B cells, macrophages, plasmacytoid dendritic cells | Perifascicular fibres | Small blood vessels | Sarcoplasmic MxA expression |
| Polymyositis | Degeneration, necrosis, regeneration | Endomysial inflammatory infiltrate with T cells often surrounding and/or invading non-necrotic muscle fibres | Diffuse distribution | No specific findings | Absence of rimmed vacuoles |
| Immune-mediated necrotizing myopathy | Necrotic fibres with scattered distribution, different stages of necrosis and myophagocytosis and regeneration, endomysial fibrosis and proliferation | Macrophage predominant, paucilymphocytic infiltrates | Diffuse distribution, sometimes only faint | Sarcolemmal and/or on small blood vessels | No specific findings |
| Antisynthetase syndrome | Oedematous and/or fragmented perimysium that stains with alkaline phosphatase, sometimes perifascicular myofibre necrosis | Scattered perimysial $CD68^+$, $CD4^+$, $CD8^+$ cells | Perifascicular predominance | Fibres adjacent to the perimysium, sarcolemmal on non-necrotic fibres | Myonuclear actin filament inclusions in electron microscopy, absence of MxA expression |
| Inclusion body myositis | Rimmed vacuoles, ragged red fibres, cytochrome oxidase-negative fibres, groups of atrophic fibres | Endomysial inflammatory infiltrate with mainly $CD8^+$ cells surrounding and/or invading non-necrotic muscle fibres | Diffuse distribution | No specific findings | TDP43, p62 aggregates, 15–18 nm filaments in electron microscopy |

***Table 3.*** *Overview of the histopathological findings across different IIM subtypes. MAC: Membrane Attack Complex; MxA: Myxovirus resistance protein 1. Adapted from Lundberg I. et al., 2021* [13].

Skin biopsy may be useful in patients with an interface of dermatitis difficult to differentiate from SLE [64].

Furthermore, a cardiac sonography should be performed as screening method with troponin-I assay and electrocardiogram in IIM patients characterized by a potential involvement of cardiac muscle. Cardiac MRI with gadolinium contrast is mandatory in patients with suspected myocarditis to evaluate the presence of specific radiologic sings [65].

Finally, in suspicion of CAM and particularly in the presence of anti- TIF1-γ positivity, it should be performed a total body imaging with total-body CT-scan or PET-CT/MRI scan beyond colonoscopy, esophagogastroduodenoscopy (EGD), and gynecologic/mammographic evaluation according to the clinical suspicion [66].

### *1.1.7 Prognosis*

Early diagnosis and treatment are essential to avoid or delay muscle atrophy and functional loss by identifying the disease subtype, the serologic markers, the age at disease onset, the disease severity at onset, the extent of the extra-muscular disease burden, and underlying malignancy.

Almost in 40% of IIM patients the immunosuppressive therapy allows to achieve clinical remission, while the rest of patients are characterized by a remitting-relapsing disease course [59].

Mortality estimates show large variations across different populations with a 10 years overall survival rate ranging from 20% to 90%, with the highest mortality peak within the first year after diagnosis [13]. The main causes of death in IIM are malignancy, cardiovascular disease, and ILD [13].

### *1.1.8 Therapy*

The aim of the therapy in IIM patients is to restore functionality and prevent further deterioration of muscle and extra-muscular organs involved in the pathogenesis.

#### *Non-pharmacological treatment*

The non-pharmacological treatment allows the recovery of physical functions and preserves the remaining self-autonomies.

Specific physiokinesiotherapy programs are fundamental in patients that present acute muscle injury for muscle strength reconditioning. During the active phases of the disease are prefer passive mobilizations than underload exercises to avoid contractures [67].

Of interest, physical exercise appears to activate several molecular pathways promoting capillary growth and muscle remodelling and reducing the immune response [13,68].

Moreover, the combination of aerobic and resistance exercises decreases muscle inflammation, increases aerobic capacity, and improves quality of life and muscle strength [69].

Regarding patients with chronic lung involvement, the preservation of the lung residual function is fundamental through respiratory physiotherapy to maintain static and dynamic lung volumes and prevent respiratory infections.

Finally, patients should be educated on skin photo-protection to interfere with the course of the disease at any level.

### *Pharmacological treatment*

The pharmacological treatment acts to arrest the inflammatory and autoimmune response. It is represented by variable combinations of glucocorticoids (GC) and immunosuppressants (IS) (**Figure 2**), but guidelines and results from clinical trials are still limited.

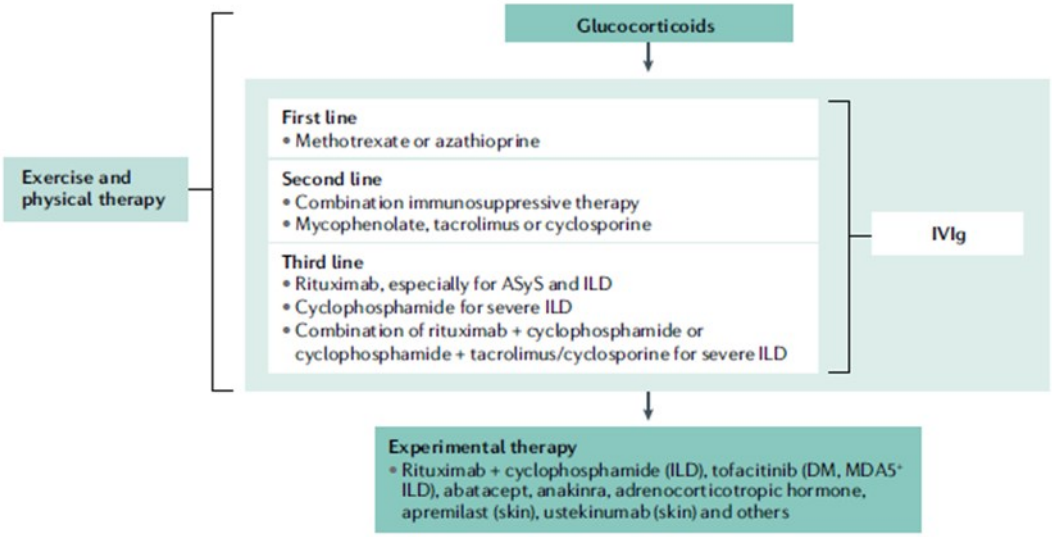


***Figure 2.*** *Guidelines for the treatment of IIM. ASyS: anti-synthetase syndrome; DM: dermatomyositis; IBM: inclusion body myositis; IIM: idiopathic inflammatory myopathies; ILD: interstitial lung disease; IVIg: intravenous immunoglobulin; MDA5: melanoma differentiation-associated gene 5. From Lundberg I. et al., 2021* [13].

### *Glucocorticoids*

Glucocorticoids (GC) still make up the first-line treatment, especially in patients characterized by severe ILD or muscle weakness. Several studies demonstrated its benefit on muscle inflammation. In fact, patients treated with GC for 3-6 months reported reduced inflammatory molecules, such as IL-1α/β, ICAM-1, MHC-I and a recovery of muscle strength [70]. A significant improvement in muscle strength is expected over the course of the second semester after GC treatment initiation.

The intravenous administration, compared to the oral one, is generally reserved for the most severe forms and extra-muscular involvement. GC treatment can trigger long-term adverse effects, and are burdened by a still high flare rate, thereby often requiring the association with an immunosuppressive agent [67].

### *Immunosuppressants*

Therapy with immunosuppressive (IS) drugs aims to reduce the GC dosage and to target disease mechanisms; yet these are slow-acting drugs which require weeks to months to reach full efficacy [71].

Methotrexate (MTX) is often used in association with cortisone as therapy of myositis and in the treatment of patients characterized by disease flares due to a reduction in the dose of glucocorticoids. A study conducted on JDM naïve patients reported a better response when treatment provided the association of prednisone and MTX compared to only prednisone administration [72,73]. Moreover, it has been demonstrated a protective effect of MTX on ILD progression [74]. Nevertheless, MTX can induce hepatotoxicity and myelodepletion and for this reason it is recommended the association with folic acid; it is also known a teratogen effect.

Azathioprine (AZA) is the immunosuppressant of choice in patients with liver or lung conditions and it is safe for use in cases of alcohol addiction and in pregnancy [72]. The AZA administration allows a better functional outcome in the long term than glucocorticoids alone [75,76]. It carries a risk for bone-marrow suppression that requires a complete blood count monitoring within the first two weeks of administration [13].

Mycophenolate mofetil (MMF) is a second-line agent for IIM treatment, while it is an increasingly valued drug in patients with severe myositis coexisting ILD where it can serve as the first-line drug. Its adverse effects are similar to the AZA's ones thus requiring the monitoring of blood cell count and liver enzymes. It could be poorly tolerated for gastrointestinal disorders, and it is teratogenic [77].

Cyclophosphamide (CYC) is a potent immunosuppressive agent for the treatment of refractory or severe disease, including rapidly progressive ILD, severe myositis or systemic vasculitis. Unfortunately, it is characterized by a multisystem toxicity, high infectious risk and teratogenicity that restricts its use to serious clinical conditions [72].

Cyclosporin A (CsA) and Tacrolimus (Tac) are second-line agents belonging to calcineurin inhibitors. They are emerging to be effective in the treatment combined with GC or MMF. They act by suppressing the T cell activation and have been demonstrated efficacy in refractory or severe myositis with or without an associated ILD. CsA and Tac require control of blood drug concentration and monitoring of renal function, but they are compatible with pregnancy [77].

***Intravenous immunoglobulins***

Intravenous immunoglobulins (IVIg) are second or third-line agents endowed with anti-inflammatory and immunomodulating functions. They are used concomitantly with other therapies, such as in

combination with GC for treating dysphagia, or subsequently to their failure. Their use in combination with immunosuppressants is useful for the management of refractory forms. IVIg are well tolerated and safe in pregnant, oncologic or infected patients and with an impact on patients' quality of life [78]. Recently, Aggarwal et al. conducted a 16-week phase III trial evaluating the IVIg Octagam 10% for the treatment of adult patients with dermatomyositis showing improvements in disease activity. The authors concluded that IVIg resulted effective compared to placebo despite being associated with adverse events, including thromboembolism [79].

***Biological drugs and small molecules***

Rituximab (RTX) is a chimerical monoclonal antibody targeting CD20+ B lymphocytes that are cells involved in the pathogenesis of several IIM subgroups. It is well tolerated and allows a significant reduction of steroid dosage. RTX demonstrated efficacy in skin manifestations, muscle weakness and ILD with a short course of disease (< 36 months) and seropositive status [80–83].

It has been reported contrasting results on anti-TNF therapies, such as Etanercept and Infliximab, maybe due to the ambiguous function of TNF-α in the muscular milieu that both impair muscle contraction and myogenesis and promote myotube development [84,85].

Abatacept is a fusion protein deriving from the combination of CTLA4 and IgG1's Fc portion able to inhibit the T cell co-stimulation. It associates with clinical and histology improvements [86].

JAK-inhibitors (JAKi) are small molecules that interfere with JAK-STAT signaling pathway which is responsible for the intracellular transduction of inflammatory signals, particularly from inflammatory cytokines and IFN-I. JAKi effects result in modulation of cell growth and immune response [87]. Recently, Tofacitinib has been proposed for the treatment of refractory cutaneous manifestations [88] as well as of ILD with progressive lung involvement [89]. Moreover, there are ongoing multicenter phase III clinical trials of baricitinib in the treatment of adult IIM and in patients with relapsing or naïve DM [90,91]. In addition, it has been demonstrated the efficacy of baricitinib in a case of refractory muscle and cutaneous juvenile DM by inducing a rapid and significant amelioration of cutaneous and joint features of DM, as well as of subjective muscle strength [92].

***Plasma exchange***

Plasma exchange (PE) allows the removal of endotoxins, circulating autoantibodies, and complement components. It is applied in outstandingly refractory disease, and it has been demonstrated efficacy in patients with rapidly progressive ILD, especially anti-MDA5 positive, with severe pharyngoesophageal muscle weakness, and in anti-SRP positive patients. PE can be performed in association with glucocorticoids, immunosuppressants, or biological drugs administration [93,94].

## 1.2 Extracellular vesicles (EVs)

### *1.2.1 Definition, classification, and nomenclature*

The extracellular vesicles (EVs) are a family of nanoparticles delimited by a lipid bilayer naturally released from all cell types. Unlike cells, they cannot replicate due to the lack of a functional nucleus [95,96]. These nanoparticles are continuously released into all body fluids, express distinctive surface markers and deliver cell-specific cargo in an organ-specific manner acting as an important mediator in cell-to-cell communication [97,98]. EVs are potent vehicles that convoy cytoplasmic components including proteins, lipids, nucleic acids, and carbohydrates influencing various pathophysiological processes [99,100]. EVs were first observed by Wolf in 1967 who defined them as "platelet dust" [101]. In 1981, Trams and colleagues attribute the term "exosomes" to plasma membrane-derived vesicles with 5'-nucleotide enzyme activity that may have physiological functions and originate from the exudation of various cell line cultures [102]. In 1987 Rose Johnstone proposed the term "exosome" [103,104] to describe the nanoparticles as an alternative pathway to eliminate waste products and maintain cellular homeostasis [105,106].

EVs that originate from cells undergoing apoptosis are called apoptotic bodies (50 - 1000 nm in diameter). EVs released from living cells include exosomes (30 - 150 nm) and microvesicles (100 - 1000 nm). Exosomes derive from endosomal origin and are released in the extracellular environment upon fusion of multivesicular bodies (MVBs) with the plasma membrane, while microvesicles (also known as ectosomes or microparticles) bud off from the plasma membrane. EVs are also subdivided into different subtypes based on size, density, content, and topology [96].

To unify the nomenclature of EVs, in 2018 the International Society for Extracellular Vesicles proposed the Minimal Information for Studies of Extracellular Vesicles (MISEV) guidelines to invite to refer to these nanoparticles using the generic term "extracellular vesicles" (EVs) discriminating by physical characterization the "small EVs" (< 200 nm) and "medium/large EVs" (> 200 nm) or depending on their biochemical composition, such as tetraspanin positive (CD63+/CD81+) EVs [107].

### *1.2.2 Biogenesis*

#### *Exosomes biogenesis*

Despite the term "exosomes" is still widely used, it has been suggested referring to them using "small EVs" according to ISEV 2018 guidelines, due to methodological difficulties of nanoparticles separation. Their biogenesis begins with the endosome formation by the invagination of the cell membrane in the early stage, and the bioactive substances accumulate in the early sorting endosomes

(ESEs). Then, the ESEs mature in late sorting endosomes (LSEs) under the control of the endocytosis sorting complex and other related proteins required for transport, and during this process they accumulate intraluminal vesicles (ILVs) in their lumen. Ultimately, after a second indentation LSEs form multivesicular bodies (MVBs) which fuse with the cell membrane, and then the cells components are released on the outside in vesicle structures. It has been reported that exosomes biogenesis can happen both via endosomal sorting complex required for transport (ESCRT)-dependent and ESCRT-independent mechanisms. However, recently it has been reported that the formation of some exosomes can also involve other components, such as four-transmembrane domain proteins and lipid rafts [99,102].

In the biogenesis process, ESCRT machinery is involved through the presence of four multiprotein subcomplexes: ESCRT-0, -I, -II, and -III that act to facilitate MVBs formation, vesicle budding, and protein cargo sorting [108,109] associated with other proteins (e.g., Vps4, VTA1, Alix) [110]. The ESCRT-0, -I, and -II complexes recognize and sequester ubiquitinated membrane proteins at the endosomal membrane, whereas the ESCRT-III complex is responsible for membrane budding and the final scission of ILVs [111]. In detail, ESCRT-0 comprises HRS that recognizes the mono-ubiquitylated proteins and associates in a complex with STAM, Eps15, and clathrin. HRS recruits tumor susceptibility gene 101 protein (Tsg101) of the ESCRT-I complex, and ESCRT-I is then involved in the recruitment of ESCRT-III through ESCRT-II or Alix, an ESCRT-accessory protein [110]. Furthermore, the formation of exosomes requires the regulation by several proteins, including protein tyrosine phosphatase (HD-PTP), the HOP complex (heat-shock protein (HSP)70-HSP90 proteins), soluble NSF attachment (SNAPs), soluble N-ethylmaleimide-sensitive factor attachment protein receptors (SNAREs) such as vesicle-associated membrane protein 7 (Vamp7), coat complex subunit, and Sec 1 proteins, GTPase Ras-related protein Rab7A, Rab GTPases proteins [112]. Rab GTPases are molecular switches that regulate intracellular vesicle transport, including EVs secretion [113]. Rab27a has been shown to play a role in both docking and fusion. Rab27b and Rab27, synaptotagmin-like 4 (SYTL4) and exophilin-5 regulate the docking of the MVBs at the plasma membrane. Meanwhile, Rab11 and Rab31, the R-SNARE protein YKT6, and the v-SNARE protein VAMP7/TI VAMP are implicated in the fusion event between MVBs and the plasma membrane [112,114]. Moreover, it has been reported that the exosomal protein Alix which is associated with several ESCRT proteins (Tsg101 and CHMP4) participates in endosomal membrane budding and abscission, as well as exosomal cargo selection via interaction with syndecan [108] and the regulation of ESCRT-membrane scission machinery [112]. Finally, the dissociation and recycling of the ESCRT machinery require interaction with the AAA-ATPase Vps4 (vacuolar protein sorting-associated protein) [110].

The exosomes biogenesis driven in an ESCRT-independent pathway is orchestrated by neutral sphingomyelinases, a family of enzymes that hydrolyses sphingomyelin in ceramide, as well as phospholipase D2 (PLD2) and ADP ribosylation factor 6 (ARF6) [112]. Then, ceramide may act generating membrane subdomains that impose a spontaneous negative curvature on the membranes, or it could be metabolized to sphingosine 1-phosphate to activate Gi-protein-coupled sphingosine 1-phosphate receptor for cargo sorting into exosomal ILVs. In addition, another ESCRT-independent pathway might be initiated by proteins of the tetraspanin family that is involved in endosomal sorting. Among these, CD63 which is particularly enriched on the surface of exosomes and the tetraspanins CD81, CD82 and CD9 are directly involved in the sorting of various cargoes to exosomes. Particularly, these proteins form clusters and dynamic membrane platforms with transmembrane and cytosolic proteins and other tetraspanins probably acting in the formation of the microdomains that will bud. Moreover, the CD81 tetraspanin has a cone-like structure probably shared by other tetraspanins with an intramembrane cavity that can accommodate cholesterol. The clustering of several cone-shaped tetraspanins could induce inward budding of the microdomain in which they are enriched. However, tetraspanins also regulate the intracellular routing of cargoes, such as integrins towards multivesicular endosomes (MVEs), suggesting their function affects different steps of exosome generation [115] (**Figure 3**).

The sorting of transmembrane cargoes into EVs is largely dependent on endosomal sorting machineries [115]. "De novo" proteins from the endoplasmic reticulum and Golgi complex may be directly sorted into the MVBs guided by either action of ESCRT-machinery (AIP1/Alix/Vps31 and Tsg101/Vps23), or by a ceramide/tetraspanin-dependent pathway [114]. For example, it has been shown that tetraspanin-enriched microdomains (TEMs) with tetraspanin CD81 play a key role in sorting target receptors and intracellular components toward exosomes [108]. In fact, exosomes are highly enriched in proteins, including tetraspanins which take part in cell penetration, invasion, and fusion events and heat shock proteins as part of the stress response that are involved in antigen binding and presentation. Exosomes also contain proteins that are involved in exosome release (Alix, TSG101), responsible for membrane transport and fusion (annexins and Rab) and in exosome biogenesis (Alix, flotillin, and TSG101) [108].

***Microvesicles biogenesis***

The biogenesis of microvesicles is less known than the exosomes one [112]. This process requires several molecular rearrangements within the plasma membrane, including changes in lipid components, protein composition and in $Ca^{2+}$ levels. $Ca^{2+}$-dependent enzymatic machineries, including aminophospholipid translocases (flippases and floppases), scramblases and calpain drive

rearrangements in the asymmetry of membrane phospholipids which causes physical bending of the membrane and restructuring of the underlying actin cytoskeleton favouring membrane budding and microvesicles formation. Moreover, cytoskeletal elements and their regulators are required for biogenesis. In addition, the RHO family of small GTPases and of the RHO-associated protein kinase (ROCK) are important regulators of actin dynamics [115]. In fact, generally, microvesicles originate via direct budding of the plasma membrane through ARF6 and RHOA-dependent rearrangement of the actin cytoskeleton. Similar to exosomes, ESCRT complex is also engaged in microvesicles biogenesis. Thus, TSG101 protein interacts with accessory proteins ALIX and arrestin domain-containing protein-1 (ARRDC1) during the last phase of the release, and ESCRT-III with ALIX are involved in cytokinetic abscission [112]. Cholesterol, an abundant lipid component in microvesicles [115] and ceramide have also been shown to play an essential role in this process [112] (**Figure 3**).

Cytosolic components fated for secretion into microvesicles require their binding to the inner leaflet of the plasma membrane through association on the plasma membrane anchors (palmitoylation, prenylation, myristoylation) and the establishment of high-order complexes to concentrate them to the small membrane domains from which microvesicles will bud [115]. Furthermore, microvesicles display unique lipid characteristics, including phospholipid phosphatidylserine which promotes uptake by recipient cells, an enrichment in phospholipid lysophosphatidylcholine, sphingolipid sphingomyelins, acylcarnitine, and fatty acyl esters of L-carnitine [112]. It is still unclear how nucleic acids found in microvesicles are targeted to the cell surface [115].

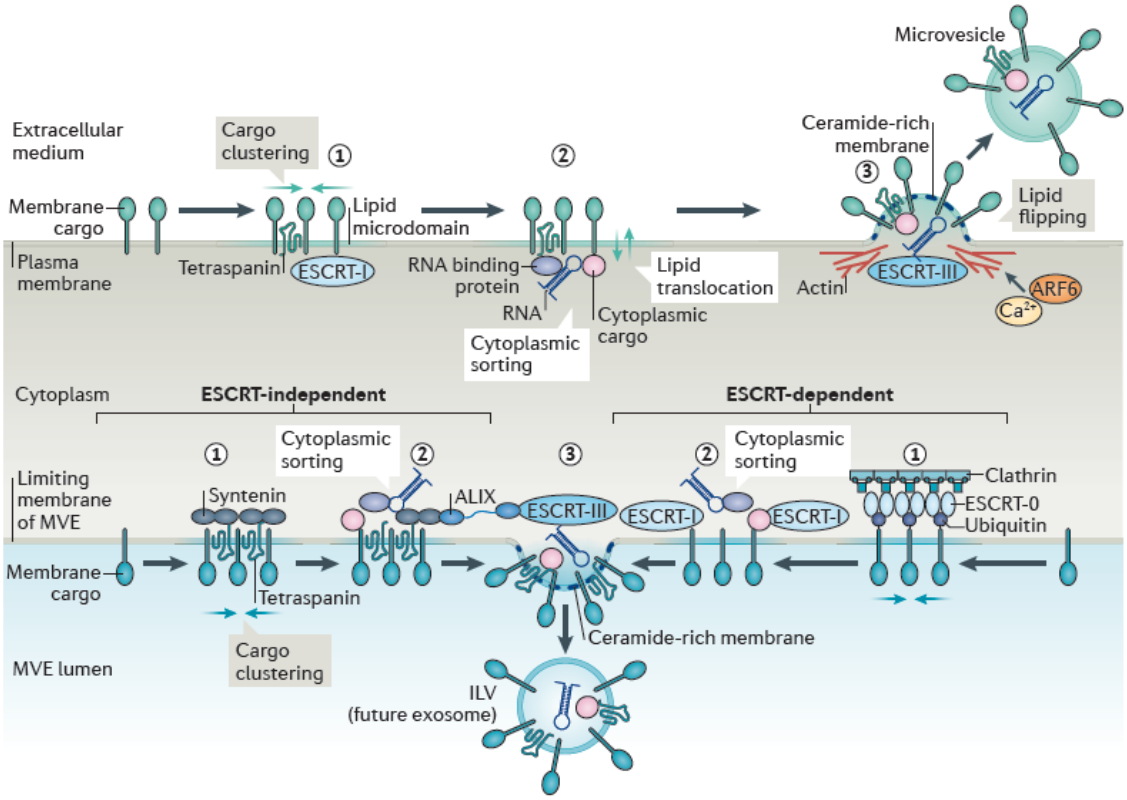


***Figure 3**. Overview of the mechanisms involved in EVs biogenesis. ESCRT: Endosomal sorting complexes required for transport; ARF6: ADP-ribosylation factor 6; MVE: multivesicular endosome; ALIX: ALG-2 interacting protein; ILV: intraluminal vesicle. From van Niel G. et al., 2018* [115].

### *1.2.3 Targeting to recipient cells and EVs uptake*

Once released into the extracellular space, EVs can reach recipient cells and deliver their contents to elicit functional responses and affect their physiological or pathological status. This process requires the docking at the plasma membrane, the activation of surface receptors and signaling, and then the vesicle internalization or fusion with target cells. However, the mechanism is complex and depends on the origin of EVs and the recipient cells [115]. EVs exert their intercellular signaling function in two ways: transmitting information to recipient cells by direct contact via their surface ligands or transferring proteins and nucleic acids to target cells.

The first mechanism depends on ligand–receptor interaction without delivery of the EVs contents into the recipient cell [113]. Target cell specificity is determined by specific interactions between proteins enriched on the EVs surface and receptors on the plasma membrane of the recipient cell. Several mediators of these interactions are known, including tetraspanins, integrins, lipids, lectins, heparan sulfate proteoglycans, and extracellular matrix (ECM) components. For example, integrins on EVs can interact with adhesion molecules such as intercellular adhesion molecules (ICAMs) at the surface of recipient cell or with extracellular matrix proteins. EVs tetraspanins can interact with integrins and promote docking and uptake of EVs by selected recipient cells [115].

The second mechanism of intercellular signaling depends on cellular internalization or membrane fusion, which facilitates the entry of the EVs contents into acceptor cells. For instance, EVs can transfer microRNAs (miRNAs) into acceptor cells to downregulate expression of target genes and deliver messenger RNAs (mRNAs) to be functionally translated. Furthermore, other functionally important molecules, including genomic DNAs (gDNAs), mitochondrial DNAs (mtDNAs), long noncoding RNAs (lncRNAs), and proteins can be delivered to recipient cells. Nevertheless, the mechanisms of EVs uptake and cargo delivery into the cytosol of recipient cells are still poorly understood [113]. When EVs are bound to recipient cells, the uptake can happen by direct membrane fusion or may be internalized by endocytosis. Endocytosis can be generally subdivided into five categories: receptor-mediated endocytosis also known as clathrin-mediated endocytosis, caveolin-mediated endocytosis, phagocytosis, micropinocytosis, and lipid raft-mediated endocytosis. Interestingly, lipid rafts disruption by cholesterol depletion reduces their uptake [113,115]. Following the uptake to the recipient cells, frequently EVs reach the lysosomes and are degraded. In other cases, EVs may escape digestion by back fusion with the limiting membrane of the MVBs, releasing their contents into the cytoplasm of the target cell [115] (**Figure 4**).

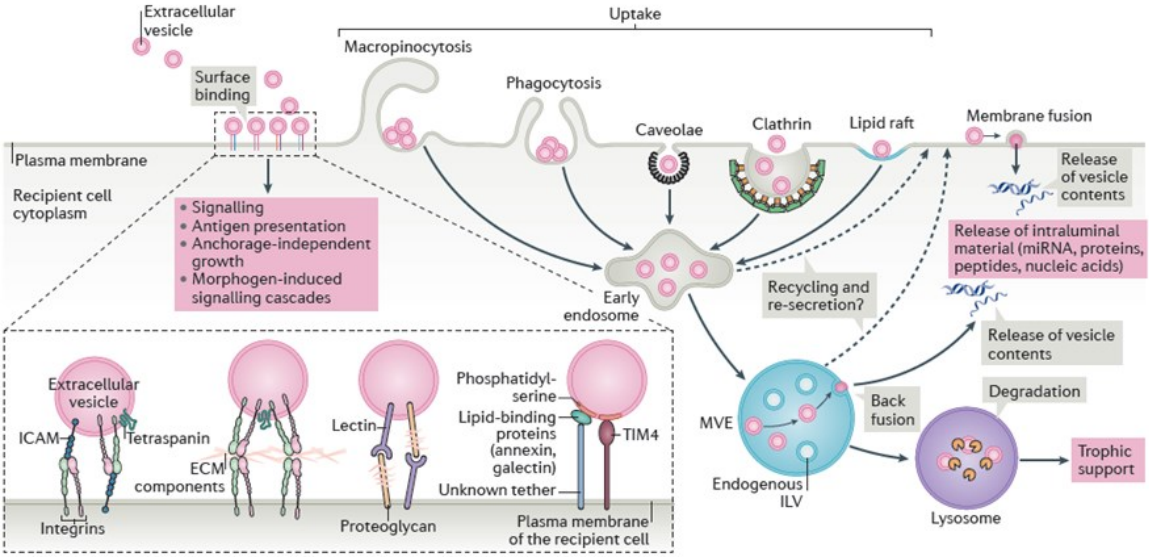


***Figure 4.*** *Mechanisms of EVs fate in recipient cells. MVE: multivesicular endosome; ILV: intraluminal vesicles; ICAM: intercellular adhesion molecules; ECM: extracellular matrix; TIM4: T cell immunoglobulin mucin receptor 4. From van Niel G. et al., 2018* [115].

### *1.2.4 EVs cargo*

EVs carry a plethora of biomolecules including proteins, lipids and nucleic acids that modulate the behavior of the recipient cells and promote tissue-specific effects [115].

The protein cargo enclosed in EVs is extremely diverse and reflects the EVs subtypes. They include proteins involved in EVs biogenesis (e.g., ALIX, TSG101, and other ESCRT components), EVs release, response to the thermic shock (e.g., RABs and ARF6), vesicular trafficking (e.g., HSP70 and HSC70), signal transduction proteins, and other transmembrane proteins co-isolated in EVs as well as transcription factors, enzymes, and extracellular matrix proteins. Of note, transmembrane α-helices proteins belonging to the tetraspanin superfamily (CD9, CD63, CD81) are high specificity EVs markers [116,117]. Interestingly, ubiquitination is a mechanism by which proteins are selectively targeted to the EVs pathways due to the role of ubiquitin to recruit proteins and form MVBs by the ESCRT-dependent system. Accordingly, ubiquitinated proteins are commonly found in EVs. Nevertheless, also non-ubiquitinated MHC class II molecules are targeted to MVBs fated for secretion as well as palmitoylation and farnesylation bring proteins to lipid rafts and are implicated in EVs biogenesis [118]. Exosomes tend to express a higher glycoprotein content compared to the donor cell, whereas microvesicles are enriched of post-translationally modified protein cargos, in particular with a predilection for glycosylations and phosphorylations [119].

Lipids are important bioactive molecules of EVs, and the lipid composition differ between EVs and donor cell. They play a fundamental role in EVs biogenesis characterizing the membranous microdomains with greater rigidity compared to the donor cell with consequently increased resistance to the extracellular environment [116,120,121]. The enzyme phospholipase D2 (PLD2) produces phosphatidic acid (PA) which regulates ILVs formation and exosome biogenesis [122,123]. In particular, the PA group may induce negative membrane curvature and the subsequent invagination of the MVBs membrane [124]. However, the direct involvement of PA in the effect of PLD2 on exosome biogenesis has not yet been demonstrated.

Moreover, lipids act in the EVs biological functions. In detail, as an example, phosphatidylserine facilitates their internalization by recipient cells and lysophosphatidylcholine allows them to acquire the ability to interact with dendritic cells causing them to undergo maturation and to perform antigen presentation more efficiently. It has been reported that phosphatidylcholine and diacylglycerol are decreased in EVs compared to the cell of origin's plasma membrane, while sphingomyelin, cholesterol, GM3 ganglioside, phosphatidylserine, and ceramide are increased in the EVs cargo [116].

Although EVs cargo of DNA (EVs-DNA) is now an essential part of the dynamics and survey of natural ecosystems, it has started to gain in importance in the last few years [125] particularly as a tool for therapeutic nucleic acid delivery to target cells in gene therapy [126]. Interestingly, many researchers have shown that cancer-derived EVs contain DNA which reflects the mutational status of parental cancer cells [125].

The EVs cargo of RNA does not mirror the composition of the donor cell as to the RNA molecules types and their relative concentration. The most prominent nucleic acid molecules enriched in EVs are small RNAs, rarely exceeding 200 base pairs (bp) in length [127,128]. Many of the RNAs found therein engage in protein synthesis like transfer RNAs (tRNAs), 18S or 28S ribosomal RNAs (rRNAs) subunits, and messenger RNAs (mRNAs) fragments. Furthermore, a considerable portion of the RNA cargo consists of regulatory RNAs such as microRNAs (miRNAs) and piwi-interacting RNAs (piRNAs) small non-coding RNA (sncRNAs), and long non-coding RNAs (lncRNAs). Small nucleolar RNAs (snoRNA) which participate in RNA post-translational processing and DNA replication, have also been detected in EVs [127,128]. The study of selective packaging of RNA into nascent EVs has discovered that some miRNAs contain a targeting sequence recognized by a sumoylated hnRNPA2B1 and that YB-1 proteins may selectively recruit specific miRNAs into newly forming exosomes [118].

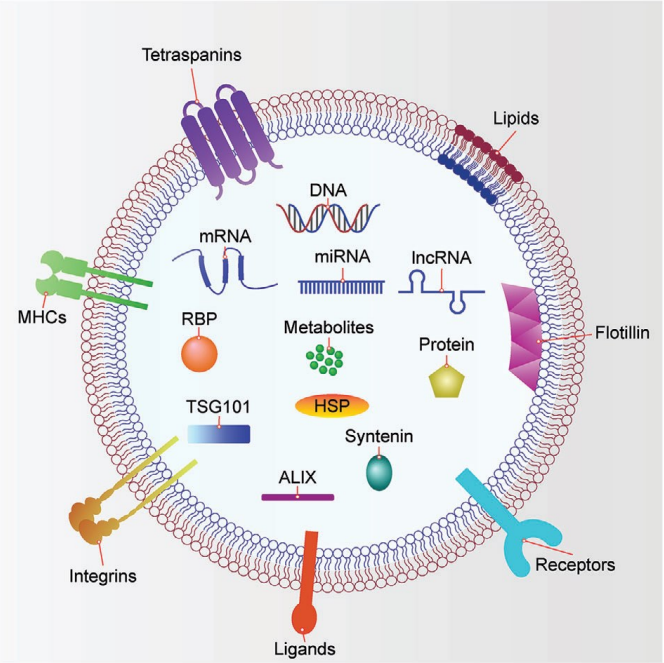


***Figure 5***. *Composition of EVs containing various nucleic acid molecules, proteins, lipids, and metabolites. mRNA: messenger RNA; miRNA: microRNA; lncRNA: long non-coding RNA; RBP: retinol binding protein; MHC: major histocompatibility complex; TSG101: tumor susceptibility gene 101 protein; ALIX: ALG-2 interacting protein X; HSP: heat shock protein. From Teng F. et al., 2021* [113].

### *1.2.5 Patophysiological functions*

It is recognized that EVs are involved in various physiological processes as well as pathological conditions [129]. A growing amount of evidence supports the role of EVs in intercellular communication either via paracrine activity on nearby cells or endocrine activity on distant target cells through the blood circulation. In fact, they also act like a platform for the presentation of ligands or antigens [130].

EVs represent an appropriate vehicle convoying molecules of nucleic acids, lipids, and proteins able to protect their cargo from the degradative action of enzymes of the extracellular environment. These nanoparticles influence the signal transduction pathways of recipient cell by releasing signal molecules, transferring regulatory or messenger RNA molecules and proteins, removing membrane receptors, as occurs in the maturation of reticulocytes, as well as removing cytosolic components, such as MAC [131].

They also can support cells to dispose of unwanted molecules such as β-amyloid and α-synuclein aggregates when the lysosome activity is impaired [127].

Several studies demonstrated the pro-coagulant, anti-coagulant and fibrinolytic properties of EVs. They promote the reticulocyte maturation into erythrocytes via recycling of transferrin and its receptor, as well as stimulate angiogenesis, regulate embryonic development and tissue regeneration, synapsis plasticity and microglia interconnection [103,132–134].

Furthermore, EVs are involved in both innate and adaptative immunity by regulating the inflammatory process, transporting pro-inflammatory cytokines, promoting the antigen presentation and controlling the functioning of the immune system. The nanoparticles loaded with MAC can be released to remove it from the cell surface and ensure cell survival representing an escape system from the complement. On the other hand, EVs can promote the complement activation in thrombotic and inflammatory diseases.

EVs released from dendritic cells express the membrane molecules of the donor cell, including MHC-I, MHC-II and adhesion molecules thus stimulating the antigen presentation to T CD8+ and T CD4+ lymphocytes [135]. The nanoparticles that originate from regulatory T (Treg) lymphocytes acquire the functions of self-tolerance and immune response modulation characteristic of the donor cells [136]. T-reg cells-EVs that contain specific miRNAs, such as miR-146a-5p or let-7d involved in the immunity pathways, can inhibit the proliferation of T CD4+ lymphocytes. These EVs can exert an immunosuppressive role also thank to CD81 tetraspanin able to bind IL-35 which combine with its receptor on T CD8+ and T CD4+ lymphocytes inducing PD-1 expression and anergy [137]. Already in 1996 it has been reported that B lymphocytes-derived EVs exhibit antigen-presenting properties, allowing the induction of T-cell responses [112].

### *1.2.6 EVs in cancer*

It is beyond doubt the role of EVs in cancer pathology where they represent key mediators in the complex interplay between tumor cells, stromal cells, and the tumor microenvironment thus influencing tumor growth, local invasion, and remote dissemination. EVs participate in the multidirectional crosstalk mediating the communication among stromal and tumor cells as well as different cells subpopulations of the tumor microenvironment, such as tumor-associated macrophages and they exchange meaningful cues within the primary tumor's niche. Many of the interactions rely on profound ECM remodelling to support local and distant invasion. For instance, KRAS and EGFR III are oncogenic molecules that represent the EVs cargo in the tumor microenvironment. They are shared amongst primary tumor subpopulations via EVs resulting in MAPK and AKT triggering [138].

Tumor-secreted EVs interact with stromal fibroblasts and endothelial cells inducing the cell differentiation to myofibroblasts and angiogenesis, respectively. It has been demonstrated that stromal cells have a dual role in the EV-mediated interaction with tumor cells. They confer apoptosis- and chemo- resistance alongside invasive properties to cancer-cells through different pathways, such as Wnt up-regulation and PTEN down-regulation due to the action of specific miRNAs. On the other hand, they display anti-tumor activities by inducing metastatic cells into a state of dormancy [139].

Moreover, tumor-secreted EVs show different functions towards the immune system displaying an increased immune-tolerance (e.g., by inducing the cytotoxic T cell apoptosis via Fas ligand and TRAIL) and an immune-stimulation (e.g., by exposing T cells to MHC I and II molecules and T cell costimulatory molecules) against the tumor [140]. An immune-suppressive status is established in tumor microenvironment also by means of tumor-derived PD-L1+ EVs that involved the PD-1/PDL-1 pathway resulting in the blockade of CD8+ T cells proliferation [137].

Furthermore, EVs loaded with vimentin and matrix metalloproteinases (MMPs) regulate another fundamental step of tumorigenesis, the epithelial mesenchymal transition (EMT) promoting the acquisition of the mesenchymal phenotype with migratory and invasive properties [141]. However, it is necessary that EVs, through a variety of mechanisms, induce a favourable pre-metastatic niche so that circulating tumor cells adhere and metastasize [142]. In particular, endothelium-targeted EVs promote loss of endothelial barrier's integrity with consequent vascular leakiness allowing the entry of circulating tumor cells [143,144].

### *1.2.7 EVs in autoimmune rheumatic diseases*

EVs are fundamental regulatory actors in innate and adaptative response and they are involved in the pathogenesis of several autoimmune diseases [116,145–147].

Systemic lupus erythematosus (SLE) reports higher plasma EVs concentration compared to healthy controls in several studies and reflects the state of immune system hyperactivation and global disease activity [148]. They transport complement proteins, immunoglobulins, phosphatases, kinases and metabolic enzymes with effects on the activation of lymphocytes, monocytes and neutrophils [149,150]. In particular, CD14+ monocyte-derived EVs appear significantly more concentrated among SLE patients with active disease compared to healthy donors [149]. Endothelium-derived EVs levels result in tight correlation with the degree of vascular involvement in these patients [151]. Podocyte-derived EVs, especially HMGB1+ EVs, collected from urinary samples of lupus nephritis (LN) patients report a strong association with glomerular damage and degree of LN activity that correlated with clinical parameters [151].

In SLE pathogenesis, EVs are crucial sources of self-antigens. For instance, it has been observed that EVs contain dsDNA which activates DNA-specific B lymphocytes [152]. EVs positive to CD46, CD55 and CD59 markers are protected from MAC assembly thus causing reduced clearance of apoptotic bodies and their subsequent accumulation, a hallmark of numerous autoimmune conditions [153]. Of interest, some subpopulations of apoptotic-derived EVs have been shown to trigger neutrophil extracellular traps (NET)-osis in dendritic cells encouraging the formation of anti-dsDNA antibodies [154]. It has been recognized that apoptotic bodies from the serum of SLE patients trigger cGMP-AMP synthase which in turn activates the stimulator of interferon genes (STING) thus increasing IFN-I secretion. Similarly, EVs-miR-574 induces the up-regulated expression of IFN-I among the plasmacytoids dendritic cells of SLE patients [155]. Finally, the EVs isolated from SLE patients are enriched in immunoglobulins and complement components, while they are relatively poor in microtubular and cytoskeletal proteins that healthy controls [156].

Findings concerning rheumatoid arthritis (RA) patients report increased EVs concentration in peripheral blood of patients than healthy donors that correlates with disease activity and progression [157] as well as in synovial fluid [158].

Leukocyte-derived and platelets-derived EVs stimulate the up-regulation of inflammatory mediators and matrix degeneration through an enhanced secretion of metalloproteinases and hypercoagulation [159]. For instance, platelets-derived EVs are elevated within the synovial fluid. They promote angiogenesis to sustain chronic inflammation by facilitating the recruitment of inflammatory cells to

the affected joint [116,157]. Furthermore, fibroblast-like synoviocyte (FLS)-EVs appear to be increased in RA than controls. They participate in B cells stimulation within the intra-articular milieu and the glycosidase hexosaminidase D contained in them show joint-damaging effects [160]. In addition, FLS-released EVs carrying TNF-α which stimulate the AKT and NF-κB pathways leading to apoptosis resistance and T cells activation [161]. Citrullinated peptide-containing EVs released from FLS have been proposed to be implicated in the development of anti-citrullinated protein antibodies (ACPA) with a primary role in the RA pathogenesis [162].

Like CD8+ T cells-EVs [163], also platelet-derived EVs CD41+ containing immunocomplexes are particularly enriched in synovial fluid of RA patients where they prompt neutrophils to release leukotrienes [164].

Interestingly, EVs derived from macrophages that enclose damage-associated molecular patterns (DAMP) molecules directly bind and activate TLR2/4 pathway. They may carry cytokines such as RANK-L, IL-15, IL-1β, and TNF-α eliciting potent pro-inflammatory effects [116].

A dysregulated concentration of serum EVs has been detected in systemic sclerosis (SSc). Their increased concentration correlates with disease flares [165]. EVs isolated from SSc patients have been shown to be involved in immune impairment, vascular damage, and fibrosis. A potential role of EVs in primary pathogenetic mechanisms has been recognized in the dysregulation of endothelial cell apoptosis [166]. Moreover, it has been supposed that EVs mediate angiogenesis and vascular remodelling with consequences in the genesis of pulmonary artery hypertension [167].

Furthermore, the increased content of pro-fibrotic miRNAs and decreased expression of anti-fibrotic miRNAs in SSc patients support the induction of a profibrotic phenotype in vitro [168]. Interestingly, cultured scleroderma fibroblasts release EVs able to induce type 1 collagen expression in normal recipient fibroblasts [165].

Sjögren syndrome (SS) condition exhibit increased EVs concentration than healthy controls. However, patients characterized by a severe disease report a drop in EVs levels, probably due to their sequestration in target tissues. Interestingly, exosomes released by the epithelial cells located in the salivary glands deliver cargo proteins, such as Ro/SSA, La/SSB and Sm ribonucleoproteins which are key antigens in SS pathogenesis [169]. Consistently, the endothelial-EVs levels correlate with disease activity. Moreover, an altered protein and miRNAs composition has been detected in the EVs cargo from the tears and saliva of SS patients [169], the more representative related to immune-innate response [170].

### *1.2.8 EVs in idiopathic inflammatory myopathies*

The current knowledge of EVs role in IIM is still limited in comparison to the other autoimmune rheumatic diseases. EVs represent a source of autoantigens and immunocomplexes; besides, they also deliver myokines, a combination of miRNA sequences and peptides that, when released from inflamed myotubes, inhibit the myogenic signals [24,171]. Studies support the involvement of EVs in the promotion of local inflammatory processes, local muscle fibrosis, loss of function, and muscle weakness in PM and DM. MSAs and MAAs antibodies are usually included in PM EVs [148].

In 2010, Baka and colleagues have reported higher levels of immune cell-derived EVs in the plasma of IIM patients compared to healthy donors [172]. Other authors have demonstrated that higher plasmatic platelet-derived EVs levels in PM/DM patients correlate with systemic inflammation [173,174] and that they were reduced by glucocorticoid treatment [173]. Moreover, Jiang and collaborators have shown that EVs taken up by human aortic endothelial cells of patients with juvenile DM carry different RNA cargo compared to healthy children suggesting a role of EVs in the alterations of gene expression, cell functions, and consequently IIM pathogenesis [175,176].

### *1.2.9 EVs in clinical application*

A growing amount of literature is raising interest around EVs as potential biomarkers across a number of diseases, including autoimmune diseases [169]. Moreover, their accessibility in body fluids such as blood i.e. within the liquid biopsy is generating significant interest in medical research, due to the minimally invasive nature of the acquisition [177].

In fact, EVs could be used as tools for early and non-invasive diagnosis of a growing number of conditions [178]. In detail, the analysis of EVs cargo might provide remarkable insights into the disease pathogenesis and allows to characterize disease activity, stratify the patient's risk and the response to therapy [179]. Indeed, given that EVs can be released by every cell in the body and their levels may increase in pathological conditions, they possess several distinct advantages compared to traditional biomarkers, including capacity to function as non-invasive biomarkers present in almost all body fluids; ability to reflect the progress of diseases and the effects of treatments through EVs origin or cargo investigation; and ability to protect their cargos during long-term storage.

For these reasons EVs have been proposed for longitudinal disease monitoring and early detection of relapse in cancer, besides the evidence that EV-associated proteins and nucleic acids may be predictive of response to treatment [180]. Moreover, EVs have been proposed as promising diagnostic biomarkers in several autoimmune diseases, such as SLE, RA, primary SS, and SSc [151,169,181].

### *1.2.10 MicroRNAs*

MicroRNAs (miRNAs) are single-stranded small non-coding RNA molecules ranging in length from 18 to 25 nucleotides (nt) [182,183]. The half-life of miRNAs is generally long persisting for 5 days or longer, however, some miRNAs have rapid turnover. They are regulated by mechanisms similar to other RNAs, such as transcriptional activation or inhibition, epigenetic repression, and controlled degradation rates. MiRNAs are secreted by cells through EVs, and they remain stable in bodily fluids. Furthermore, their expression profiles differ between disease and normal conditions and multiple studies have used miRNAs in diagnostics [184].

Their biogenesis begins with the transcription from genomic DNA into primary-miRNA (pri-miRNA) composed of two stem-loop structures. The complex of RNase III enzyme Drosha with the RNA-binding protein DGCR8 cleaves the flanking regions of pri-miRNA to form a single stem-loop of precursor-miRNA (pre-miRNA). Then, the RNase III enzyme Dicer cleaves the loop region of the pre-miRNA to create a double-stranded miRNA: one of which is subjected to degradation [185–187].

A single miRNA can target hundreds of mRNAs and influence the expression of many genes post-transcriptionally often involved in a functional interacting pathway, likewise, a target mRNA can be bound by many different miRNAs to enable more diverse signaling patterns [182,185]. The binding of miRNA to mRNA requires the ribonucleoprotein complex RNA-induced silencing complex (RISC) with the core containing a miRNA loaded onto an Argonaute (AGO) protein (miRISC complex) to target in a sequence-specific manner the mRNA [182,184–186]. It is often sufficient a complementarity of ~7–8 bases in the miRNA-dependent manner. The guide strand of miRNA (mature miRNA strand) is incorporated into the RISC complex to mediate gene silencing and the passenger strand is degraded [182,188] (**Figure 6**). MiRNAs can act by targeting the 3′ untranslated (3' UTRs) region of target mRNA, with the seed region in nucleotide 2–7 in the 5′ end of miRNA being the crucial sequence [182] as well as a base pairing in the central region (bases ~9–12) causing mRNA cleavage and subsequent degradation [184]. The sequence-specific degradation depends on RNA hydrolysis with consequent silencing. However, generally miRNAs do not act to completely silence their target expression genes, but rather decrease their expression. Moreover, any given mRNA 3' UTR presents binding sites for many miRNAs allowing miRNAs to work together to increase the target repression. Different mechanisms which not mutually exclusive are involved in reducing the expression of target mRNA or proteins by means of miRNAs, including RNA degradation, induced decapping, induced deadenylation, altered cap protein binding, reduced ribosome occupancy, and sequestration of the mRNA from translational machinery. On the other hand, it has been reported that under certain cellular conditions miRNA binding to the promoter can even increase target expression. Interestingly, it has been recognized the ability of a single miRNA to have opposing functions in different systems,

illustrating that miRNA communication is context dependent. Finally, the complementarity between miRNAs and other non-coding RNAs has been identified to be involved in miRNAs and cell signaling conversation [184].

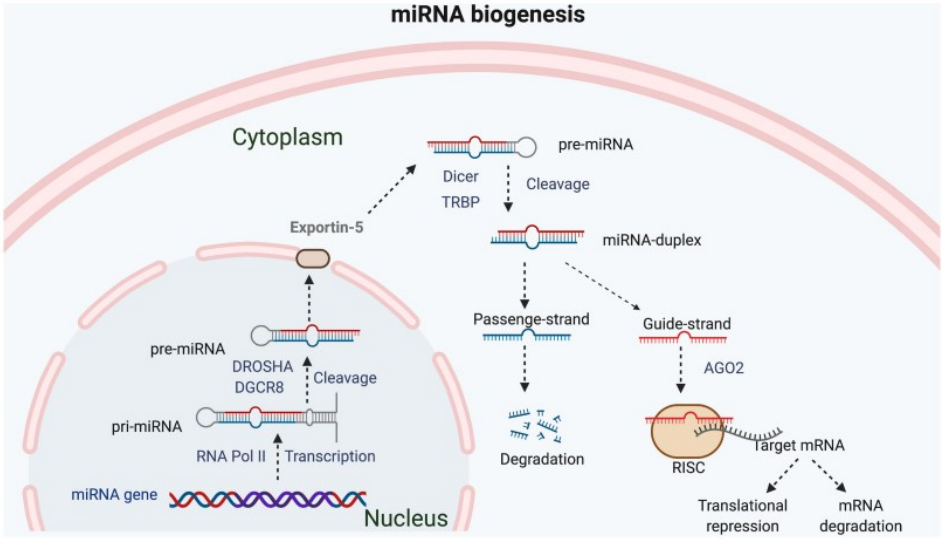


***Figure 6**. Schematic diagram of miRNAs biogenesis and their mechanism of action. miRNA: microRNA; pri-miRNA: primary microRNA; pre-miRNA: precursor-miRNA; RNA pol II: RNA polymerase II; AGO: Argonaute; RISC: RNA-induced silencing complex. From Shang X. et al., 2022* [189].

### *1.2.11 EV-microRNAs*

In the last decade, EVs have been shown to be efficient carriers of genetic information, including miRNAs that can be transferred between cells and regulate gene expression and function on the recipient cell [190]. EV-associated RNAs (EV-RNAs) are under intense investigation due to their potential role in health and disease. To date, there is a lack of standardized protocols for the EV-RNAs extraction and very little consensus on the technological platforms and normalization tools for assessing the expression levels of different RNA species. However, miRNAs isolation from EVs as well as their subsequent analysis through a variety of techniques such as qRT-PCR, miRNA arrays or Next-Generation Sequencing (NGS) is well documented. Moreover, the majority of circulating EVs from plasma are released from red and white blood cells and might carry RNA species (e.g., miRNAs) shared with tissue-derived EVs [115].

Importantly, cells can selectively sort RNA and miRNA into EVs for secretion and this content is markedly different compared to the parent cell. Thus far, research has identified several miRNA sorting mechanisms, but the specific details remain incompletely understood. RNA-binding proteins (RBPs) such as heterogeneous nuclear RNPA2B1, Argonaute 2, Y-Box Binding Protein 1, MEX3C,

Major Vault Protein, and La protein appear to bind specific RNA molecules and facilitate their transfer into EVs [191].

It has been demonstrated that EVs biological activity depends also on their cargo of non-coding RNAs, such as miRNAs, silencing RNAs, and long non-coding RNAs that appear to mediate pathological conditions [192] and disease progression [147]. For instance, in cancer and immune response have been identified dysregulated EV-miRNAs content, shedding light on the potential role of selective sorting in pathogenesis. In some cases, selective shuttling of miRNAs into EVs has been directly implicated in the disease pathological process, for example, miR-92a-3p with atherosclerosis [191]. A growing body of evidence associates EV-miRNAs with different functional roles in cancer such as metastatic progression or response to therapeutic agents [115]. Other research demonstrated differential expression of EV-derived miRNAs without a clear mechanism of pathogenic control, such as miR-320a and miR-221 over hyperoxia. In particular, the EVs-mediated transfer of mRNA and miRNA has been shown to induce effects on recipient cells such as regulating protein expression, suggesting an in vivo functional role. However, another main theory indicates that cells might secrete EVs to eliminate unnecessary RNAs [191].

Of interest, like EVs are gaining increased recognition as a reliable source of autoimmune disease biomarkers, recent studies indicated the diagnostic/prognostic potential of dysregulated EV-miRNAs in adult rheumatic patients. EV-miRNAs are proposed as powerful means for new non-invasive biomarker discovery thanks to their high stability, concentration, and integrity coupled with tissue specificity [193].

### *1.2.12 MicroRNAs in cancer*

A growing amount of research studies aims to identify the dysregulated miRNAs in several diseases and subtypes of neoplasia with the scope of using these microRNAs as early biomarkers. In addition, circulating miRNAs enclosing in EVs are detected in bodily fluids [194] and could facilitate their detection.

It has been reported the dysregulated expression profile of miRNAs that target regulatory genes critical to cancer development, including E2F and RAS in several types of cancer, such as lymphoma, colorectal cancer, lung cancer, breast cancer and glioblastoma [195]. MiRNAs can act both as onco-suppressors and onco-genes depending on the target mRNA to which they bind. For instance, miRNAs belonging to the hsa-let-7 family represent onco-suppressors in lung, breast, urothelial and cervical cancer [196]. They negatively regulate RAS, one of the most important oncogenes mutated in human tumors and they resulted down-regulated in cancer compared to healthy controls [197]. On the

other hand, examples of onco-genes are hsa-miR-222 and hsa-miR-221 which regulate p27 stimulating cell proliferation in glioblastoma. Similarly, hsa-miR-155 acts on HGAL, FOXO3A, SOCS1, JMJD1A in various neoplasms contributing to tumor progression and resistance to chemotherapy [198].

### *1.2.13 MicroRNAs in autoimmune rheumatic diseases*

MiRNAs are largely involved in the immune system regulation and their dysregulation may contribute to predisposition to immune system abnormalities and development of autoimmune conditions.

In SLE patients the research is addressed to the definition of new biomarkers for better identification of disease activity and prognosis. In the context of lupus nephritis, increasing evidence leads interest toward urine proteome and transcriptome. Urinary hsa-miR-146a and hsa-miR-26a result associated with renal damage suggesting these miRNAs to be useful in discriminating the potential renal involvement [146,199]. In detail, EV-miR-146 is a promising urinary marker for kidney sclerosis [151]. This miRNA reduces the expression of several components of the IFN-I signaling pathway, such as TRAF6, IRAK1, IFN-5, STAT1, thus attenuating the numerous effects that this cytokine has on all cells of the immune system [200]. In addition, hsa-miR-21 with a key role in macrophage polarization has been proposed as potential biomarker for discriminating kidney fibrosis and injury [201]. Serum hsa-miR-451a has been suggested to correlate with SLE disease activity and kidney damage [202].

Among RA disease, several studies are aiming for the molecular profile of miRNAs to define an additional tool for early diagnosis and prognosis of the disease. In detail, recent findings have reported that in activated fibroblast-like synoviocytes of RA patients characterized by active disease hsa-miR-346, which negatively regulates the IL-18 response, is up-regulated [203]. Moreover, hsa-miR-146a with the potential function to induce the production of pro-inflammatory cytokines (TNF and IL-1β), has been detected as over-expressed in the synovial tissue of RA patients [204]. Circulating hsa-miR-155, hsa-miR-146, and hsa-miR-16 have been observed to be up-regulated in RA and, particularly the last two, in association with active disease [205].

The miRNAs profile in SSc concerns dysregulated expression of miRNAs involved in pro-fibrotic pathways that act on TGFβ expression, metalloproteinases, collagen production, and fibroblast

survival, including hsa-miR-21, hsa-miR-145, hsa-miR-92a, hsa-miR-4458, hsa-miR-155, and hsa-miR-202-3p. Indeed, miRNAs that play a role in SSc pathogenesis mediate the interaction between the immune system, microvasculature, and extracellular matrix. Of interest, circulating miRNAs signature differ in patients characterized by a diffuse cutaneous form compared to those with a limited cutaneous manifestation. Moreover, promising prognostic biomarkers have been identified in SSc patients with ILD [206].

To date, studies analyzing the association between miRNAs and SS as both a biomarker and as players in the pathophysiology of SS are limited. The recent interest in the definition of miRNAs profile in patients affected with SS focused on tears, saliva, salivary glands, and peripheral blood. In particular, hsa-miR-146a and hsa-miR-155 were up-regulated in peripheral blood mononuclear cells (PBMC) of SS patients [205]. Furthermore, hsa-miR-181a was dysregulated in SS compared to healthy controls, sustaining its role in an impaired maturation of B lymphocytes and consequent impossibility of these cells to recognize autoantigens [207]. Finally, lymphocyte-derived hsa-miR-30b-5p inversely correlated with BAFF expression suggesting its role in SS pathogenesis [208].

### *1.2.14 MicroRNAs in idiopathic inflammatory myopathies*

In recent years, an increasingly important role has been given to epigenetic alterations in the context of the etiopathogenesis of PM/DM. However, the study of the role of miRNAs, especially EV-miRNAs, in IIM is still limited.

In muscle tissue from PM patients, hsa-miR-146a was found to be down-regulated as well as in PBMCs from PM/DM patients. The role of this miRNA reflects its function in regulating macrophage infiltration and signaling pathways in both innate and adaptive immunity [209]. Similarly, the down-regulation of serum miR-409-3p and miR-381 in PM patients results in increased infiltration of macrophages into muscle tissue contributing to the pathogenesis of the disease [210,211]. Moreover, miR-146a, miR-221, and miR-222 are over-expressed in muscle tissue biopsy of PM and IBM that appear to inhibit differentiation into myocytes, while miR-1, miR-133a and miR-133b that are implicated in the control of muscle tissue differentiation are down-regulated in IIM, especially IBM, and miR-206 in DM [212].

Evidence concerning the epigenetic alterations in the whole blood of IIM patients reported dysregulated expression of miRNAs involved in the innate immune response and anti-viral response, especially belonging to the IFN pathway. In anti-Jo1-positive IIM patients, DM, and PM, hsa-miR-96-5p was up-regulated. It negatively affects the production of adenosine kinase provoking a

mitochondrial disfunction and inducing oxidative stress which may contribute to muscle damage and weakness in IIM [213]. Furthermore, it has been detected a down-regulation of circulating hsa-let-7 and hsa-miR-21 which were proposed as potential biomarker of PM and DM with a peculiar feature of differential diagnosis: hsa-let-7 seem to characterize patients affected with ILD, while hsa-miR-21 DM patients [214,215].

In addition, circulating hsa-miR-4442 has been reported dysregulated in the plasma of DM/PM patients with lower expression after pharmacological treatment. Its up-regulation was also confirmed in IIM patients compared to other connective tissue diseases and correlate with disease activity [216].

Recently, it has been observed an up-regulated expression of circulating EV-miR-30a-5p and EV-miR-29c-3p in the plasma of ASyS-ILD patients compared to those without lung involvement, confirming higher levels of miR-29c-3p in idiopathic pulmonary fibrosis patients with respect to both ASyS and ASyS-ILD. These miRNAs are involved in numerous processes, including inflammatory response and fibrinogenesis. In detail, miR-29c displays pro-inflammatory activity and antifibrotic action. It is a regulator of B-cell maturation, it is implicated in the positive regulation of NK cells cytotoxicity, and it also modulates the activity of NF-kappa B in T cells. MiR-30a-5p inhibits the proliferation and diffusion of many tumors, seems to play a double-edged role in inflammation, and it could also display an antifibrotic action with ambiguous data suggesting that it can undergo organ-specific and disease-specific variations in its expression, possibly due to the local balance between proinflammatory and antifibrotic triggers [217].

### *1.2.15 EV-microRNAs in clinical application*

The role of miRNAs and particularly EV-miRNAs in clinical applications has not yet been fully elucidated in various pathologies. It is still in an early stage and several challenges remain to overcome. However, growing attention to this research area is defining interesting proposals due to the potential advantages and application of EV-miRNAs.

For instance, EV-miRNAs have been suggested as biomarkers of several cancer types, such as lung and endometrial cancer to assist in diagnosis or prognosis [218–220].

Moreover, abnormal expression levels of EV-miRNAs have been suggested as ideal diagnostic biomarkers in the renal injury of SLE [221]. In particular, EV-miR-21 and EV-miR-155 have been proposed as potential biomarkers for the diagnosis of SLE and lupus nephritis [222]. EV-miRNA profiling of RA has been suggested as useful for the detection of diagnostic and predictive biomarkers and to evaluate RA progression, including the down-regulation of serum EV-miR-548a-3p, EV-miR-548a-3p, and EV-miR-6089 or up-regulation of EV-miR-17, EV-miR-19b, and miR-121 in East

Asian populations [223]. Moreover, a combination of EV-miRNAs from mouthrinse samples including the up-regulation of let-7b-5p, miR-1290, miR-34a-5p, and miR-3648 have been demonstrated to detect SS patients and monitor the disease progression [224].

Recently, in addition to the evidence reported in paragraph **1.2.14** concerning the circulating miRNAs altered expression in PM and DM patients, a research study has suggested that plasma-derived EV-miR-29c-3p and EV-miR-30a-5p could be useful in identifying ASyS patients at risk of developing ILD [217].

# 2 Aims of the study

The main aim of the study is to investigate the potential role of circulating EVs and EV-miRNAs as biomarkers of disease in IIM. Detailed aims are as follows:

1) validating a methodological approach for the isolation of EVs from human blood samples not defined as a "gold standard" through the combination of SEC and UF;

2) characterizing the isolated EVs samples by evaluating the integrity of isolated nanoparticles by TEM, their constitutive surface markers through IFC and measuring their concentration and size by NTA;

3) evaluating the presence of surface markers to speculate EVs cellular origin;

4) analyzing the EVs cargo of microRNAs through NGS to evaluate a possible peculiar epigenetic expression that could suggest altered molecular pathways involved in IIM;

5) comparing EVs features in IIM patients, IIM subgroups, and healthy donors to assess their association with clinical and laboratory parameters in an observational cross-sectional study.

# 3 Patients and methods

## 3.1 IIM patients and healthy donors

Human plasma samples were collected from adult (≥18 years old) patients affected with IIM followed up at the Unit of Rheumatology, University Hospital of Padua and healthy donors (HDs). The eligibility criteria for patients entailed a documented diagnosis of any IIM subtype performed by an experienced rheumatologist on the grounds of clinical, laboratory, and histology data if available. This study was conducted in accordance with the Declaration of Helsinki and approved by the local ethics committees (protocol code 5349/AO/22). All participants gave written and oral informed consent. The anonymity of the samples was ensured by using a randomly generated personal identification code.

## 3.2 Human platelet-free plasma collection

Peripheral blood venous samples (6 mL) were collected from non-fasting subjects in sodium-citrate tubes and platelet-free plasma (PFP) was prepared within 1 hour. Briefly, the blood samples were centrifuged at 1500x g for 20 min and then supernatants were centrifuged twice at 3000x g for 15 min. PFP samples were aliquoted in microtubes and stored at -80°C.

## 3.3 Size-exclusion chromatography (SEC)

PFP samples were defrosted at room temperature (RT) to perform EVs isolation steps. The SEC procedure was performed using qEV original®/70 nm columns (Izon Science), following the manufacturer's instructions. Briefly, the Izon column was removed from +4 °C and the storage solution was allowed to run. The column was equilibrated with Phosphate Buffered Saline (PBS) (pH 7.4; ThermoFisher Scientific) filtered through a 0.22 µm filters unit (Millex – GP; Merck Millipore) (fPBS), and 0.5 mL of PFP sample was added on the top. The eluate was subsequently subdivided into 25 fractions (Fr.). Fr. 1-6 were the void volume, which was disposed of, Fr. 7-10 containing the vesicular fraction were collected for further processing, and Fr. 11-25 containing the protein fraction were eliminated.

## 3.4 Ultrafiltration (UF)

The EVs fractions collected by SEC were enriched through ultrafiltration (UF) using Amicon® Ultra-4 mL, 100 Kda centrifugal filter unit (Merck Millipore). Each filter was sterilized by centrifugation

with 1 mL of ethanol 70% at 2800x g for 1 min. The ethanol residues were removed by centrifugation with 2 mL of fPBS at 2800x g for 2 min. EVs fractions (2 mL + 1 mL of fPBS) were added above previously ethanol-sterilized filter and centrifuged at 4000x g for 10 min according to the manufacturer's instructions to collect the samples held on the filter. The collected samples were adjusted to 0.5 mL volume by adding fPBS, aliquoted in microtubes and frozen at -80°C.

### 3.5 Nanodrop spectrophotometer

Protein concentration of both PFP and SEC-eluted EVs samples was quantified by NanoDrop 2000C® Spectrophotometer (Thermo Fisher Scientific).

### 3.6 Transmission electron microscopy (TEM)

One drop of EVs samples (about 25 µL) was placed onto a 400 mesh holey film grid. After staining with 2% uranyl acetate (for 2 minutes) the sample was observed with a Tecnai G2 (FEI) transmission electron microscope operating at 100 kV. Images were captured by a Veleta (Olympus Soft Imaging System) digital camera.

### 3.7 Imaging flow cytometry (IFC)

Fluorescent signals acquisition of EVs samples were performed using Amnis ImageStream$^X$ MkII (ISx; EMD Millipore, Seattle, WA, USA) instrument. EVs samples were diluted in fPBS (1:100) and then incubated for 30 minutes in the dark at RT with the following fluorophore-conjugated antibodies previously centrifuged at 20000x g for 10 minutes at 10 °C to prevent the formation of antibody-antibody aggregates: calcein-acetoxymethyl ester (calcein-AM) 10 µM (Abcam) collected in channel 2 (505-560 nm filter); or anti-human CD63 (Brilliant Violet 421; BioLegend, clone H5C6; RRID: AB_2687004) in channel 1 (435-505 nm filter), anti-human CD81 (FITC; BioLegend, clone 5A6; RRID: AB_10642825) in channel 2 (505-560 nm filter), anti-human CD9 (Alexa Fluor 647; Exbio, clone MEM-61; RRID: AB_10733480) in channel 5 (642-745 nm filter), and anti-human CD11c (PE; BioLegend, clone 3.9; RRID: AB_314176) in channel 3 (560-595 nm filter). Channel 4 (595-642 nm filter) was set to brightfield (BF) and channel 6 (745-780 nm filter) to side-scatter (SSC). Further acquisitions of EVs labelled with the following fluorophore-conjugated antibodies were perform: anti-human CD3 (Brilliant Violet 711; BioLegend; RRDI: AB_2562907) in channel 5, anti-human CD19 (Brilliant Violet 421; BioLegend; RRID: AB_2564227) in channel 1. Channel 3 was set to BF and channel 6 to SSC. The acquisition settings were applied for a fixed time of 2 min with low-speed fluidics, all used laser (405 nm, 488 nm, 642 nm, 785 nm) at maximum power to ensure maximal

sensitivity, magnification at 60X, core size 7 µm, the numerical aperture of 0.9, a DOF of 2.5 µm, and the "Remove Beads" option unchecked to include Speed Beads (1000 nm) in the analyses. Technical controls included: labelled EVs with 0.1% Triton X-100 (Merck), unlabelled EVs, single antibody-labelled EVs, and mixed samples of single antibody-labelled EVs, fPBS with the addition of fluorophore-conjugated antibodies, and fPBS only. An improved masking setting (NMC, not in the MC mask) was used to optimize the SSC resolution and efficacy of the detection of dim fluorescent single EVs compared to the "masks combined" (MC) standard setting. EVs gating strategy was performed by applying the "Intensity_MC Or NMC" of SSC (channel 6) versus the "Normalized Frequency" in a histogram to identify the Low SSC area limited to the area under the Speed Beads. The following dot-plot graphs provide "Intensity of SSC channel" in the Y axis and "Intensity_MC Or NMC" for each used channel in the X axis to detect the fluorescent-positive particles. Upon each start-up, the instrument calibration tool ASSIST® was performed to optimize performance and consistency. Samples were acquired using INSPIRE® software. Data analyses and spectral compensation matrices were performed using IDEAS® software (version 6.3). The advanced ISx fluidic control coupled with the continuously running Speed Beads enable particles enumeration using the "objects per mL" feature within the IDEAS® software.

### 3.8 Nanoparticle tracking analysis (NTA)

EVs quantification and size were measured in samples diluted in filtered PBS through a 0.1 µm filters unit (Millex – GP; Merck Millipore) to the concentration range of $10^6$ – $10^8$ particles/mL using the NanoSight NS300 (Malvern Panalytical) instrument as specified by the manufacturer for optimal assessment of particle concentration and size distribution. The ideal detection threshold was determined to include particles with the restriction concentrations of 20 – 120 particles per frame while indistinct particles were limited to 5 per frame. According to the manufacturer's manual, the camera level was increased to visibly distinguish all particles not exceeding a particle signal saturation over 20% and autofocus was adjusted to avoid indistinct particles. For each sample, particles moving under Brownian motion were recorded on three 1-min videos captured with a 20X magnification. EVs concentration and size were calculated by NTA software (version 3.4). To minimize data skewing based on single large particles, the ratio between total valid tracks and total complete tracks was always ≤ 1:5.

## 3.9 Statistical analysis

Data are expressed as mean and standard deviation (SD) for continuous variables; categorical data are expressed as numbers and percentages. Shapiro-Wilk test was performed to test normality. Student's t test was used to compare the differences between parametric variables and one-way ANOVA with Bonferroni's correction was used when more than two groups were considered. Pearson's correlation was used to evaluate strength and direction of the correlation. A two-tailed p-value (p) $\leq 0.05$ was considered statistically significant. Data were analyzed using SPSS software version 20.0 (SPSS, Chicago IL, USA) and GraphPad Prism® version 9.

## 3.10 Next-generation sequencing (NGS)

### *3.10.1 RNA extraction and quantification*

Total RNA from isolated EVs samples was extracted using the miRNeasy Serum/Plasma Advanced kit (Qiagen, Germany), according to the manufacturer's protocol that combines sample guanidine-based lysis, an inhibitor removal step, and silica-membrane–based purification of total RNA. Briefly, buffer RPL containing guanidine thiocyanate as well as detergents to facilitate the lysis and denaturation of protein complexes and RNases was added to 350 µL of the EVs sample. After thoroughly mixing, buffer RPP was added to precipitate inhibitors, mostly proteins, by centrifugation. The supernatant containing the RNA was transferred into a new tube and isopropanol was added to provide appropriate binding conditions for all RNA molecules from approximately 18 nucleotides (nt) upwards. The sample was then transferred into the RNeasy UCP MinElute spin column, where the total RNA binds to the membrane and all contaminants are efficiently washed away. RNA was eluted in 20 µL of RNase-free water and then stored at -80 ˚C.

The concentration of extracted miRNAs (ng/µL) was quantified by fluorometric spectroscopy through the Qubit® 3.0 Fluorimeter (Thermo Fisher Scientific, Massachusetts, USA) instrument using Qubit microRNA assay kit (Thermo Fisher Scientific) according to the manufacturer's manual.

### *3.10.2 sncRNA NGS libraries preparation and quantification*

Universal complementary DNA (cDNA) synthesis and sequencing libraries of sncRNAs were generated using QIAseq miRNA Library kit (Qiagen, Germany) according to the manufacturer's manual. Briefly, specially designed adapters are ligated to the 3' and 5' ends of sncRNAs to prevent undesired side products. Universal cDNA synthesis with Unique Molecular Index (UMI) assignment

and cDNA clean-up using a magnetic bead-based method was performed. Finally, libraries amplification and clean-up were applied (**Figure 7**).

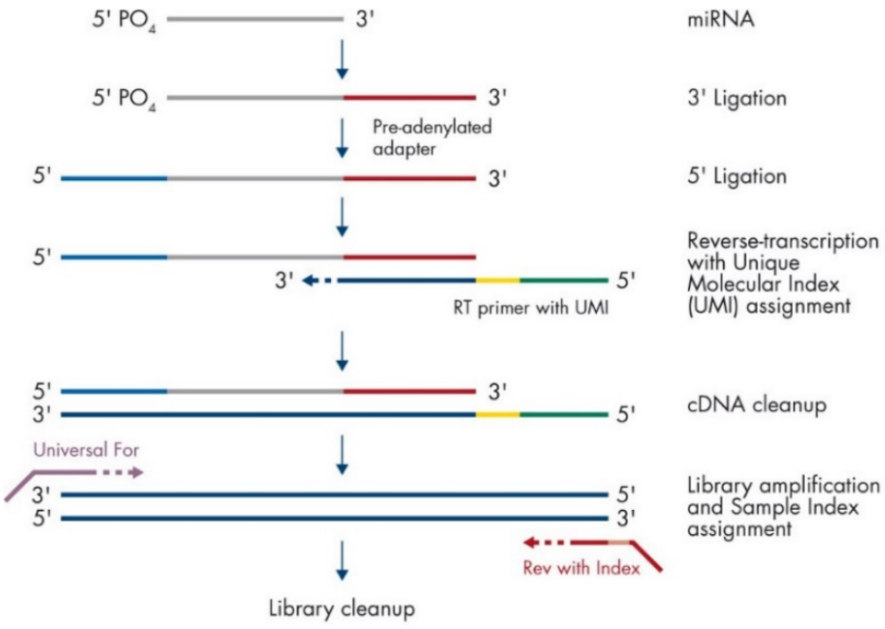


***Figure 7.*** *Workflow of sncRNA libraries preparation using the QIAseq miRNA Library Kit (Qiagen).*

In detail, the adapters ligation step provides that a pre-adenylated DNA adapter was ligated to the 3' end of sncRNAs incubating for 1 hour at 28°C, 20 min at 65°C, and finally at 4 °C the sample and the reaction mix containing the Ligation Activator buffer with enzymes. Then, the RNA adapter and specific reagents were added to the product of the first reaction and incubated for 30 min at 28°C, 20 min at 65°C, and finally at 4 °C to allow the ligation to the 5' end of all sncRNAs. For the reverse transcription (RT) reaction to occur, RT primer containing a UMI and universal sequence binds to a region of the 3' adapter to perform the conversion in cDNA. During this step, each UMI is assigned to every sncRNA molecule to ensure accurate quantification of sncRNAs through NGS adding molecular tags to each molecule to eliminate the bias due to the number of reads that could result in an overestimation of expression. Moreover, a universal sequence is added to be recognized by the sample indexing primers during library amplification.

In the first RT reaction, the mix containing RT Initiator was added to the sample and incubated for 2 min at 75 °C, 2 min at 70 °C, 2 min at 65 °C, 2 min at 60 °C, 2 min at 55 °C, 5 min at 37 °C, 5 min at 25 °C, and then at 4 °C. The second step provides a reaction by incubating the sample with RT primer and enzyme for 1 hour at 50 °C, 15 min at 70 °C, and 5 min at 4 °C. After the RT step, a cDNA clean-up was performed using a magnetic bead-based method, in order to enrich the samples

in cDNA fragments with the adapters and remove the exceeded reagents. The library amplification occurs through the use of a universal reverse primer and a specific primer forward primer containing a barcode index dried into a microplate to assign each sample a unique custom index. During the sequencing step, the barcode is recognized to collect the sequences derived from the same sample. The library amplification needs the primers and HotStartTaq DNA polymerase which was activated by a heating step incubation for 15 min at 95 °C. Consequently, 22 cycles of denaturation, annealing, and extension steps (15 sec at 95 °C, 30 sec at 60 °C, 15 sec at 72 °C) were provided, and then incubation for 2 min at 72 °C and 5 min at 4 °C. Finally, a sncRNA library magnetic bead-based method clean-up was performed to enrich the library with specific size RNA and to remove contaminants, adapter dimers, and inhibitors. Libraries were stored at -20°C.

The concentration of sncRNAs libraries (ng/μL) was quantified by fluorometric spectroscopy through Qubit® 3.0 Fluorimeter (Thermo Fisher Scientific) instrument using the Qubit 1X dsDNA HS kit (Thermo Fisher Scientific) according to the manufacturer's protocol.

### *3.10.3 sncRNA libraries quality control (QC) by High Sensitivity DNA electrophoresis*

sncRNA libraries were subjected to quality control through LabChip GX Nucleic Acid Analyzer (PerkinElmer, Massachusetts, USA) using HT DNA 5K/RNA LabChip kit (D-MARK Biosciences, Canada, USA), following the manufacturer's manual to verify that the constructed libraries contained miRNAs sequences (**Figure 8**). Briefly, a chip composed of an interconnected set of microchannels was filled with buffer, sieving gel, and a marker. A microchannel is connected to a capillary that sips the sample libraries labelled with fluorescent dye from the wells of the microplate during the assay. The chip functions as an integrated electrical circuit driven by the 7 electrodes that contact solutions in the chip's wells. Fragments into the samples separate by size driven by means of electrophoresis, then they pass the laser which excites the fluorescent dye bound to the molecule. The LabChip GX software provides an Optical Calibration function using Test Chip C to calculate a correction factor which will be applied to all samples run on the instrument to provide a common absolute fluorescence across different instruments. The measurement of fragments' concentration and size is achieved by comparing against a sizing ladder and running internal standards or "markers" of known concentration mixed with each sample. The software plots fluorescence intensity versus time and produces electropherograms for each sample. A typical electropherogram referred to sncRNA library reports a peak of 170-180 bp corresponding to the miRNA-sized library. A peak approximately of 188 bp corresponds to a piRNA-sized library and a peak approximately of 157 bp represents adapter–dimer.

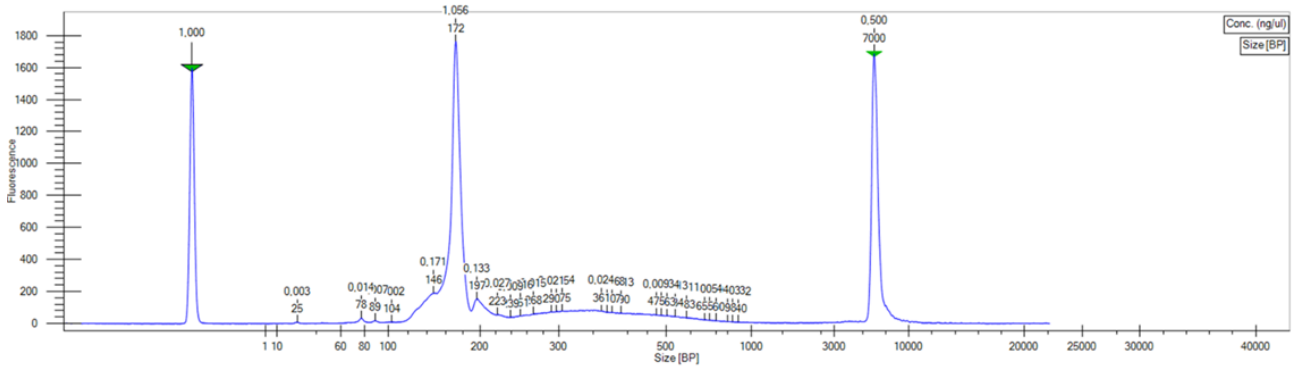


***Figure 8.*** *sncRNA libraries were analyzed before sequencing to verify the quality of the sequences obtained and their enrichment in small non-coding RNAs. The figure shows a representative electropherogram of the sncRNA library characterized by an evident and a net peak in the range of 170-180 bp corresponding to the miRNA-sized library.*

### *3.10.4 Next Generation Sequencing (NGS) on sncRNA libraries*

The molarity of each library was calculated using the following equation: (X ng/µL)($10^6$)/(112450) = Y nM according to the manufacturer's manual. Libraries to sequence in multiplexing were generated in equimolar amounts diluting each sample in RNAase-free water to reach the final pool concentration of 1.2 pM as recommended by the "Standard Normalization Method" protocol for the sequencing run in the NextSeq550 instrument (Illumina). The correct libraries concentration optimizes cluster density to avoid the phenomenon of "over-clustering" or "under-clustering" which would not discriminate the brightness of the reads.

Then, libraries pool concentration was quantified through Qubit® 3.0 Fluorimeter (Thermo Fisher Scientific) instrument as previously described.

SncRNA libraries were sequenced using the NextSeq550 Illumina Platform following the manufacturer's instructions. This platform is a system of sequencing by synthesis technology that uses two-colours chemistry to sequence in parallel millions of clusters obtained from bridge amplification. Two bases are labelled with single dyes, a third with both dyes, and the fourth with no dye. Only two pictures are taken and, in each one, each cluster either appears in a single channel red or green (T or C), in both channels (A), or in no channel at all (G).

Briefly, a pool of NGS library fragments was denatured following the Illumina manufacturers' protocol and diluted as previously described. Fragments were flowed across a flow cell (NextSeq™ High Output Flow Cell v2.5, Illumina) and hybridized on complementary adapter oligos. Fragments were amplified via bridge amplification PCR, denaturated, and linearized by cleavage within an adaptor sequence, resulting in clusters of single-stranded templates for sequencing. During each

sequencing cycle, a labelled deoxynucleoside triphosphate (dNTP) is added to the nucleic acid chain and it acts as a terminator for polymerization. The fluorescent dye is useful to identify the base and then enzymatically cleaved to allow incorporation of the following nucleotide. Sequencing fragments are immobilized on the flow cell surface designed to facilitate access to enzymes ensuring high stability of surface-bound template and low non-specific binding of fluorescently labelled nucleotides. Base pairs are identified after laser excitation and fluorescence detection. Finally, the analysis was performed using the tool CLC Genomics Workbench from NGS platforms that provide quality control, alignment, quantification, statistics, and visualization tasks.

The bioinformatic analysis provides the upload of the data of fragments sequences from each sample as FastQ files. To make use of the UMIs it was used the protocol of sequencing in single reads of 75 bp for the sncRNA library. Adapter sequences should be trimmed from reads through the cut-adapt tool because they interfere with downstream analyses. Sequences with less than 15 bp or without adapters or without UMI are discarded and are not used for the analysis. Using the UMI counts for each miRNA, the software performs differential expression analysis evaluating the Fold Change value and presents the results. The platform produces output from the images: extracts intensities, performs base calling, and assigns a quality score (Q-score) to the base call that acts as internal quality control. It is generated a template that defines the position of each cluster in a tile using X and Y coordinates. Intensities extracted and compared to another image result in four distinct populations, each corresponding to a nucleotide. The Q-score indicates a prediction of the probability of an incorrect base call to communicate small error probabilities. It is defined as a property that is logarithmically related to the base calling error probabilities (P): $Q(X) = -10 \log10 P$, where X is the score. A higher Q-score implies that a base call is higher quality and more likely to be correct. Low Q scores can lead to increased false-positive variant calls, resulting in inaccurate conclusions. To avoid systematic variation, the analysis requires normalization. The data were subjected to filter by setting a cut-off to consider the sncRNAs with a minimum number of reads count. Finally, it is performed the differential expression analysis of small RNA sequences data.

# 4 Results

## 4.1 Patient cohort and healthy donors

A total of 65 adult (≥18 years old) patients affected with IIM (male:female ratio 1:2) and 65 sex- and age- matched HDs (male:female ratio 1:2) were included in the present study. IIM patients were distributed across different disease subsets and their main clinical and demographic features are reported in **Table 4**. The clinical characteristics of the patients' cohort are described in **Table 5**.

| Diagnosis | Number (%) | Mean age ± SD | Males | Females |
|---|---|---|---|---|
| **IIM patients** | 65 (100) | 60.97 ± 12.70 | 22 | 43 |
| **DM** | 19 (29.23) | 59 ± 14.24 | 3 | 16 |
| **PM** | 8 (12.31) | 62 ± 7.02 | 1 | 7 |
| **IBM** | 2 (3.07) | 62 ± 9.19 | 2 | 0 |
| **AsyS** | 17 (26.15) | 56 ± 14.50 | 7 | 10 |
| **CAM** | 16 (24.61) | 67 ± 7.92 | 9 | 7 |
| **Unspecified** | 3 (4.61) | 76.50 ± 4.95 | 1 | 2 |
| **HDs** | 65 (100) | 49.94 ± 18.56 | 22 | 43 |

***Table 4.*** *Cohort composition reported demographic features of IIM patients and HDs and the distribution of disease subtypes. 3 subjects were diagnosed with an idiopathic inflammatory myopathy whose exact subtype could not be ascertained due to the lack of histologic data at the time of sampling. DM: dermatomyositis; PM: polymyositis; IBM: inclusion body myositis; ASyS: anti-synthetase syndrome; CAM: cancer-associated myositis; HD: healthy donors.*

| | |
|---|---|
| **Disease duration at sampling time, mean ± SD (years)** | 3.01 ± 2.39 |
| **MMT-8 score median (IQR)** | 144 (134 – 150) |
| **Serology ever (n, %)** | |
| Myositis-specific autoantibodies (MSAs) | |
| Anti-Mi2 | 7 (10.77 %) |
| Anti-t-RNA synthetase * | 17 (26.15 %) |
| Anti-SRP | 3 (4.61 %) |
| Anti-MDA-5 | 5 (7.68 %) |
| Anti-TIF1-γ | 5 (7.68 %) |

| | |
|---|---|
| Anti-HMGCoAR | 1 (1.54 %) |
| <u>Myositis-associated autoantibodies (MAAs)</u> | |
| Anti-SSA | 13 (20 %) |
| Anti-SSB | 3 (4.61 %) |
| Anti-Ku | 3 (4.61 %) |
| Anti-PM/Scl-100 | 5 (7.69 %) |
| Other ** | 9 (13.85 %) |
| Unknown | 3 (4.61 %) |
| **Clinical manifestations ever (n, %)** | |
| Cutaneous | 40 (61.54 %) |
| Grotton's sign and papules | 21 (32.31 %) |
| Heliotropic rash | 15 (23.08 %) |
| Mechanic's hand | 18 (27.68 %) |
| Raynaud's phenomenon | 17 (26.14 %) |
| Other *** | 33 (50.77 %) |
| Arthritis | 21 (32.31 %) |
| Myositis | 49 (75.38 %) |
| ILD | 38 (58.45 %) |
| Dyspnea | 26 (40 %) |
| Cough | 17 (21.54 %) |
| Dysphagia | 18 (27.68 %) |
| **Clinical manifestations upon sampling (n, %)** | |
| Cutaneous | 24 (39.91 %) |
| Grotton's sign and papules | 11 (16.91 %) |
| Heliotropic rash | 6 (9.22 %) |
| Mechanic's hand | 9 (13.84 %) |
| Other **** | 17 (26.14 %) |
| Articular activity | 6 (9.22 %) |
| Muscular activity | 22 (33.84 %) |
| Pulmonary activity | 8 (12.31 %) |

| | |
|---|---|
| **No clinical activity** | 29 (44.61 %) |
| **Ongoing treatment** | |
| Oral glucocorticoids (n, %) | 46 (70.77 %) |
| Dose of prednisone, mean ± SD, (mg/die) | 14.55 ± 10.03 |
| Immunosuppressant drugs | 42 (64.61 %) |
| Mycophenolate mofetil | 15 (23.08 %) |
| Methotrexate | 19 (29.23 %) |
| Azathioprine | 1 (1.54 %) |
| Cyclosporine A/ Tacrolimus | 2 (3.08 %) |
| Rituximab | 4 (6.14 %) |
| Abatacept | 1 (1.54 %) |
| **Untreated** | 7 (10.77 %) |

***Table 5.*** *Clinical characteristics of the patients' cohort. MMT: manual-muscle test; IQR: interquartile range; ILD, interstitial lung disease.*
*Anti-t-RNA synthetase *: 12 cases of anti-Jo1 positivity (18.45 %), 4 cases of anti-PL12 positivity (6.14 %), 1 case of anti-PL7 positivity (1.54 %).*
*Other **: 1 case of anti-PM1 positivity (1.54 %), 2 cases of anti-U1RNP (3.08 %), 4 cases of anti-PM/Scl75 positivity (6.14 %) and 1 case of anti-SMA positivity (1.54 %).*
*Other ***: 11 cases with nailfold changes (16.91 %), 5 cases with holster sign (7.69 %), 1 case with poikilodermatomyositis (1.54%), 5 cases with mid-facial erythema (7.69 %), 5 cases with V-neck sign (7.69 %), 2 cases with livedo reticularis (3.08 %), 15 cases with shawl rash (23.08 %).*
*Other ****:11 cases with shawl rash (16.91 %), 4 cases with holster sign (6.14 %), 4 cases with nailfold changes (6.14 %), 8 cases with mid-facial erythema (12.31 %), 5 cases with V-neck sign (7.69 %), 1 case with livedo reticularis (1.54 %).*

## 4.2 Significantly reduced protein concentration in isolated EVs compared to PFP samples

The protein concentration measured in both IIM patients and HDs was significantly reduced in EVs samples collected after SEC step (mean 0.066 ± 0.054 SD [mg/mL] vs. 0.073 ± 0.069 SD [mg/mL], respectively) compared to the corresponding PFP samples (52.71 ± 4.537 SD [mg/mL] vs. 52.30 ± 4.419 SD [mg/mL], respectively) ($p<0.0001$) (**Figure 9**).

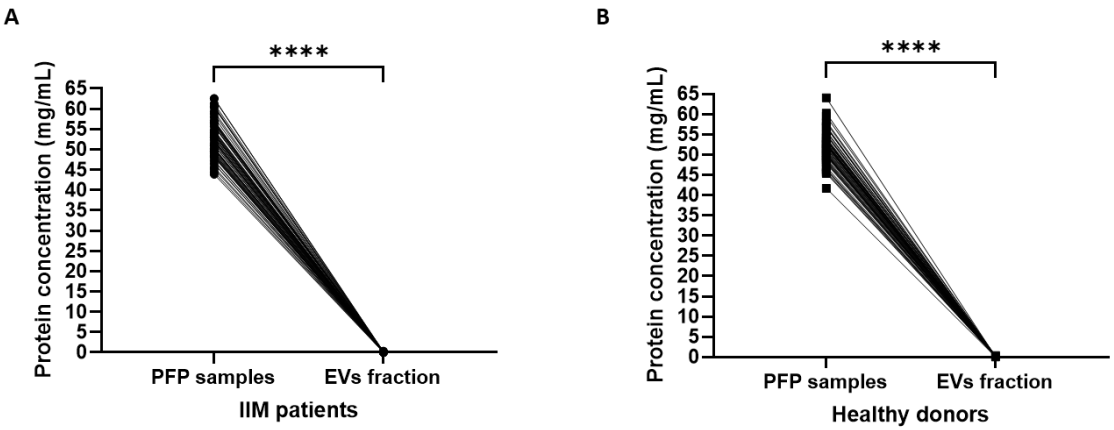


***Figure 9**. Graphs representing the protein concentration before SEC isolation (PFP samples) and after SEC isolation (EVs fraction) **A)** in IIM patients (n=65) and **B)** in HDs (n=65); **** p<0.001.*

## 4.3 Typical EVs morphology by TEM observations

TEM images of isolated EVs samples (n=9) showed a population of intact and roundish nanoparticles which appear heterogeneous in size with a diameter range of 30 – 200 nm and a prevalence of small EVs (**Figure 10A** and **Figure 10B**). Fresh and frozen/thawed (4 or 8 months) EVs samples did not display morphological differences (**Figure 10C**).

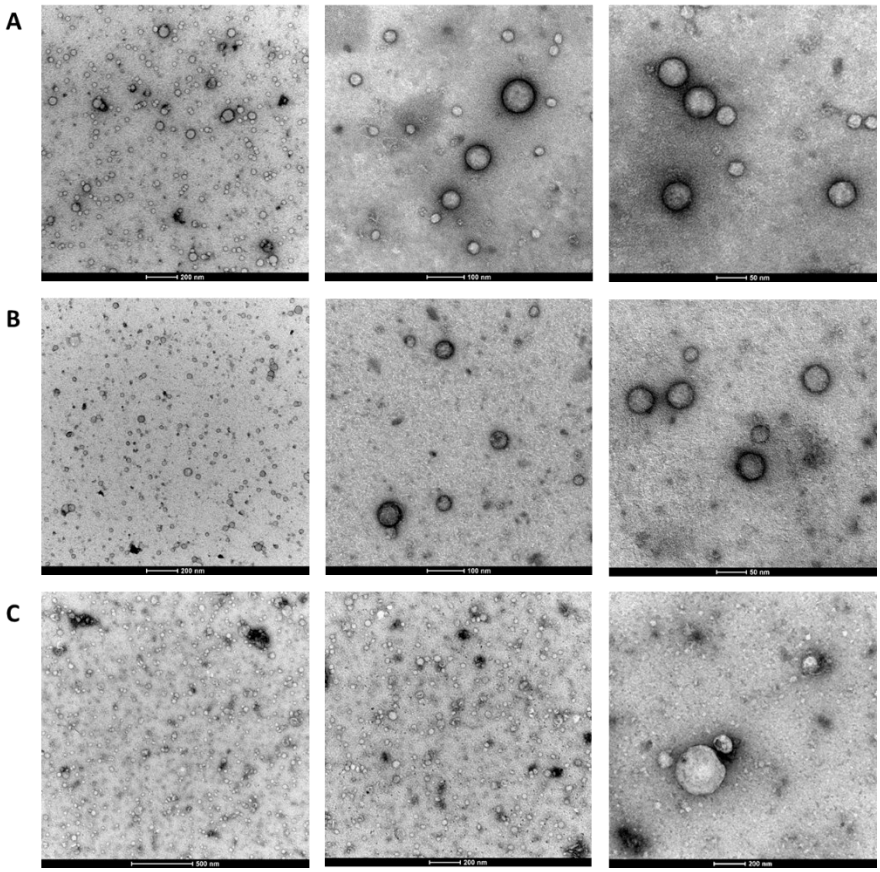


***Figure 10.*** *Representative images of EVs observed by TEM of* ***A)*** *IIM patient (n=1) and* ***B)*** *HD (n=1) fresh samples (dilution 1:10) and* ***C)*** *IIM patient (n=1) after freeze (8 months) and thawed sample cycle (undiluted) captured at high magnification (scale bar: 50 nm; 100 nm; 200 nm; and 500 nm).*

## 4.4 IFC characterization determines the presence of EVs markers on isolated nanoparticles

EVs characterization through calcein-AM marker for the purpose of verifying the EVs integrity reported comparable values of EVs concentration in both IIM patients (n=20) ($5x10^5 \pm 1.03x10^6$ [EVs/mL]) and HDs (n=20) ($3.10x10^5 \pm 3.81x10^5$) (p=0.4465) (**Figure 11**).

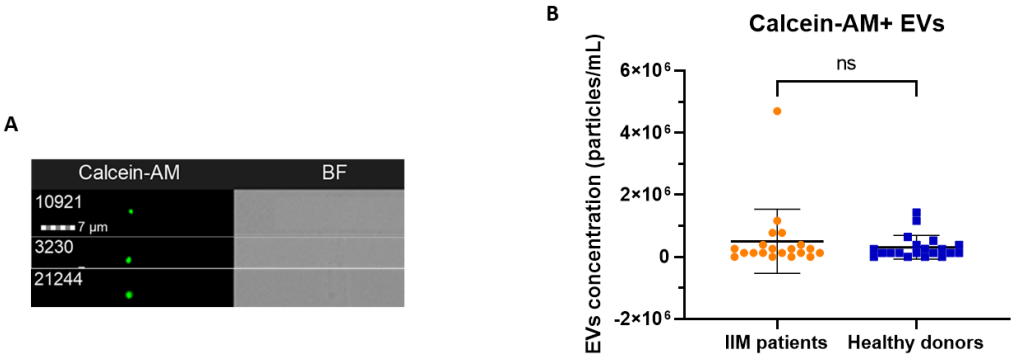


***Figure 11.*** ***A)*** *shows representative particles captured through the ImageStreamX MkII instrument with a positive signal for calcein-AM.* ***B)*** *the graph reports the calcein-AM+ EVs concentration ± SD in IIM patients (n=20) and HDs (n=20) isolated EVs samples.*

The EVs immuno-characterization by means of the constitutive surface tetraspanins CD63, CD81, CD9 and integrin CD11c reported higher levels of CD63+ EVs both in IIM patients (n=30) and HDs (n=30) compared with CD81+, CD9+, and CD11c+ EVs (p<0.0001) (**Table 6**) (**Figure 12**).

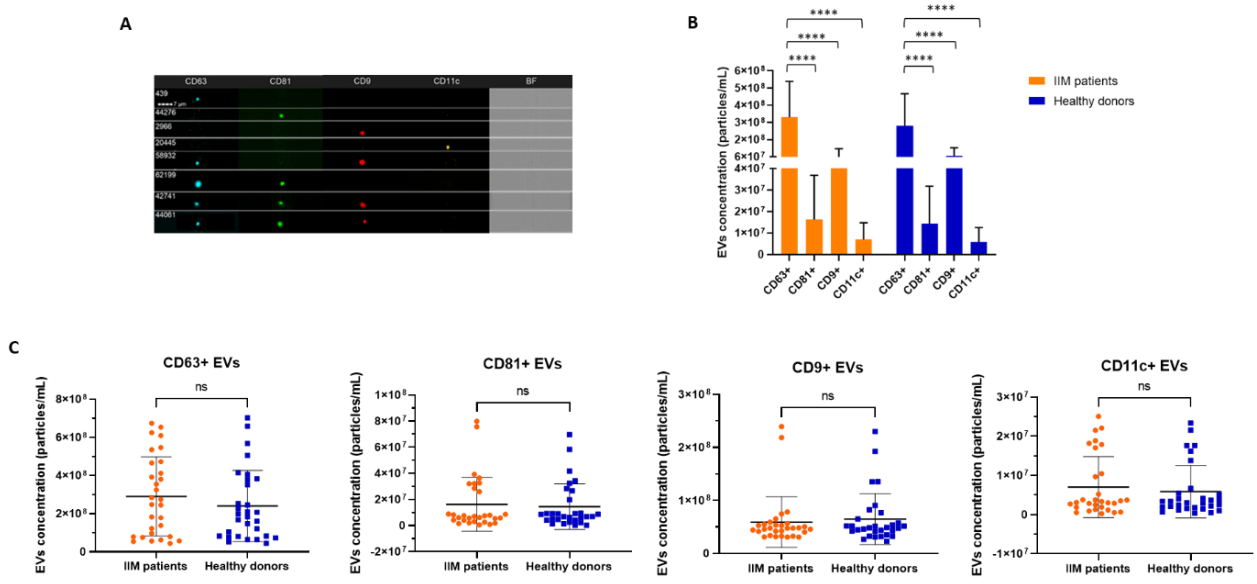


***Figure 12. A)*** *shows representative captured particles with a positive signal to the tetraspanins CD63, CD81, CD9 and the integrin CD11c.* ***B)*** *represents the EVs concentration (mean [EVs/mL] ± SD) of EVs positive to single marker in IIM (n=30) and HDs (n=30).* ***C)*** *the graphs report the EVs concentration ± SD of single-positive particles to the EVs surface markers in IIM vs. HDs. BF: Brightfield; **** p<0.001.*

The mean EVs concentrations for the multiple-markers positivity reported higher values of CD63/CD11c+ compared to the other multiple-markers positive EVs in both IIM and HDs. Significant differences emerged in the comparison between CD63/CD11c+ vs. CD81/CD9+ EVs (p=0.0007 in IIM and p=0.0298 in HDs), CD63/CD11c+ vs. CD81/CD11c+ (p=0.0003 in IIM and p=0.0265 in HDs), and CD63/CD11c+ vs. CD63/CD81/CD9+ EVs (p=0.0003 in IIM and p=0.0220 in HDs) (**Table 6**) (**Figure 13**).

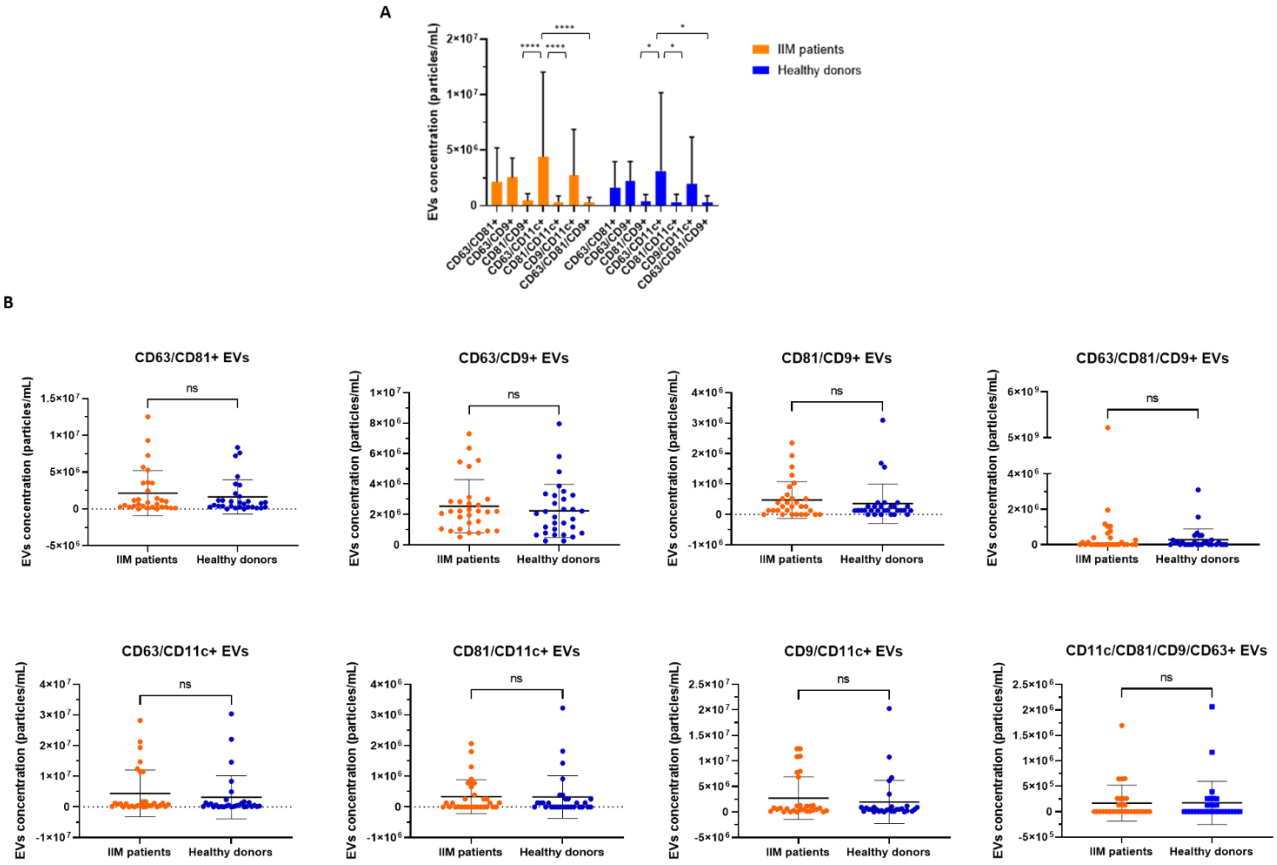


***Figure 13***. *Graphs reporting **A)** the EVs concentration (mean [EVs/mL] ± SD) of multiple-positive particles to the EVs surface markers in IIM (n=30) and HDs (n=30) and **B)** the EVs concentration ± SD of multiple-positive EVs in IIM vs. HDs; **** p<0.001; * p<0.05.*

| | **IIM vs. HDs [EVs/mL] ± SD** |
|---|---|
| **CD63+** | $2.91x10^8 \pm 2.07x10^8$ vs. $2.40x10^8 \pm 1.85x10^8$ (p=0.3272) |
| **CD81+** | $1.62x10^7 \pm 2.06x10^7$ vs. $1.44x10^7 \pm 1.73x10^7$ (p=0.7093) |
| **CD9+** | $5.89x10^7 \pm 4.78x10^7$ vs. $6.46x10^7 \pm 4.83x10^7$ (p=0.6472) |
| **CD11c+** | $7x10^6 \pm 7.78x10^6$ vs. $5.85x10^6 \pm 6.68x10^6$ (p=0.5413) |
| **CD63/CD81+** | $2.14x10^6 \pm 3.06x10^6$ vs. $1.63x10^6 \pm 2.32x10^6$ (p=0.4675) |
| **CD63/CD9+** | $2.53x10^6 \pm 1.75x10^6$ vs. $2.23x10^6 \pm 1.74x10^6$ (p=0.5071) |

| | |
|---|---|
| **CD81/CD9+** | $4.71x10^5 \pm 6.06x10^5$ vs. $3.54x10^5 \pm 6.47x10^5$ (p=0.4711) |
| **CD63/CD11c+** | $4.40x10^6 \pm 7.62x10^6$ vs. $3.12x10^6 \pm 7.04x10^6$ (p=0.5032) |
| **CD81/CD11c+** | $3.33x10^5 \pm 5.50x10^5$ vs. $3.24x10^5 \pm 6.96x10^5$ (p=0.9555) |
| **CD9/CD11c+** | $2.71x10^6 \pm 4.16x10^6$ vs. $1.96x10^6 \pm 4.21x10^6$ (p=0.4934) |
| **CD63/CD81/CD9+** | $2.77x10^5 \pm 4.83x10^5$ vs. $2.76x10^5 \pm 6.22x10^5$ (p=0.9940) |
| **CD63/CD81/CD9/CD11c+** | $1.68x10^5 \pm 3.52x10^5$ vs. $1.72x10^5 \pm 4.24x10^5$ (p=0.9696) |

***Table 6**. Mean concentration ([EVs/mL] ± SD) of tetraspanins and integrin positive EVs in IIM patients (n=30) vs. HDs (n=30).*

Altogether, by comparing the concentration of differently combined tetraspanins-positive and integrin-positive EVs in the two groups, significant differences are found in IIM patients between CD63+ vs. CD81+; CD63+ vs. CD9+, CD63+ vs. CD11c+, CD63+ vs. CD63+CD81+, CD63+ vs. CD63+CD9+, CD63+ vs. CD81+CD9+, CD63+ vs. CD63+CD11c+, CD63+ vs. CD81+CD11c+, CD63+ vs. CD9+CD11c+, CD63+ vs. CD63+CD81+CD9+ EVs ($p<0.0001$), CD9+ vs. CD63+CD81+ ($p=0.0425$), CD9+ vs. CD63+CD9+ ($p=0.0460$), CD9+ vs. CD81+CD9+ ($p=0.0297$), CD9+ vs. CD81+CD11c+ ($p=0.0288$), CD9+ vs. CD9+CD11c+ ($p=0.0478$) and CD9+ vs. CD63+CD81+CD9+ ($p=0.0317$).

Within the HDs group significant differences are reported in the following comparisons: CD63+ vs. CD81+, CD63+ vs. CD9+, CD63+ vs. CD11c+, CD63+ vs. CD63+CD81+, CD63+ vs. CD63+CD9+, CD63+ vs. CD81+CD9+, CD63+ vs. CD63+CD11c+, CD63+ vs. CD81+CD11c+, CD63+ vs. CD9+CD11c+, CD63+ vs. CD63+CD81+CD9+ EVs ($p<0.0001$), CD9+ vs. CD11c+ ($p=0.0062$), CD9+ vs. CD63+CD81+ ($p=0.0020$), CD9+ vs. CD63+CD9+ ($p=0.0024$), CD9+ vs. CD81+CD9+ ($p=0.0014$), CD9+ vs. CD63+CD11c+ ($p=0.0030$), CD9+ vs. CD81+CD11c+ ($p=0.0014$), CD9+ vs. CD9+CD11c+ ($p=0.0022$) and CD9+ vs. CD63+CD81+CD9+ ($p=0.0014$) (**Figure 14**).

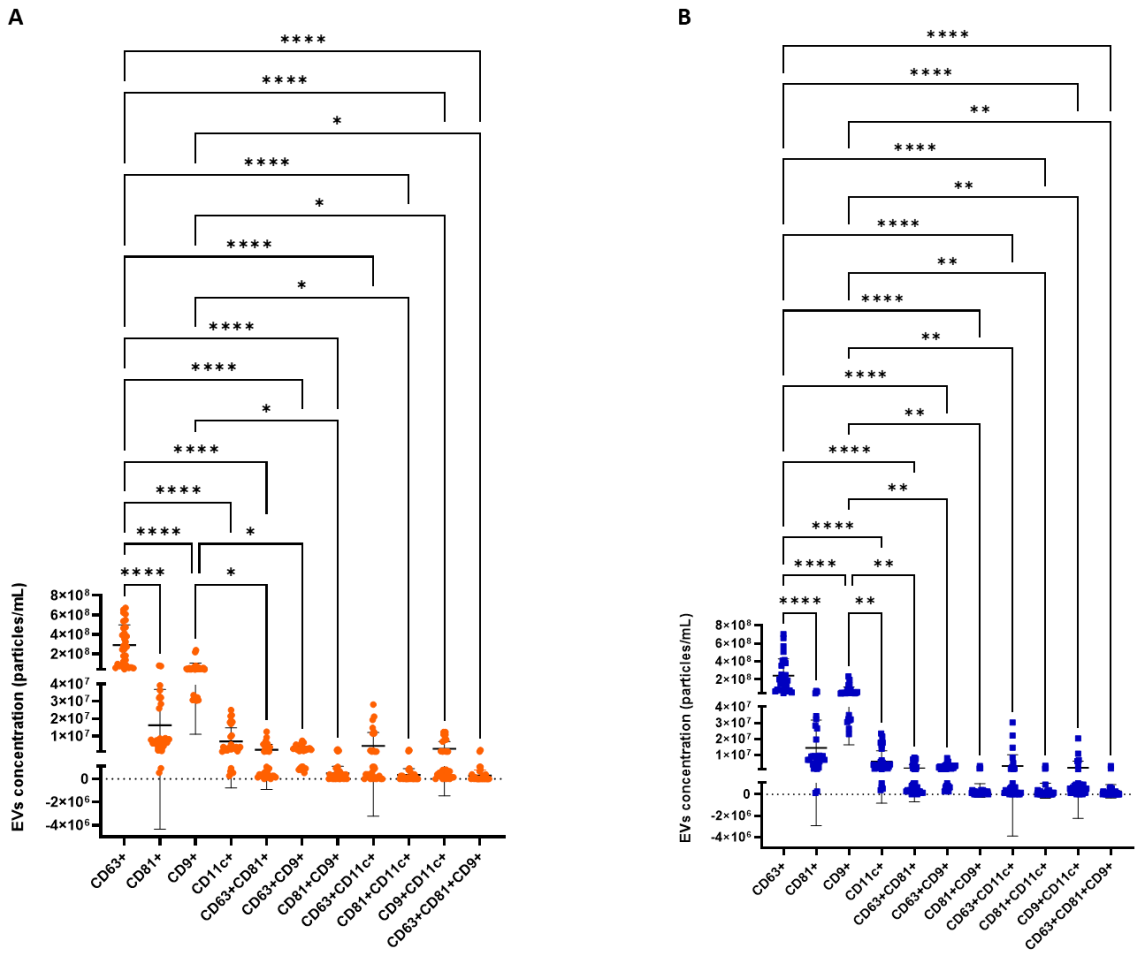


***Figure 14***. *Graphs representing the EVs concentration ± SD positive to tetraspanins and integrin markers **A)** in IIM (n=30) and **B)** in HDs (n=30); **** p<0.001; **p<0.01; * p<0.05.*

## 4.5 IFC detects immune cells markers on the EVs surface

By investigating the presence of T and B lymphocytes markers on the surface of EVs isolated from IIM patients (n=26) and HDs (n=25), IFC analysis demonstrated a prevalence of CD3-CD19+ EVs compared to CD3+ EVs, in both groups (p<0.0001) (**Table 7**) (**Figure 15**).

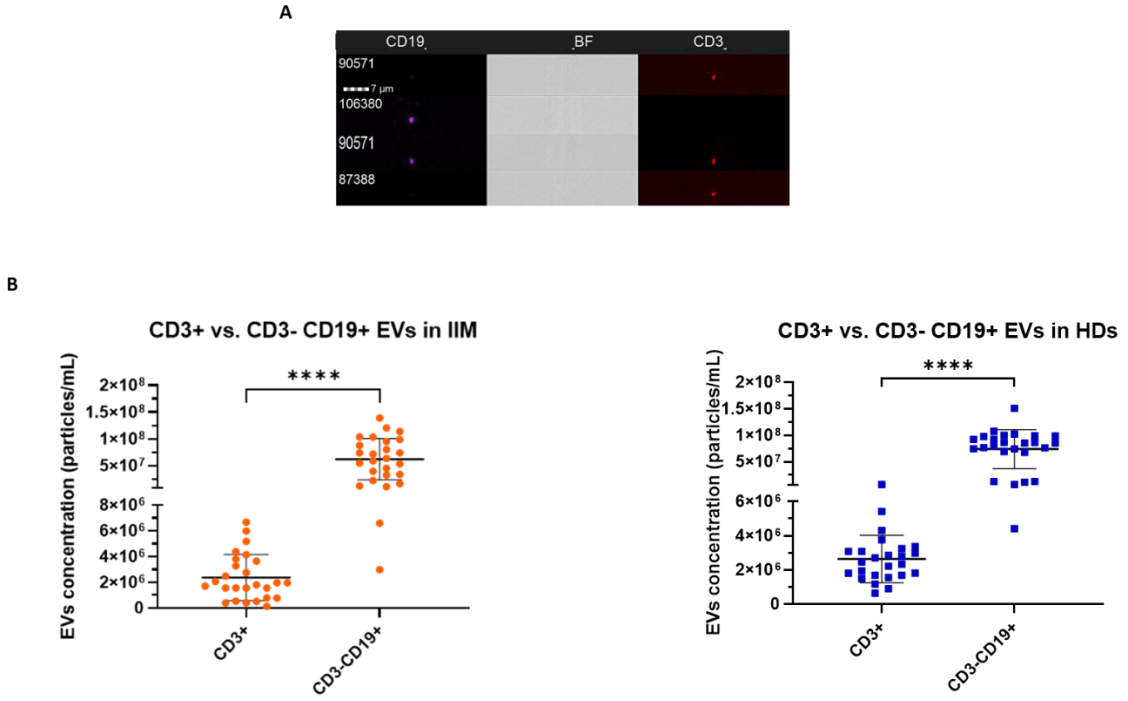


***Figure 15. A)*** *shows representative captured particles with a positive signal to CD3 and/or CD19 markers.* ***B)*** *the graphs report the EVs concentration ± SD of CD3+ EVs and CD3-CD19+ EVs in IIM patients (n=26) on the left and HDs (n=25) on the right. BF: Brightfield; **** p<0.001.*

| | **IIM vs. HDs [EVs/mL] ± SD** |
|---|---|
| **CD3+** | $2.35x10^6 \pm 1.78x10^6$ vs. $2.64x10^6 \pm 1.38x10^6$ (p=0.5262) |
| **CD3-CD19+** | $6.20x10^7 \pm 3.85x10^7$ vs. $7.38x10^7 \pm 3.67x10^7$ (p=0.2704) |

***Table** 7. Mean concentration [EVs/mL] ± SD of lymphocytes markers positive EVs in IIM patients (n=26) vs. HDs (n=25).*

## 4.6 Abnormal EVs levels in IIM patients by NTA measurements

NTA measurements of nanoparticles concentration and size reported a significantly higher mean EVs concentration in IIM patients than in HDs ($1.71x10^{10} \pm 1.29x10^{10}$ vs. $1.31x10^{10} \pm 7.17x10^9$ SD [EVs/mL], p=0.0306) with EVs mean size of 199 ± 20.02 vs. 204.1 ± 17.78 SD nm (p=ns) and mode size of 151.9 ± 19.81 vs. 154.8 ± 16.89 SD nm (p=ns), respectively (**Figure 16**).

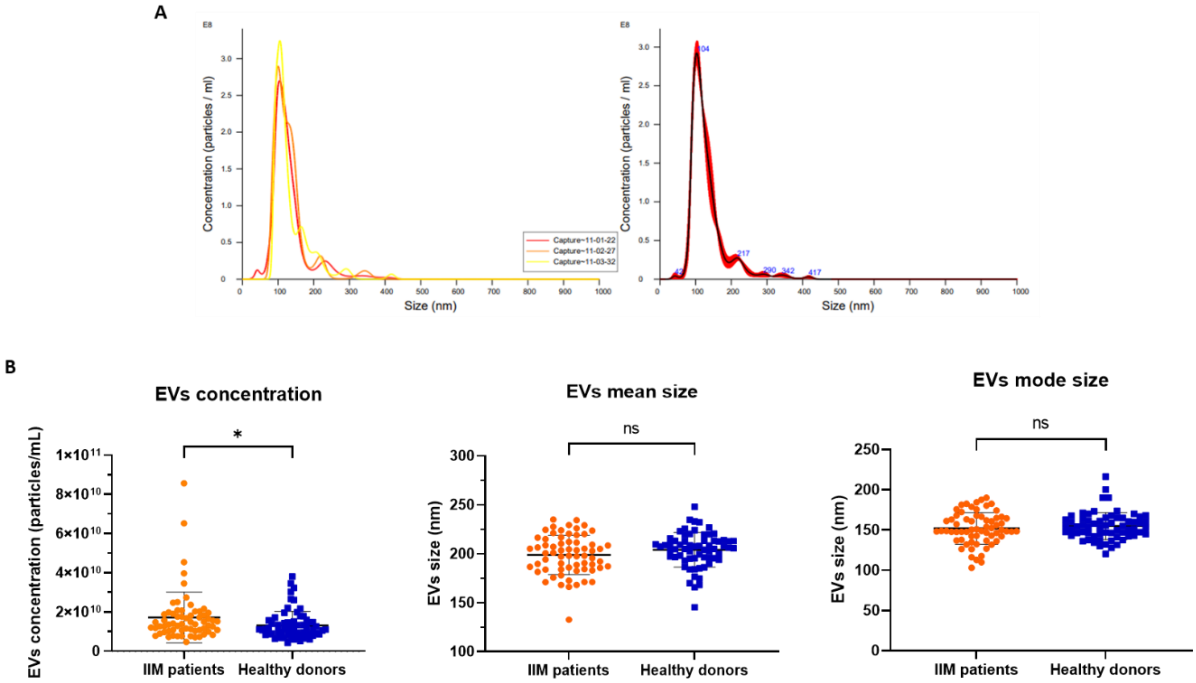


***Figure 16**. A) a representative graph (n=1) of NTA measurement through NanoSight NS300 (Malvern Panalytical) obtained by NTA Software version 3.4 reporting the values of particles concentration in relation to their size. On the left, the three curves show the data captured in three 1-min videos for the same sample. On the right, the merged data. **B**) graphs representing the EVs mean concentration ± SD, EVs mean size, and EVs mode size ± SD in IIM patients (n=65) and HDs (n=65); * $p<0.05$.*

After splitting IIM patients into subsets of disease, patients affected with CAM (n=16) stood out for the highest levels of circulating EVs ($2.35x10^{10}$ ± $2.20x10^{10}$) showing a significant difference compared to HDs (p=0.0026) and to no CAM patients ($1.51x10^{10}$ ± $7.51x10^{9}$, p=0.0206). Besides, a concurrent diagnosis of ILD (n=39) in IIM patients was associated with a significantly increased concentration of circulating EVs ($1.86x10^{10}$ ± $1.38x10^{10}$) compared to HDs (p=0.0320) and no ILD group (n=25), despite not reaching statistical significance in this case ($1.52x10^{10}$ ± $1.16x10^{10}$, p=0.6225) (**Figure 17**).

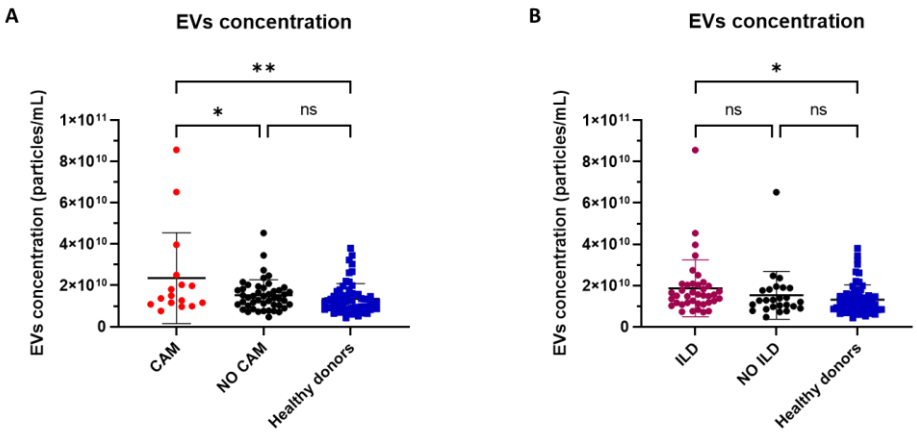


***Figure 17.*** *Graphs reporting the EVs concentration ([EVs/mL] ± SD)* ***A)*** *referred to CAM (n=16), no CAM (n=46) and HDs; and* ***B)*** *in ILD (n=39), no ILD (n=25) and HDs; **p<0.01; * p<0.05.*

A significantly increased EVs concentration was displayed in seropositive IIM patients (n=41) ($1.78x10^{10}$ ± $1.51x10^{10}$) compared to HDs (p=0.0328) and numerically increased EVs levels compared to seronegative patients (n=22) ($1.62x10^{10}$ ± $8.37x10^{9}$). Moreover, patients in clinical remission (n=26) displayed significantly higher levels of circulating EVs compared to those with active disease (n=35) ($2.13x10^{10}$ ± $1.60x10^{10}$ vs. $1.46x10^{10}$ ± $1.02x10^{10}$, p=0.0452) and HDs (p=0.0029) (**Figure 18**).

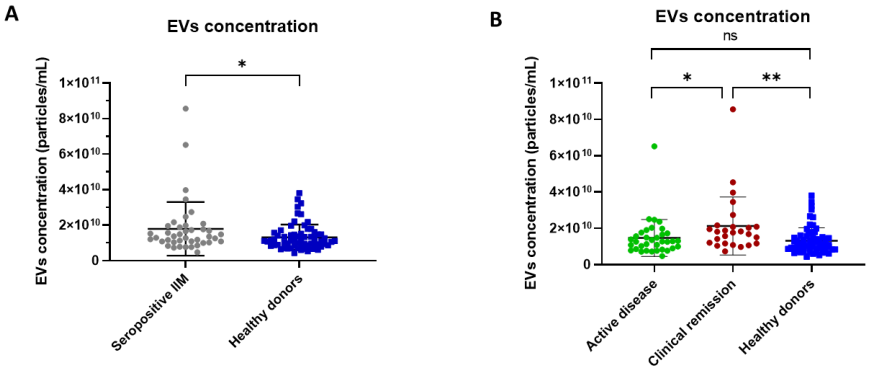


***Figure 18****. Graphs showing the EVs concentration ([EVs/mL] ± SD)* ***A)*** *in seropositive IIM patients (n=41) and* ***B)*** *in patients with active disease (n=34) vs. clinical remission (n=25) vs. HDs; * p<0.05; **p<0.01.*

Lastly, we verified a potential correlation between EVs levels and pharmacological treatment. IIM patients receiving pharmacological treatment (n=57) maintained a significant higher EVs concentration ($1.76x10^{10}$ ± $1.37x10^{10}$) compared to HDs (p=0.0231). Specifically, by splitting up the treated IIM group into patients treated with GC (n=21) and GC with IS (n=36), the former group displayed greater EVs concentration ($2.23x10^{10}$ ± $1.99x10^{10}$) compared to GC + IS treated patients

($1.49x10^{10} \pm 7.25x10^{9}$, p=0.0482). Finally, EVs levels were significantly reduced in IIM patients treated with RTX (n=12) than in patients receiving other treatments (n=45) ($9.63x10^{9} \pm 3.26x10^{9}$ vs. $1.96x10^{10} \pm 1.46x10^{10}$, p=0.0228) (**Figure 19**).

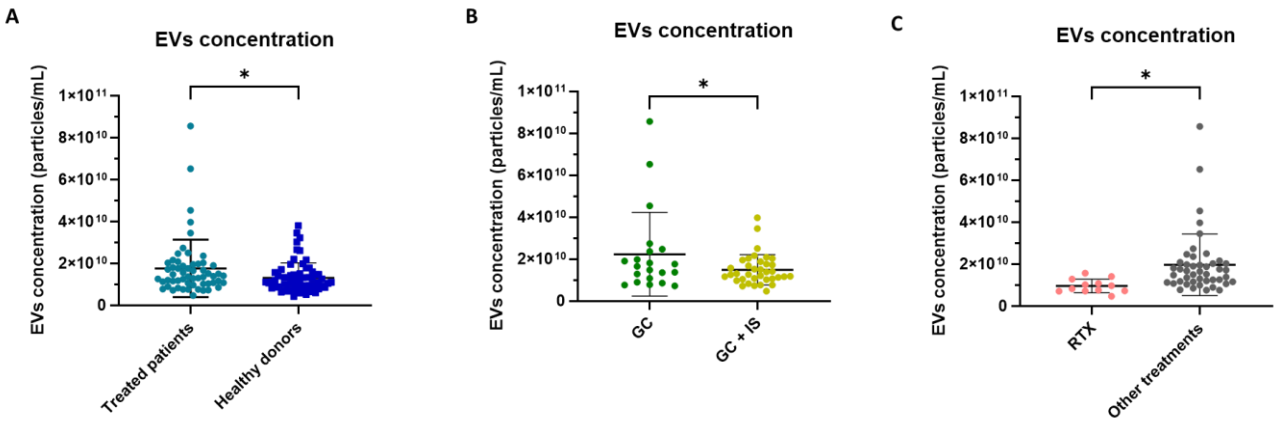


***Figure 19**. Graphs representing the EVs concentration ([EVs/mL] ± SD) **A)** in pharmacological treated IIM patients (n=57) vs. HDs, **B)** in patients treated with GC (n=21) vs. GC +IS (n=36), and **C)** in patients treated with RTX (n=12) vs. other treatments (n=45). GC: glucocorticoids; IS: immunosuppressants; RTX: rituximab; * p<0.05.*

## 4.7 EV-microRNAs differential expression in IIM patients detected by NGS

The data obtained by NGS analysis highlighted the miRNAs expression profile that characterized the EVs cargo of IIM patients (n=21) and HDs (n=21). The total number of circulating EV-miRNAs detected and analysed reached 100. **Figure 20** displays the expression level (total reads) of the 20 most representative EV-miRNAs both in IIM patients and HDs. Hsa-miR-16-5p miRNA was the most expressed (1480 ± 1287 in IIM vs. 886 ± 1078 in HDs) followed by hsa-miR-126-3p (780 ± 644 vs. 652 ± 1105, respectively).

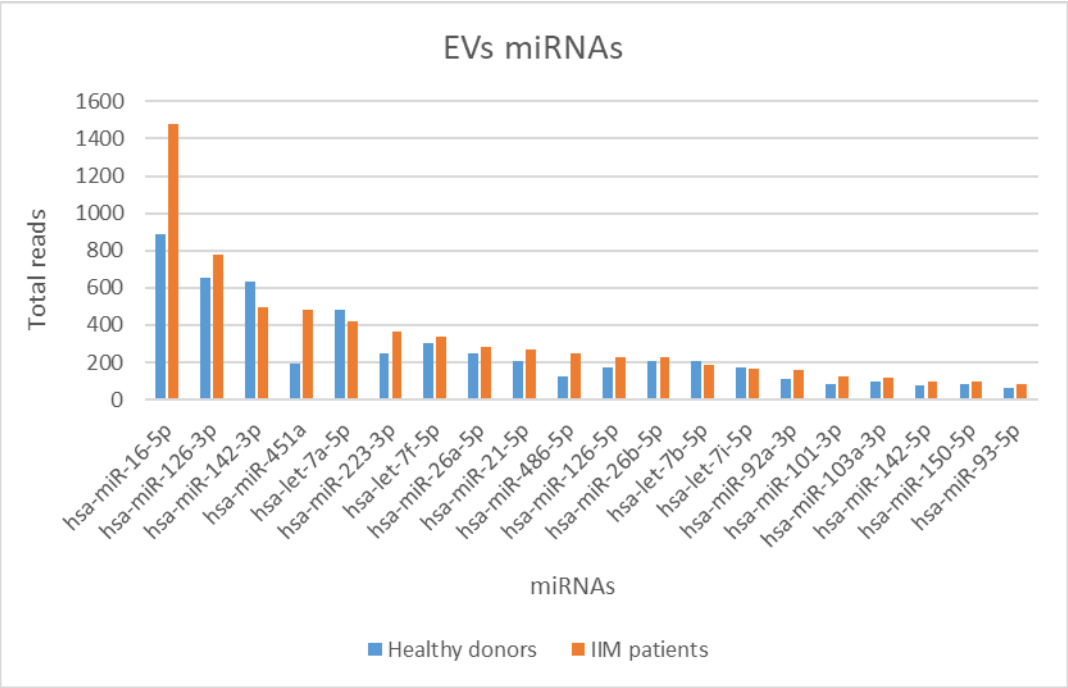


***Figure 20***. *Expression profile of the 20 most representative circulating EV-miRNAs from IIM patients (n=21, in orange) and HDs (n=21, in blue).*

The EV-miRNAs expression comparison among IIM patients and HDs was performed by the CLC Genomics software which provides the "Fold Change" value and the "p-value". The "Fold Change" is calculated as the ratio between the average value of the normalized reads among the two groups for each miRNA. Fold Change values > 1 indicate an increased miRNA expression (up-regulation) whereas values < -1 indicate a decreased expression (down-regulation). A Fold Change value included between 1 and -1 indicates no difference change in miRNA expression. The "p-value" has been calculated through the "Trimmed Mean of M" (edge R) normalization method by CLC Genomics software. **Table 8** shows the Fold Change and p-values relative to EV-miRNAs that reported significant differences in the comparison between IIM and HDs.

| EV-miRNAs | Fold Change | p-value | IIM vs. HDs |
|---|---|---|---|
| **hsa-miR-451a** | 1.919321 | 0.0000759 | Up-regulated |
| **hsa-miR-15a-5p** | 1.275568 | 0.022154 | Up-regulated |
| **hsa-miR-486-5p** | 1.446866 | 0.00114 | Up-regulated |
| **hsa-miR-222-3p** | 1.845142 | 0.001526 | Up-regulated |
| **hsa-miR-32-5p** | 1.778544 | 0.018901 | Up-regulated |
| **hsa-miR-185-5p** | 1.454742 | 0.00529 | Up-regulated |
| **hsa-let-7e-5p** | -1.56348 | 0.00157 | Down-regulated |
| **hsa-let-7a-5p** | -1.55167 | 0.001512 | Down-regulated |
| **hsa-let-7f-5p** | -1.29617 | 0.018207 | Down-regulated |
| **hsa-let-7b-5p** | -1.50724 | 0.000313 | Down-regulated |

***Table 8**. List of EV-miRNAs with significantly different expressions in IIM (n=21) vs. HDs (n=21) comparison with respective indicated Fold Change and p values.*

To perform a comparative analysis of the miRNAs differential expression (DE) among the groups, the total reads value has been normalized into counts per million (CPM) by dividing the value of total counts of the reads of a miRNA by the total counts of the reads of the sample and then multiplying by $10^6$. By analyzing the miRNAs DE between IIM patients and HDs it was reported an up-regulated expression in the first group referring to: **hsa-miR-451a** (46146 ± 25901 vs. 23893 ± 12213 [CPM], respectively, p=0.0010), **hsa-miR-486-5p** (27153 ± 9402 vs. 18936 ± 5357, p=0.0012), **hsa-miR-222-3p** (961.3 ± 828.3 vs. 427.5 ± 358.3, p=0.0098), **hsa-miR-185-5p** (2084 ± 882.9 vs. 1438 ± 87, p=0.0217), **hsa-miR-32-5p** (926.6 ± 641.6 vs. 443.2 ± 326.5, p=0.0038), **hsa-miR-15a-5p** (2432 ± 1122 vs. 1598 ± 808.9, p=0.0086). The following miRNAs were found to be downregulated in IIM patients: **hsa-let-7b-5p** (24784 ± 11158 vs. 37575 ± 15988, p=0.0046), **hsa-let-7a-5p** (49910 ± 17929 vs. 77529 ± 36163, p=0.0032), **hsa-let-7e-5p** (1167 ± 529 vs. 1873 ± 1143, p=0.014), **hsa-let-7f-5p** (35943 ± 14566 vs. 47198 ± 13218, p=0.0123) (**Figure 21**).

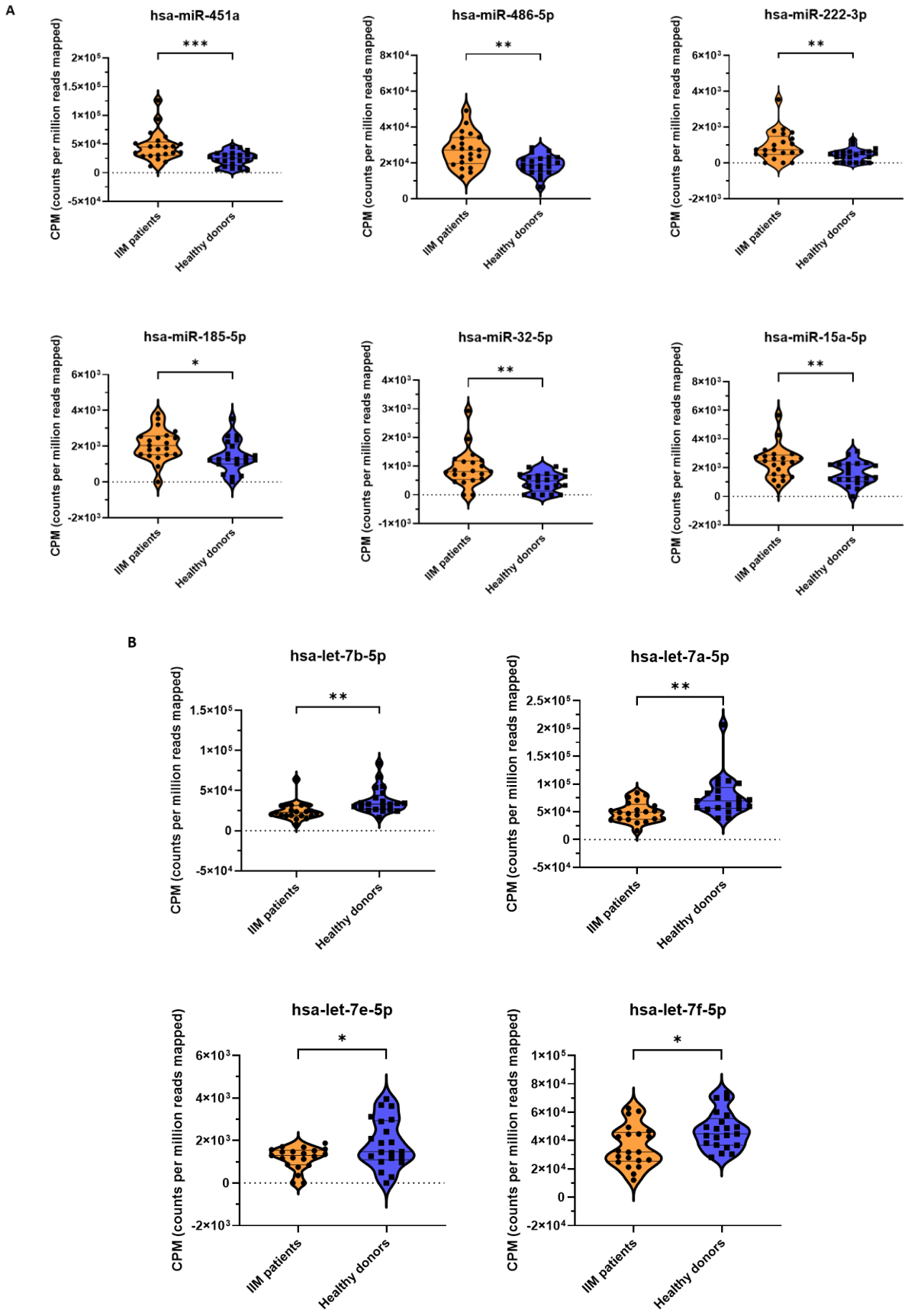


***Figure 21***. *Graphs representing the miRNAs differential expression when **A**) up-regulated (hsa-miR-451a, hsa-miR-486-5p, hsa-miR-222-3p, hsa-miR-185-5p, hsa-miR-32-3p, hsa-miR-15a-5p) and **B**) down-regulated (hsa-let-7b-5p, hsa-let-7a-5p, hsa-let-7f-5p, hsa-let-7e-5p) in IIM patients (n=21) vs. HDs (n=21); *** p<0.001; **p<0.01; * p<0.05.*

After splitting the IIM patients group into DM (n=6), PM + ASyS (n=7) and CAM (n=6) to compare the expression of the 10 miRNAs previously resulted significantly different in IIM vs. HDs it was observed an up-regulated expression for **hsa-miR-451a** in CAM (54631 ± 36145 [CPM], p=0.0120) and PM + ASyS (52325 ± 26170, p=0.0142) compared to HDs (23893 ± 12213); for **hsa-miR-486-5p** in CAM than HDs (30215 ± 8415 vs. 18936 ± 5357, p=0.0061); for **hsa-miR-222-3p** in DM than HDs (1258 ± 1285 vs. 427.5 ± 358.3, p = 0.0408) and for **hsa-miR-32-5p** in PM + ASyS than HDs (1284 ± 884.4 vs. 443.2 ± 326.5, p=0.0019) (**Figure 22**).

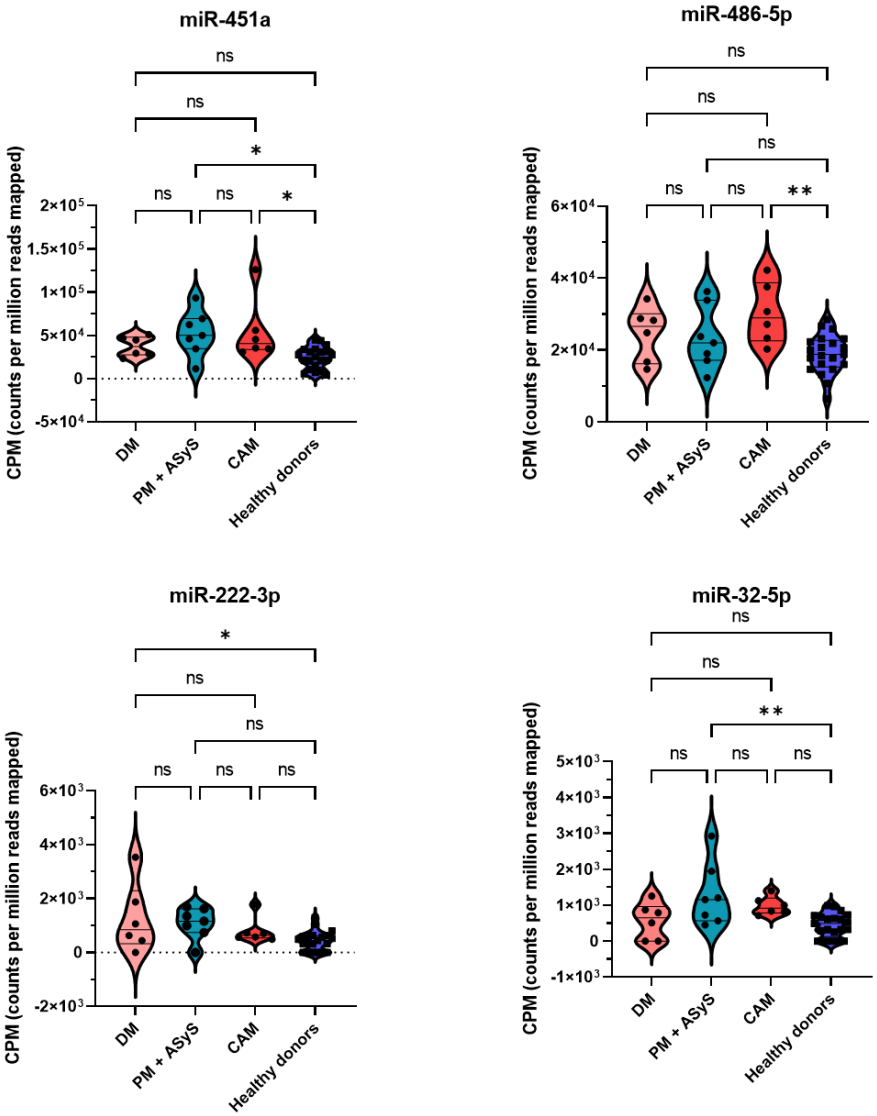


***Figure 22***. *Graphs representing the miRNAs differential expression (hsa-miR-451a, hsa-miR-486-5p, hsa-miR-222-3p, hsa-miR-32-3p) in DM (n=6), PM + ASyS (n=7), CAM (n=6), and HDs (n=21); **p<0.01; * p<0.05.*

Moreover, by comparing these subgroups it was revealed a significant difference in **hsa-miR-186-5p** that appear up-regulated in PM + ASyS compared to HDs (2325 ± 607.9 vs. 1337 ± 580.3, p=0.0119) (**Figure 23**).

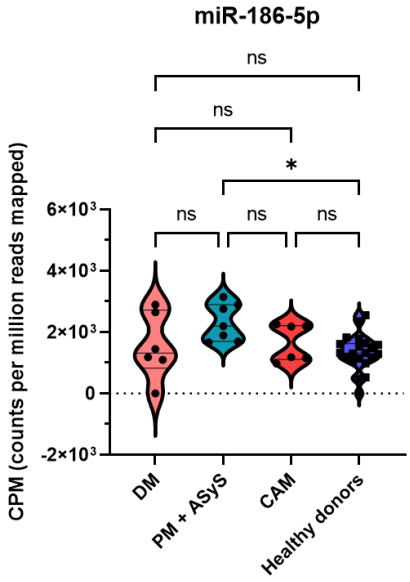


***Figure 23**. Graph reporting the differential expression of hsa-miR-186-5p in DM (n=6), PM + ASyS (n=7), CAM (n=6), and HDs (n=21); * p<0.05.*

Furthermore, it was shown a significantly lower expression of **hsa-miR-23b-3p** in CAM compared to DM patients (1681 ± 638.4 vs. 737.2 ± 260, p=0.0073) and greater expression of **hsa-miR-223-3p** in the former subgroup (28.584 ± 8.758 vs. 44.775 ±14.627, p=0.0423) (**Figure 24**).

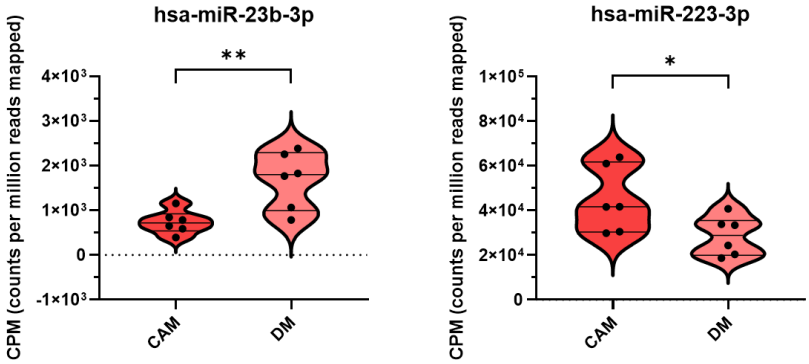


***Figure 24**. Graph showing the differential expression of hsa-miR-23-3p and hsa-miR-223-3p in DM (n=6) vs. CAM (n=6); **p<0.01; * p<0.05.*

By comparing ASyS (n=5) and CAM subgroups **hsa-miR-23b-3p** miRNA was detected higher in the first group (1311 ± 467.3 vs. 737.2 ± 260, p=0.0295) and **hsa-miR-374a-5p** in the latter group (1472 ± 845.7 vs. 2621 ±406.8, p=0.0159) (**Figure 25**).

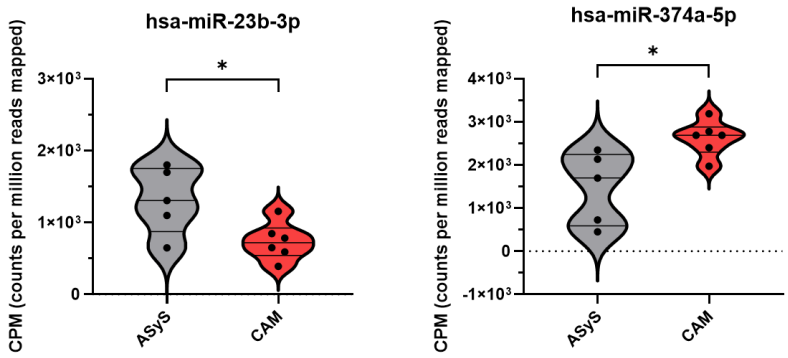


***Figure 25**. Graphs representing the miRNAs differential expression of hsa-miR-23b-3p and hsa-miR-374a-5p in ASyS (n=5) vs. CAM (n=6); * p<0.05.*

In the statistical analysis between PM + ASyS and DM patients **hsa-miR-29c-3p** appeared down-regulated in the first subgroup (2798 ± 877 vs. 4097 ± 1133, p= 0.0471) (**Figure 26**).

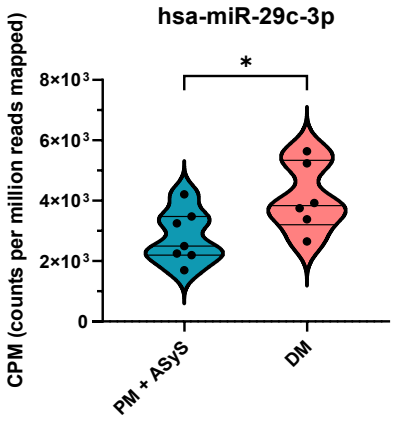


***Figure 26.** Graph showing the down-regulated expression of hsa-miR-29c-3p miRNA in PM + ASyS patients (n=7) vs. DM (n=6); * p<0.05.*

Then, by comparing separately the IIM subgroups with HDs it emerged significantly higher miRNAs expression in PM + ASyS than HDs referred to: **hsa-miR-451a** (52325 ± 26170 vs. 23893 ± 12213, p=0.0279), **hsa-miR-185-5p** (2257 ± 899.4 vs. 1438 ± 870, p=0.0420), **hsa-miR-186-5p** (2325 ± 607.9 vs. 1337 ± 580.3, p=0.0007), **hsa-miR-144-3p** (8931 ± 4236 vs. 5664 ± 3294, p=0.0439), **hsa-miR-15a-5p** (2726 ± 1575 vs. 1598 ± 808.9, p=0.0194) and **hsa-miR-22-3p** (1082 ± 583.6 vs. 427.5

± 358.3, p=0.0014). Down-regulated miRNAs were found in the first group both for **hsa-let-7f-5p** (33748 ± 15398 vs. 47198 ± 13218, p=0.0338) and **hsa-let-7e-5p** (1122 ± 562.2 vs. 1873 ± 1143, p=0.0320) (**Figure 27**).

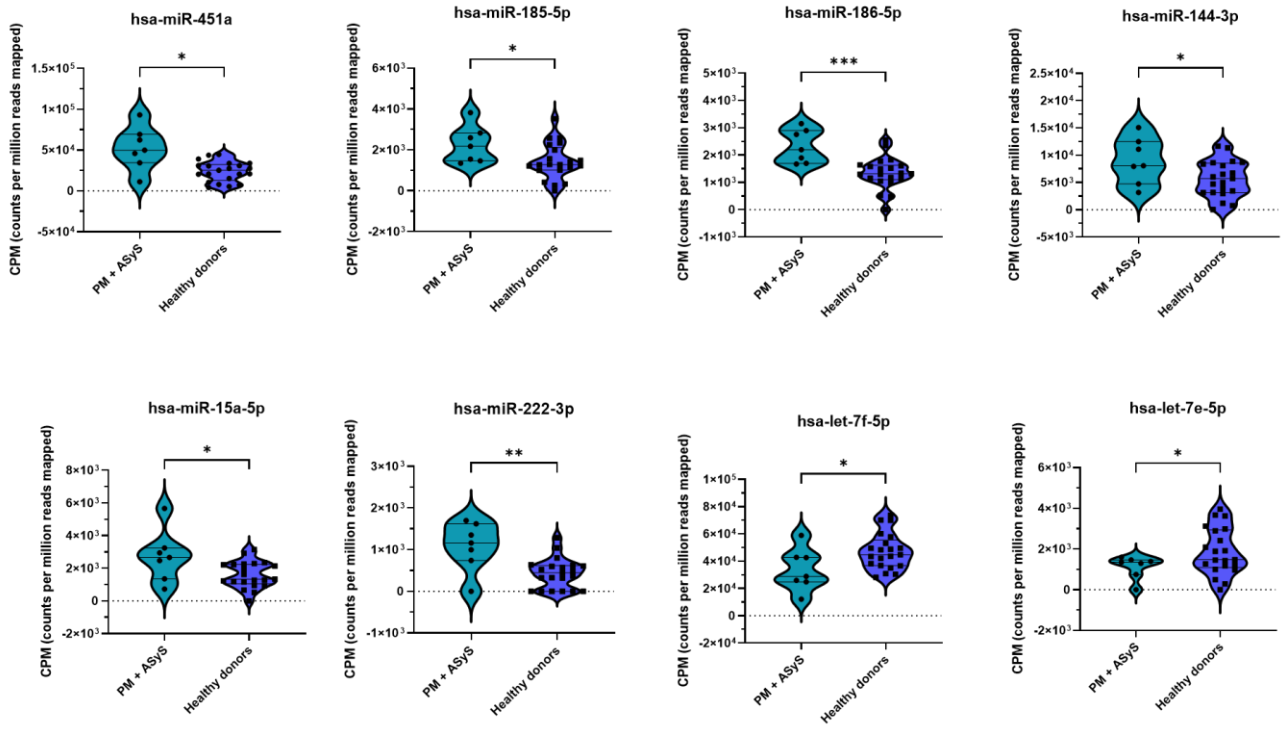


***Figure 27**. Graphs displaying the miRNAs differential expression when up-regulated (hsa-miR-451a, hsa-miR-185-5p, hsa-miR-186-5p, hsa-miR-144-3p, hsa-miR-15-5p, hsa-miR-222-3p) and down-regulated (hsa-let-7f-5p, hsa-let-7e-5p) in PM + ASyS patients (n=7) vs. HDs (n=21); *** p<0.001; ** p<0.01; * p<0.05.*

Moreover, by comparing the DM subgroup of disease with HDs a significant different expression was detected for **hsa-miR-451a** (37321 ± 11545 vs. 23893 ± 12213, p=0.0241), **hsa-miR-486-5p** (24594 ± 7546 vs. 18936 ± 5357, p=0.0474), **hsa-miR-222-3p** (1258 ± 1285 vs. 427.5 ± 358.3, p=0.0115) that were up-regulated in patients while **hsa-let-7f-5p** (33692 ± 15769 vs. 47198 ± 13218, p=0.0442) was down-regulated compared to HDs (**Figure 28**).

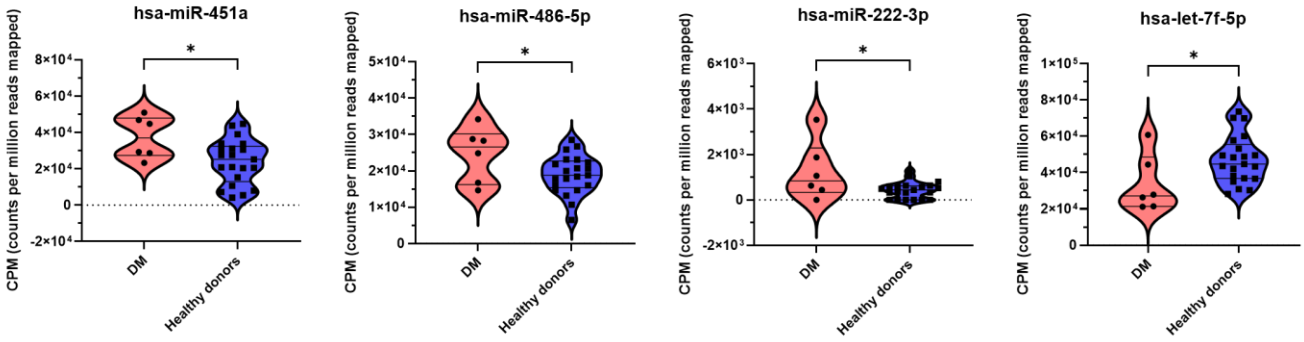


***Figure 28.*** *Graphs representing the up-regulated EV-miRNAs (hsa-miR-451a, hsa-miR-486-5p, hsa-miR-222-3p) and down-regulated (hsa-let-7f-5p) in DM patients (n=6) vs. HDs (n=21); * p<0.05.*

It was found up-regulated expression in CAM than HDs for: **hsa-miR-486-5p** (30215 ± 8415 vs. 18936 ± 5357, p=0.0005), **hsa-miR-223-3p** (44775 ± 14627 vs. 29311 ± 13113, p=0.0199), **hsa-miR-16-5p** (171642 ± 27905 vs. 130804 ± 38372, p=0.0233), **hsa-miR-185-5p** (2179 ± 423 vs. 1438 ± 870, p=0.0099), **hsa-miR-374a-5p** (2621 ± 406.8 vs. 1747 ± 877.8, p=0.0275) and **hsa-miR-23b-3p** (2375 ± 708.1 vs. 1549 ± 912.9, p=0.0398). Conversely, down-regulated expression was reported in: **hsa-let-7b-5p** (21072 ± 3886 vs. 37575 ± 15988, p=0.0205) and **hsa-let-7a-5p** (44929 ± 10217 vs. 77529 ± 36163, p=0.0409) (**Figure 29**).

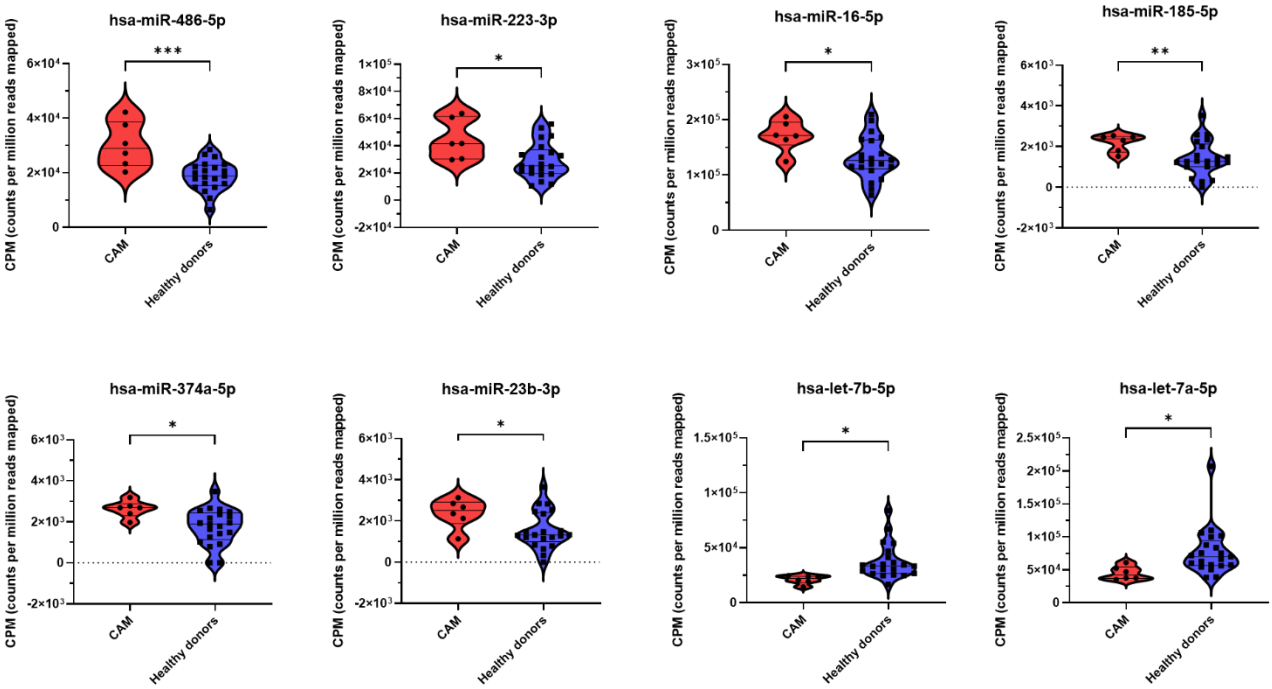


***Figure 29****. Graphs showing the miRNAs differential expression when up-regulated (hsa-miR-486-5p, hsa-miR-223-3p, hsa-miR-16-5p, hsa-miR-185-5p, hsa-miR-374a-5p, hsa-miR-23b-3p) and down-regulated (hsa-let-7b-5p, hsa-let-7a-5p) in CAM patients (n=6) vs. HDs (n=21); *** p<0.001; **p<0.01; * p<0.05.*

Subdividing the IIM group in patients affected with CAM and IIM not associated with cancer (n=15) it was highlighted a dysregulated expression profile referred to different miRNAs (**Table 9**).

| EV-miRNAs | Mean ± SD | | p-value | CAM vs. No CAM |
|---|---|---|---|---|
| | CAM | No CAM | | |
| **hsa-miR-374a-5p** | 2621 ± 406.8 | 1726 ± 940.3 | 0.0068 | Up-regulated |
| **hsa-miR-26b-5p** | 28189 ± 3376 | 22605 ± 7236 | 0.0270 | Up-regulated |
| **hsa-miR-23b-3p** | 737.2 ± 260 | 1357 ± 935.2 | 0.0303 | Down-regulated |
| **hsa-miR-361-5p** | 438.5 ± 253.7 | 930.1 ± 799.2 | 0.0468 | Down-regulated |
| **hsa-miR-143-3p** | 1541 ± 305.6 | 2434 ± 1391 | 0.0312 | Down-regulated |

***Table 9.*** *Table reporting the values of significantly differential expression miRNAs in IIM patients associated with CAM (n=6) vs. without cancer-association (n=15).*

Likewise, by comparing PM + ASyS vs. no PM + ASyS patients (n=12) (**Table 10**), DM vs. no DM patients (n=14) (**Table 11**), and patients with a concurrent diagnosis of ILD (n=11) vs. no ILD subgroup (n=10) (**Table 12**) we found differential expressions of peculiar miRNAs.

| EV-miRNAs | Mean ± SD | | p-value | PM + ASyS vs. No PM + ASyS |
|---|---|---|---|---|
| | PM + ASyS | No PM + ASyS | | |
| **hsa-miR-30c-5p** | 1325 ± 764.5 | 697.3 ± 458.2 | 0.0333 | Up-regulated |
| **hsa-miR-186-5p** | 2390 ± 592.2 | 1603 ± 835.3 | 0.0241 | Up-regulated |

***Table 10.*** *Table reporting the values of significantly differential expression miRNAs in IIM patients affected with PM + ASyS (n=8) vs. no PM + ASyS (n=12).*

| EV-miRNAs | Mean ± SD | | p-value | DM vs. No DM |
|---|---|---|---|---|
| | DM | No DM | | |
| **hsa-miR-125b-5p** | 4714 ± 3861 | 1757 ± 1514 | 0.0215 | Up-regulated |
| **hsa-miR-29c-3p** | 4097 ± 1133 | 2986 ± 868.7 | 0.0275 | Up-regulated |
| **hsa-miR-361-5p** | 1281 ± 791.3 | 557.9 ± 612.7 | 0.0394 | Up-regulated |

***Table 11.*** *Table reporting the values of significantly differential expression miRNAs in IIM patients affected with DM (n=6) vs. no DM (n=14).*

| EV-miRNAs | Mean ± SD | | p-value | ILD vs. No ILD |
|---|---|---|---|---|
| | ILD | No ILD | | |
| **hsa-miR-122-5p** | 6414 ± 4941 | 2923 ± 1855 | 0.0482 | Down-regulated |
| **hsa-miR-423-5p** | 3168 ± 1290 | 4546 ± 1821 | **0.0581** | Not significantly down-regulated |
| **hsa-miR-222-3p** | 638.9 ± 441.7 | 1316 ± 1020 | **0.0592** | Not significantly up-regulated |

***Table 12.*** *Table reporting the values of significantly or slightly differential expression miRNAs in IIM patients with a concurrent diagnosis of ILD (n=11) vs. no ILD (n=10).*

Interestingly, by comparing the IIM patients with active disease in at least a clinical domain (cutaneous, articular, pulmonary, or muscular) (n=10) and those in clinical remission (n=11) at the sampling time, an up-regulation of **hsa-miR-155-5p** (1375 ± 774.4 vs. 696.7 ± 495.8, p=0.0259) and a down-regulation of **hsa-miR-347a-5p** (1564 ± 949.6 vs. 2361 ± 720.8, p=0.0420) emerged among active patients (**Figure 30**).

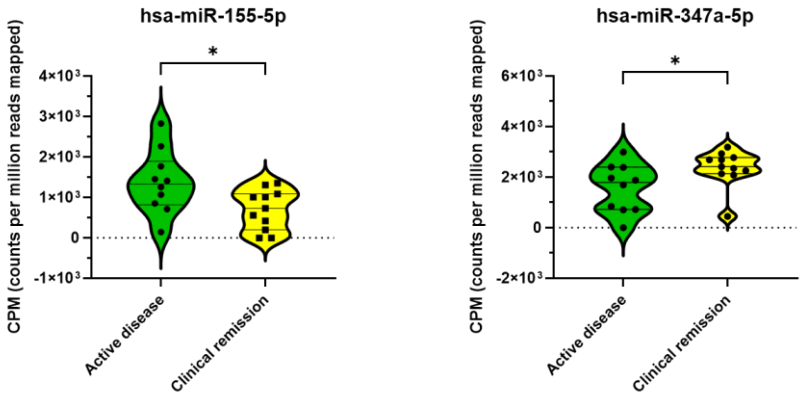


***Figure 30.*** *Graphs representing the up-regulated (hsa-miR-155-5p) and down-regulated (hsa-miR-347a-5p) miRNAs in IIM patients with active disease (n=10) compared to patients in clinical remission (n=11); * p<0.05.*

Finally, we verified that the up- or down-regulation trend of each detected EV-miRNAs did not correlate with the circulating EVs concentration (data not shown).

# 5 Discussion

To date, the involvement of EVs in various physiological and pathological conditions is recognized thanks to their central role as mediators in intercellular communication. The evolving EVs research area is generating significant interest for their potential use as biomarkers both in the diagnosis and treatment of diseases [119,177,225]. However, EVs isolation method is still an open field for methodological approaches ensuring the preservation of the EVs original profile and the purity of the samples [96,107,226,227]. Among the modern EVs isolation techniques size-based, charged-based, and affinity-based methods are included [96,228,229] despite the ultracentrifugation is defined as the gold standard technique [119].

In this study, in keeping with our recent research article [230], we demonstrated an efficient methodology for EVs separation through SEC combined with UF, as confirmed by different characterization techniques showing the presence of intact EVs in pure samples. To ensure accessibility to the biological sample to be reproduced in clinical practice, the starting material we used was venous blood and, according to the International Society on Thrombosis and Haemostasis guidelines on plasma EVs, processed to PFP samples to avoid the presence of platelet-derived EVs released after sample collection [231]. We collected blood samples in sodium citrate tubes to minimize in vitro platelet activation and consequent EVs release. Moreover, as recommended [232,233] we isolated EVs from a small amount of PFP (500 µL) to avoid co-enrichments of other plasma molecules. As suggested in the literature [107,229] we propose to combine different techniques, especially SEC followed by UF with the aim of excluding contaminations.

According to evidence in the literature [234], the protein concentration was found to be significantly reduced in isolated EVs than the relative PFP samples, thereby testifying an efficient separation of vesicular and protein fractions in our assay development and the obtainment of pure samples of EVs.

Images of isolated EVs fractions obtained by TEM revealed the presence of nanoparticles with a prevalence of small-size EVs characterized by their typical “cup-shape” morphology, standing for EVs integrity. No contaminants were observed. These results confirm the evidence of SEC as a method to preserve vesicles structure, integrity, and biological activity [119] and we conclude that also UF step does not destruct the EVs morphology. Furthermore, the EVs structure maintenance before and after the freezing cycle supports that samples storing at –80 °C does not compromise their original profile. Therefore, we confirm that TEM is a helpful method for EVs characterization to discriminate single EV, EVs aggregates and non-EV particles [235].

Then, to specifically confirm the EVs nature of the isolated nanoparticles we verified the presence of constitutive EVs markers in IFC analysis by immuno-characterizing their biochemical composition. The goal of our first IFC analysis was to test the EVs integrity by means of calcein-AM. Nevertheless, the data referred to calcein-AM-positive particles reported lower EVs levels compared to the surface tetraspanin- and integrin- positive EVs obtained by the same method and compared to NTA quantification in both IIM patients and HDs groups. In this context it should be specified that calcein-AM marker is a non-fluorescent membrane permeable dye that involves the intra-vesicular esterases to catalyze the hydrolysis to convert it into a membrane-impermeable fluorescent [236]. Of interest, a study conducted by De Rond and colleagues reported that calcein-AM has a low sensitivity in EVs samples, which may be due to an insufficient brightness of the marker or to the EVs insufficient esterase activity. They conclude that none of the generic EVs markers detected all and only EVs in plasma [236]. In agreement, we speculate the need for different integrity indicators to detect intact EVs.

IFC analysis performed using specific surface markers confirmed that our samples contain EVs characterized by an expression profile belonging to small EVs of endosomal origin, in accordance with TEM observations and NTA measurements. In fact, the tetraspanins CD63, CD81, and CD9 are specific markers for EVs of endosomal origin, while the integrin CD11c is a generic marker associated to the plasma membrane and/or endosomes in a non-tissue specific manner [107]. Particularly, we reported a prevalence of CD63+ EVs compared to CD9+, CD81+ and integrin CD11c+ EVs in both IIM patients and HDs. This is in keeping with previous evidence showing a major recovery of CD63+ and CD9+ EVs after isolation of EVs by qEV columns SEC approach from plasma samples [237] which we speculate could be due to the isolation technique or to the biological starting material. Recently, a study conducted by Veziroglu and colleagues reported that CD9 and CD81 were consistent EVs markers while CD63 expression depended on the experimental parameters [226]. Moreover, by comparing the EVs positive to single surface markers or to combined markers the latter presented lower concentration, proposing that a single EV does not express together all the three tetraspanins. Besides, current evidence suggests that a given cell only expresses certain EVs subtypes even when considering these common markers [226].

Moreover, the absence of signals in the Bright Field corroborates that the EVs belong to the lower size spectrum, and they fall under the camera resolution power of the instrument. This feature even indicates that no contaminants or clustering of multiple EVs are in our samples, as is desirable. These data, beside to define the nanoparticles as small EVs allowed to define the nanoparticles as EVs and perform a biochemical characterization of circulating EVs. Indeed, IFC operates with a lower detection limit respect to canonical flow cytometry [226,237] demonstrating high sensitivity to facilitate

multi-parametric single EV analysis [238] and the characterization of specific EVs phenotypes [239]. Despite the small size of the EVs requires the use of fluorescent markers, the ImageStream$^X$ MKII instrument combines increased fluorescence sensitivity, low background, and powerful data analysis [240].

Of interest, we investigated the surface expression of CD3 and CD19 markers on EVs, respectively specific markers of T and B lymphocytes to speculate their cellular origin. We demonstrated a prevalence of CD3-CD19+ EVs compared to CD3+ EVs in both IIM patients and HDs, suggesting that the majority of circulating EVs collected from human plasma are released by B lymphocytes, cell involved in the adaptive immunity. This aspect may add up to the central role of adaptive immunity in IIM pathogenesis disclosed by the several specific autoantibodies. Furthermore, increasing evidence demonstrated that EVs are principal actors in different autoimmune diseases because they carry various antigens, including DNA and nucleosomes, α-enolases, citrullinated peptides, SS-A and SS-B antigens and Smith antigens capable of trigger and amplify autoimmunity mechanisms [241]. In fact, EVs participate in abnormal activation of the autoimmune system by acting in different immune-related processes, such as antigen presentation in that they express MHC-peptide complexes, T-cell stimulation, cytokine transport, Treg cells differentiation, cell killing and inducing antigen-specific tolerance [242]. In particular, it has been demonstrated that B cell derived-EVs are involved in the antigen presentation activity by transporting MHC-II-peptide complexes, co-stimulatory and adhesion molecules able to activate T cells in a specific manner [243,244]. Similarly, the role of EVs as autoantigens presenters and the immune complexes formation has been demonstrated in RA and SLE [157,245]. Moreover, in the IIM contest it has been highlight that EVs isolated from DM patients are potent inducers of the release of pro-inflammatory cytokines of the IFN type I family, especially IFN-β through the STING pathway activated by the content of dsDNA into the EVs [246]. These results suggest that EVs could be immuno-phenotyped through IFC analysis taking advantage of a complex flow cytometry panel within subpopulations to study their role in diseases pathogenesis. Further speculation regarding the cellular origin of EVs should be confirmed and would be a different aim than the one set for this study.

In our study the data obtained by IFC did not detect differences in the concentration of EVs subpopulation among the IIM and HDs groups. This aspect may reflect a peculiar characterization of circulating EVs from platelet-free plasma samples. On the other hand, in accordance with Botha and colleagues, we speculate that in clinical studies with expected small differences in EVs concentrations between groups, platforms with higher reproducibility would be preferable to highlight slight differences [239].

Our EVs isolation protocol included an enrichment step through UF after the SEC step and then the samples were adjusted at the initial PFP volume to measure the circulating EVs concentration which led to determine the real EVs levels in recruited human subjects. EVs quantification introduced several challenges, predominantly due to their small size and the availability of various technologies each one having its own limitations [237]. We performed EVs measurements using NTA technology which is a mainstay for EVs counting and sizing [226]. However, one of the limitations of NTA is that it is not capable of distinguishing between EVs and similar-sized contaminants from blood samples and it could lead to an overestimation of the EVs concentration [234,247]. In keeping with former reports on human blood plasma from healthy subjects [234] the data obtained by NTA measurements in the present study reported EVs concentration values of ~ $10^{10}$ EVs/mL confirming the efficiency of our EVs isolation methodology and a general qualitative homogeneity that should guarantee the reliability of the isolation techniques.

The diameter of isolated EVs in our samples is registered to be consistently lower than 200 nm in both the IIM and HDs groups confirming the predominance of small EVs isolated using SEC columns to resemble the picture of circulating EVs pool in plasma samples. In fact, former evidence reported the vast majority of circulating EVs to be smaller than 200 nm in diameter [226] in addition to the observation that smaller EVs are detected when isolated by SEC than ultracentrifugation [229].

Of interest, the data obtained through NTA highlighted differences between IIM patients and HDs supporting a good sensitivity of the technique. NTA measurements detected a circulating EVs concentration significantly increased in IIM patients with respect to HDs in accordance with the evidence in the literature [172–174]. The reason of this data resides in the role of EVs that are involved in several immune processes, including inflammation (by promoting the endothelial activation and the leukocyte diapedesis and by carrying various pro-inflammatory cytokines), antigen presentation, and T lymphocytes activation [24,241], mechanisms dysregulated in autoimmune diseases.

Interestingly, by comparing different subsets of diseases within the patients group we observed significantly higher levels of circulating EVs in IIM patients affected with CAM compared to HDs and no CAM patients. Cancer is a source of aberrant antigens characterized by a dysregulated microenvironment which acts in local tissue organization, activates a specific immune response, and participates in pre-metastatic and metastatic niches to alter distant tissues. Moreover, EVs probably play a pathogenic role facilitating the spreading of post-translationally modified self-antigens from the neoplastic milieu through a prolonged and extensive antigen presentation which could trigger potent immune responses resulting in paraneoplastic myopathic manifestations [42]. In paraneoplastic forms, the EVs may induce autoimmunity and cancer self-propagating products by inducing dysregulated antigen trafficking that culminate in CAM [42].

Furthermore, after clustering patients on their clinical spectrum of disease activity we identified a statistically increased EVs concentration in IIM patients with a concurrent diagnosis of ILD compared to HDs and a numerical significance with respect to no ILD. This feature highlights the importance of EVs in lung microenvironment signaling where these nanoparticles mediate the crosstalk of cell types involved in ILD pathogenesis (alveolar epithelial cells, lung fibroblasts, leukocytes, and endothelial cells) in the context of the injured lung and disease-propagation through inflammatory and fibrotic processes [248]. For instance, alveolar macrophage-, neutrophil-, and epithelial cell-derived EVs transfer proinflammatory cytokines such as TNF-α, IL-6 and IL1-β, carries MHC and co-stimulatory molecules supporting their role in immune regulation [248].

In addition, evaluating the serological status of IIM patients we showed significantly elevated circulating EVs concentration in seropositive patients regardless of antibody specificity than HDs. In fact, a pathological pool of active B cells may be at the root of both an increase in EVs release (according to out IFC analysis on the prevalence of B cells-derived EVs) and parallel abnormal antibody production. Moreover, we reported significantly increased EVs levels among IIM patients characterized by a quiescent status of clinical remission than in those with clinical disease activity. Similar findings of lower EVs levels coinciding with peaks of disease activity were previously demonstrated suggesting an EVs migration within sites of inflammation during diseases flares [249]. No other significant associations emerged upon patient stratification between circulating EVs levels and laboratory data, including serological muscle enzymes as an expression of active myositis, such as CPK, or myoglobin, aldolase, AST, ALT, and LDH. In accordance, no significant correlation between EVs concentrations and creatin-kinase levels was established by Shirafuji and colleagues either [173].

Taking into consideration the pharmacological therapy of IIM patients, significantly increased EVs levels in treated patients were still observed with respect to HDs. IIM patients receiving only GC displayed higher EVs concentrations compared to patients treated with GC in combination with IS. Shirafuji and colleagues observed a significant reduction of platelet-derived EVs in PM and DM patients treated with steroid drugs than controls [173]. Of note, it has been demonstrated that immunosuppressive therapy in SLE patients decreases the number of circulating endothelial derived-EVs reducing the cardiovascular risk [250]. Finally, among the pharmacologically treated patients we showed significantly lower EVs levels in patients that received RTX compared to the other treatments, suggesting that this anti-CD20 monoclonal antibody confers advantages in EVs levels normalization which hints at the potential involvement of B lymphocytes derived-EVs in IIM pathogenesis, in accordance with results obtained by IFC characterization. Accordingly, extensive research illustrates that B cells are considerably involved in EVs secretion [172,243,251]. These results

propose a role of pharmacological therapies in reducing the circulating EVs levels potentially normalizing them in IIM patients and IS therapy seems to be more effective on the reduction of EVs, probably acting at the level of their origin and mechanisms of biogenesis. However, the observational design of the study restricts our ability to infer causation in terms of the effect of treatment on EVs concentration.

Taken together, these findings suggest that EVs could be involved in the pathogenesis of IIM where they could differentiate diverse IIM disease subtypes, with a fundamental function in the immune regulation determining an impact on the serologic profile of the patients, thereby playing a potential role as biomarkers of disease and treatment response.

The final step of our study was to investigate the cargo of EVs, in particular their content of miRNAs (EV-miRNAs) to evaluate further mechanisms of EVs involvement in IIM pathogenesis and to confirm their potential role as disease biomarkers. Evidence about EV-miRNAs is still limited due to the recent research area, especially for rare diseases such as IIM.

The detection of miRNAs is challenging as they are short and highly homologous molecules. Current traditional methodologies used for detecting miRNAs include quantitative PCR, northern blotting, in-situ hybridization, microarrays, and RNA-sequencing, each one with its own individual limitations [182,183]. Various methods are currently being developed, such as nanoparticle-derived probes isothermal amplification and electrochemical methods [183]. Through throughput sequencing technology, a small RNA sequencing library can be constructed and sequenced to enable quantitative identification of all small RNA species in a particular sample and to enable the discovery of novel miRNAs and other small non-coding RNAs [182]. In fact, nucleic acids sequencing is a method for determining the exact order of nucleotides present in a DNA or RNA molecule. The development of NGS, or second-generation sequencing methods [252] has revolutionized genomic research employing different platforms able to perform sequencing of millions of small fragments of nucleic acid. NGS performs massively parallel sequencing during which millions of DNA fragments from a single sample are sequenced at the same time, facilitating high-throughput sequencing which allows an entire genome to be sequenced in less than one day [252]. Indeed, each of the three billion bases in the human genome is sequenced multiple times providing high depth to deliver accurate data. Moreover, NGS can be used to sequence entire genomes or constrained to specific areas of interest, including a whole exome (22000 coding genes) or small numbers of individual genes [253].

In the present study we performed the NGS analysis by using Illumina NextSeq/550 platform that provides template preparation, sequencing and imaging and data analysis. Template preparation consists in the building of a library of nucleic acids, such as cDNA followed by the amplification of

the library. Sequencing libraries are constructed by ligating adapter sequences (synthetic oligonucleotides of a known sequence) onto the ends of the RNA fragments and subsequently reverse transcribed to cDNA. Once constructed, library molecules are hybridized to grafted primers onto the surface of a flow cell and then clonally amplified in situ using bridge amplification to form template clusters. To obtain nucleic acid sequence from the amplified libraries the platform relies on sequencing by synthesis. In detail, the library fragments act as a template off which a new DNA fragment is synthesized through the addition of known nucleotides in a sequential order that are digitally recorded as sequence once incorporated into the growing DNA strand. This platform takes advantage of the detection of the fluorescence generated by the incorporation of fluorescently labeled nucleotides into the growing strand of DNA (**Figure 31**).

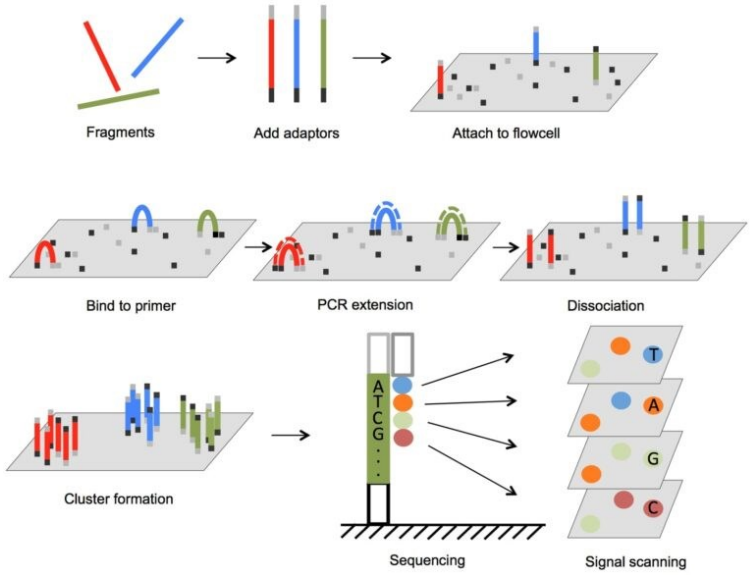


***Figure 31***. *Illustration of NGS sequencing by Illumina technology. From Lu Y. et al., 2016* [254].

The bioinformatics data analysis includes pre-processing the data to remove adapter sequences and low-quality reads, mapping the data to a reference genome or de novo alignment of the sequence reads and analysis of the sequence [252,253,255]. NGS analysis can include a wide variety of bioinformatics assessments, including genetic variants calling for detection of single-nucleotide polymorphisms (SNPs) or indels (such as insertion or deletion of bases), detection of novel genes or regulatory elements, assessment of transcript expression levels, identification of both somatic and germline mutation events. This technology can be employed in clinical practice to discover genes and regulatory elements associated with disease or to identify disease-causing mutations for the diagnosis of pathological conditions [252]. However, although in genome research NGS has mostly superseded conventional Sanger first-generation sequencing it has not yet translated into routine clinical practice [253].

The ability to identify miRNA molecules in our samples further confirmed the efficiency of our EVs isolation method. We highlighted the 20 miRNAs most expressed into the cargo of circulating EVs which not completely correspond to a differential expression between the groups and subgroups of NGS analysis conducted in IIM patients and HDs. The differential expression profile of EV-miRNAs between IIM and HDs showed 6 up-regulated (hsa-miR-451a, hsa-miR-15a-5p, hsa-miR-486-5p, hsa-miR-222-3p, hsa-miR-32-5p, hsa-miR-185-5p) and 4 down-regulated (hsa-let-7e-5p, hsa-let-7a-5p, hsa-let-7f-5p, hsa-let-7b-5p) miRNAs expression in IIM.

Among those up-regulated in IIM, **hsa-miR-451a** under physiological conditions plays anti-inflammatory and anti-migratory effects mediated by the suppression of IL-6 and TNF-α expression. It has been described that high levels of hsa-miR-451a in PBMC of RA patients in a pre-clinical phase of disease (positivity to anti-citrullinated peptide antibodies in the absence of clinical signs of disease) are potential biomarkers of a higher risk of developing RA in the manifest form [256]. Moreover, it has been reported that a down-regulation of EV-hsa-miR-451a from the synovial fluid of RA patients correlates with low-grade joint inflammation [257]. On the other hand, its down-regulation in the serum of SLE patients associates with active disease and kidney involvement [202]. An up-regulation of **hsa-miR-222-3p** leads to a pro-inflammatory stimulus guided by TNF-α e IFN-α/β and it regulates the innate immunity. Hsa-miR-222-3p (transcriptionally induced by NF-kB) can negatively regulate TNFAIP3 which inhibits TNF-α signaling, or it can target the transcription factor IRF-2 which inhibits the IFN-α/β activation [258]. Moreover, dysregulated hsa-miR-222-3p has been detected in T and B lymphocytes from anti-SSA positive patients with primary Sjögren's syndrome and the authors propose it to be involved in the regulation of T and B cells function within the tissue of salivary glands [208]. To date, there are still little evidence in the literature about the hsa-miR-222-3p as EVs cargo, particularly referred to connective tissue diseases. However, it has been reported that in the context of epithelial-type ovarian cancer the EVs carry high levels of hsa-miR-222-3p capable of inducing a polarization towards the M2 phenotype of the macrophages associated with the neoplasia [259]. Of interest, the serological cytokine profile in patients affected with PM/DM associated to ILD showed increased levels of cytokines related to macrophage M2 phenotype (M-CSF and IL-10) compared to cytokines related to macrophage M1 phenotype in DM patients positive to anti-MDA5 compared to ASyS [260]. Furthermore, hsa-miR-222-3p can form a complex with SOCS1 which activates the JAK/STAT signaling and then promote the synthesis of pro-inflammatory cytokines, including IFN, IFNα and IL-6 [261]. Of note, in DM phenotype an important pathogenic role involves JAK/STAT signaling and IFN-I, such as IFN-β pathway. The up-regulation of hsa-miR-222-3p promotes cutaneous lesions and rapidly progressive ILD [262]. Within IIM pathology, hsa-miR-222-3p as well as hsa-miR-221 and hsa-miR-146a have been reported over-expressed in the muscle tissue biopsy of

PM and IBM patients [212]. These findings correlate with the up-regulated expression of hsa-miR-222-3p founded in PM + ASyS and DM vs. HDs. **Hsa-miR-185-5p** is involved in signaling pathways mediated by cytokines and among its target genes there are TGFB1, IGF1R e VEGFA. Its expression has been disclosed up-regulated in EVs from synovial fluid of RA patients characterized with high degree of joint inflammation, suggesting the flogistic action although the precise mechanisms are not yet been defined [257]. The clear role of **hsa-miR-32-5p** has not been identified and it is not investigated in systemic autoimmune diseases. However, a study has been founded an over-expression of EV-hsa-miR-32-5p that activates the PI3K/Akt pathway through the suppression of PTEN and it induces chemo-resistance promoting angiogenesis and epithelium-mesenchymal transition in the metastatic process [263]. Besides, it has been reported that hsa-miR-32-5p contributes to neuropathic pain by degrading the Dusp5 protein, a phosphatase that negatively controls the pathway of MAPK signaling in microglia. Furthermore, it is involved in neuroinflammation and endothelial disfunction and increases the production of pro-inflammatory cytokine [264]. A dysregulated expression of **hsa-miR-15a-5p** has been detected in SLE where it acts with immuno-regulatory functions, in particular referred to adaptive immunity. It targets genes involved in cellular cycle (cyclin D1) and apoptosis (Bcl-2) promoting the persistence of reactive B lymphocytes and increasing the production of anti-dsDNA autoantibodies [200]. We speculate analogue role in IIM regarding the importance of antibodies production in the pathogenesis. On the other hand, in the literature the miRNAs hsa-miR-15a-5p, hsa-miR-451a and hsa-miR-185-5p have been described also as anti-inflammatory and onco-suppressive actors that negatively regulate the cell proliferation and neo-angiogenesis [265–268]. These findings contrast with the up-regulated expression detected in our samples, but we propose that it may be a consequence of the heterogeneity of our cohort.

Among miRNAs down-regulated in IIM than HDs appeared those of hsa-miR-let-7 family, in particular **hsa-let-7a-5p**, **hsa-let-7b-5p**, **hsa-let-7e-5p** and **hsa-let-7f-5p**. This miRNAs family play a role in anti-inflammatory mechanisms modulating the production of IL-6, TNF-α and Toll-like receptor signaling [258,269] and its dysregulated expression has been observed in several autoimmune diseases, including SLE and systemic sclerosis [270,271]. The clear role of these miRNAs is not well defined; however, our congruent results support their anti-inflammatory function.

The picture of several dysregulated miRNAs in CAM (i.e., hsa-miR-23b-3p, hsa-miR-361-5p, hsa-miR-143-3p, hsa-miR-374a-5p, hsa-miR-26b-5p) may reflect the complex mechanism that act between the immune system and neoplastic cells in this paraneoplastic manifestation. In fact, tumor biology differs among cancer types and challenging evidence is often found in the literature about the role of a miRNA in different cancer. A special mention should be spent for **hsa-miR-23b-3p** that was

down-regulated in CAM compared to DM, ASyS and no CAM patients, suggesting a potential role in differential diagnosis that could be useful to targeted screening since the paraneoplastic form can show musculocutaneous characteristics up to two years before the clinical onset of the neoplasia. This miRNA is involved in the regulation of several mechanisms, including the cellular cycle, growth factors signaling, cytoskeleton remodeling, cell survival and apoptosis, autophagy, cell migration and adhesion and cell differentiation [272]. Despite some conflicting evidence on the roles of hsa-miR-23b-3p in cancer, it has been described that it negatively regulates the MET oncogene acting as onco-suppressor. Its down-regulation promotes neoplastic transformation and metastasis in various neoplasms such as hepatocellular carcinoma, bladder carcinoma, squamous cell carcinoma of the oral cavity and cervical carcinoma. Moreover, it has been proposed the role of EV-hsa-miR-23b-3p in the tumor environment to induce invasiveness and metastasis [272]. Furthermore, hsa-miR-23b-3p participates in a signaling regulation of several inflammatory cytokines, such as TNF-α, IL-1β, IL-17 and NF-kB. Its down-regulation has been detected in DM where it could be involved in muscle damage by increasing cytokine levels and consequently immune cells that induce the injury. Finally, it has been emerged that the expression of hsa-miR-23b-3p negatively correlate with CPK levels [273]. **Hsa-miR-374-5p** was up-regulated in CAM patients compared to ASyS, no CAM and HDs. Although its role is not well defined, it has been proposed to act in anti-inflammatory roles [274] with anti-phlogistic effects in inflammatory bowel disease, in the improvement of neuroinflammation and hypoxic-ischemic damage [275]. Moreover, hsa-miR-223-3p, hsa-miR-451a, hsa-miR-486-5p, hsa-miR-185-5p, hsa-miR-16-5p were up-regulated and hsa-let-7a and hsa-let-7b were down-regulated in patients affected with CAM versus HDs. Of interest, EV-**hsa-miR-486-5p** has been detected up-regulated in lung adenocarcinoma proposing it as biomarker of early diagnosis [276]. In addition, it has been proposed that hsa-miR-486-5p regulates the EVI5 oncogene and it is responsible for the migration and invasiveness of NSCLC (Non-Small Cell Lung Cancer) through the TGF-β/Smad signaling pathway [277]. Furthermore, it was reported an up-regulation even in prostatic carcinoma where hsa-miR-486-5p involves several oncogenic pathways by suppressing FOXO1 e PTEN, negative regulators of PI3K/Akt signaling [278]. It has been recognized as a pro-tumorigenic factor even in small cell lung cancer, invasive and metastatic pancreatic ductal carcinoma and renal cell carcinoma [279]. Conversely, Ninawe et al. reported an onco-suppressive role of this miRNA in NSCLC, breast cancer, oesophageal and gastric carcinoma and squamous cell carcinoma [279] underling the dual role of hsa-miR-486-5p in carcinogenesis both as tumor promoter and tumor suppressor. It also performs immunomodulatory functions due to the involvement in MAPK, PI3K/Akt and mTOR signaling pathways which are crucial in immune cells. Indeed, CAM are paraneoplastic forms likely descending from enhanced immune response against aberrant tumor antigens, thus explaining the

dysregulated miRNA expression to link cancer and immune-mediated injury. **Hsa-miR-451a** suppresses the invasive and migration capacity of cancer cells in various cancer forms where it often appears down-regulated. In our results, the finding of an up-regulation of hsa-miR-451a in CAM patients could reflect the characteristic of this manifestation with respect to the onset of the neoplasm, as it was suggested that the development of a clinically evident CAM correlates with an enhanced yet insufficient response of the immune system in contrasting the neoplasm [280]. **Hsa-miR-185-5p** role in cancer is ambiguous with more evidence that sustains its role as a tumor suppressor due to its down-regulation in several neoplasms, such as NSCLC, breast cancer, gastric cancer and glioblastoma to guarantee the invading and metastasizing capacity [281]. However, as already mentioned CAM are paraneoplastic forms in which during the immune response the exposed neo-antigens act as triggers in muscle and skin. The immune-mediated injury in presence of neoplasm could reflect the EVs cargo of miRNAs. Further investigation might be useful to differentiate neoplasms and paraneoplastic CAM. Finally, the down-regulation of **hsa-let-7b-5p** in several neoplasms has been associated with onco-suppressor function and negative regulation of cancer stem cells [282].

In PM + ASyS subgroup, two miRNAs resulted up-regulated compared to the others subset of disease supporting them to be potentially used to differentiate the IIM subgroups. **Hsa-miR-186-5p** was up-regulated in PM + ASyS even in comparison with HDs. It negatively acts on the expression of SMAD6 and SMAD7 by suppressing the cellular cycle. Its overexpression inhibits the epithelial-mesenchymal transition, migration and tissue invasion [283]. Evidence has been showed its up-regulation in PBMC of SLE patients [284], although information is limited as an immuno-regulatory actor [258]. Furthermore, it has been hypothesized a role as tumor suppressive biomarker and potential therapeutic target [285]. In fact, hsa-miR-186-5p may act a protective role against neoplasia in patients affected by PM and ASyS with a lower risk of cancer. **Hsa-miR-30c-5p** has been demonstrated to display a role in atherosclerosis and vascular smooth muscle cells calcification [286] without evidence in immune-regulation functions. Hsa-miR-451a, hsa-miR-222-3p, hsa-miR-185-5p, hsa-miR-32-5p, hsa-miR-15a-5p, hsa-miR-144-3p, hsa-miR-186-5p were over-expressed, while hsa-let-7e and hsa-let-7f were down-regulated in PM + ASyS versus HDs. **Hsa-miR-144-3p** maintains the mitochondrial function by preserving the ATP levels. Of note, mitochondria are present in muscle fibers and their functional alterations has been demonstrated in IIM patients associated with the progression of disease [287]. In fact, oxidative and hypoxic damage affect the endothelial disfunction and vasculopathy [288]. The dysregulation of hsa-miR-144-3p may induce the tissue fibrosis promoting the epithelial-mesenchymal transition [289]. This evidence support that non-immune mechanisms are

involved in the pathogenesis of IIM and tissue damage [24] suggesting a potential role of biomarker also for miRNA not involved in immune responses.

In DM subgroup hsa-miR-125b-5p, hsa-miR-29c-3p, hsa-miR-361-5p were significantly up-regulated compared to no DM patients. **Hsa-miR-125b-5p** shows inhibitory effect on the proliferation of keratinocyte by targeting the Akt3 gene [290]. It has also been described an action in the inhibition of angiogenesis by down-regulating the vascular endothelial growth factor (VEGF) expression through thermal injury [291], suggesting to induce skin injury in DM patients. **Hsa-miR-223-3p** expression was down-regulated in DM patients than CAM. Its down-regulation is involved in the manifestation of Gottron's papules in DM [292]. It would be interesting to evaluate in a larger patients' cohort whether the expression of this miRNA correlates with the disease activity of DM and whether its down-regulation in DM phenotypes correlates with the exclusive skin involvement. Furthermore, hsa-miR-223 has been detected to be down-regulated in Gottron's papules of patients affected with clinical amyopathic dermatomyositis (CADM) compared to HDs and absent in DM. This feature induces the over-expression of PCKε (protein kinase epsilon) in basal keratinocytes of the proliferative layer of the epidermis promoting acanthosis and hyperproliferation observed in the histopathology of Gottron's papules. This evidence supports the role of hsa-miR-223 in cutaneous manifestations of DM and CADM, despite after the comparison between the different disease phenotypes the significance compared to the healthy was maintained only for the CADM patients [292]. Moreover, hsa-miR-451a, hsa-miR-486-5p, hsa-miR-222-3p were up-regulated and hsa-let-7f down-regulated in DM versus HDs.

Patients characterized by active disease reported an up-regulated expression of hsa-miR-155-5p and a down-regulated expression of hsa-miR-347a-5p than those in clinical remission. **Hsa-miR-155-5p** plays a key role as mediator in inflammatory and adaptive immunity mechanisms. The up-regulation of this miRNA is associated to IFN-γ-induced apoptosis and inflammation in salivary gland epithelial cells of patients affected with SS with an increased production of IL-6 and TNF-α [293]. Moreover, hsa-miR-155-5p is involved in germinal center formation and antibodies production in myasthenia gravis: its down-regulation resulted in a limited production of anti-acetylcholine antibodies [294]. It would be interesting know if it acts similar functions in IIM pathogenesis to propose it as a potential target of therapies. In fact, it has been reported a down-regulated expression of hsa-miR-155-5p in AR patients responsive to MTX treatment [295], allowing us to propose it as a useful biomarker of treatment response in IIM.

Other miRNAs resulted dysregulated within IIM phenotypes, including hsa-miR-122-5p in ILD patients. The functional analysis of each miRNA goes beyond the scope of this work. Furthermore, the sample size is still limited to affirm the potential involvement of these miRNAs in the IIM pathogenesis and diagnosis.

Our findings sustain a role for miRNAs encapsulated into EVs to regulate several molecular pathways involved in the immune response [296]. Moreover, these results support the interesting potential role of miRNAs as biomarkers in a variety of diseases, including autoimmune diseases. In fact, serum miRNAs derive both from circulating blood cells and from other tissues directly affected by diseases [297]. These results suggest a potential involvement of the EV-miRNAs in IIM pathogenesis. Moreover, the lack of correlation between EVs concentration and miRNAs expression suggests that each EV carries a peculiar cargo based on the cells of origin and the stimuli that induced its release in the pathological condition.
Overall, the results of the present study support the proposal of EVs and EV-miRNAs as biomarkers of IIM and IIM differential phenotypes with a perspective as a biomarker for treatment response.

Our study has some limitations which must be considered. We did not directly compare different techniques for the EVs isolation. Consequently, the prevalence of small EVs in our samples could be due to a real representation of the circulating particles or to a dimensional selection of the particles during the SEC step despite the range of size selection of the used Izon columns is 70-1000 nm. Furthermore, the efficiency of particles isolation in terms of EVs concentration was proposed by comparing our results with the data in the literature. Finally, the study section referred to the EVs cargo of miRNAs includes preliminary data in a small samples size due to the monocentric study and heterogeneous cohort of patients. We look forward to reproducing data of the differential expression profile of miRNAs in a larger, homogenous cohort of patients, in order to test their suitability as potential biomarkers of IIM and specific IIM subsets. Overall, it will be necessary to increase the sample size of the IIM patient cohort at the onset of the disease, being ideally treatment- free at the time of the first sample collection, notwithstanding hurdles related to the rarity of IIM and to real-life therapeutic management.
On the other hand, the main strength of our study consists in the efficacy and reproducibility of the EVs isolation through the SEC followed by UF approach, whose reliability to obtain pure EVs was confirmed by the subsequent application of different characterization techniques (TEM, IFC, and NTA) to verify multiple features of EVs. Besides, isolated EVs were proven comparable in the cohort in terms of concentration, size and immunophenotyping. We documented a compelling difference in

EVs concentration when comparing health and disease, submitting evidence for our isolation technique to reliably separate HDs from other phenotypes and NTA technique able to accurately identify nanoparticles. Finally, the investigation of EV-miRNAs by NGS was conducted through a sequencing methodology defined to be reliable and have high output.

# 6 Conclusions

This study was paramount to propose a newly-conceived EVs isolation method consisting of SEC followed by UF as a reliable and reproducible approach to obtain pure EVs fractions with preserved morphological integrity from complex biological fluids such as plasma.

Moreover, the results of the subsequent analyses suggested the involvement of EVs in the pathogenesis of IIM, supporting their potential role as prognostic biomarkers of disease, differential diagnosis, and treatment response.

In particular, circulating EVs appear to be released predominantly from B lymphocytes, suggesting the implication of adaptive immunity in their biogenesis.

The abnormal EVs concentration according to the presence of IIM associates with disease phenotype and clinical features, activity, and treatment, supporting what would be the important utility of EVs as biomarkers in the complexity of this pathology.

The preliminary data concerning the EVs cargo of miRNAs support the fundamental epigenetic regulation in the initiation and maintenance of the IIM autoimmune process through immunoregulatory functions of innate and adaptive immunity. The dysregulated expression profile of EV-miRNAs in IIM patients proves further promising specific biomarkers of disease and subsets of disease.

In conclusion, EVs and EV-miRNAs could represent a utility in clinical practice as biomarkers to solve the complicated diagnosis and monitor the treatment response of a heterogeneous pathology such as IIM.

# 7 References


1. Mariampillai, K. *et al.* Development of a New Classification System for Idiopathic Inflammatory Myopathies Based on Clinical Manifestations and Myositis-Specific Autoantibodies. *JAMA Neurol* **75**, 1528–1537 (2018).
2. Punzi, L. & Doria, A. *Core curriculum - Reumatologia*. vol. Unico (2014).
3. Schmidt, J. Current Classification and Management of Inflammatory Myopathies. *J Neuromuscul Dis* **5**, 109–129 (2018).
4. Lundberg, I. E. *et al.* EULAR/ACR Classification Criteria for Adult and Juvenile Idiopathic Inflammatory Myopathies and their Major Subgroups. **69**, 2271–2282 (2017).
5. Mahler, M., Miller, F. W. & Fritzler, M. J. Idiopathic inflammatory myopathies and the anti-synthetase syndrome: A comprehensive review. *Autoimmun Rev* **13**, 367–371 (2014).
6. Troyanov, Y. *et al.* Novel classification of idiopathic inflammatory myopathies based on overlap syndrome features and autoantibodies: Analysis of 100 French Canadian patients. *Medicine* **84**, 231–249 (2005).
7. Lundberg, I. E. *et al.* 2017 European League Against Rheumatism/American College of Rheumatology classification criteria for adult and juvenile idiopathic inflammatory myopathies and their major subgroups. *Ann Rheum Dis* **76**, 1955–1964 (2017).
8. Bottai, M. *et al.* EULAR/ACR classification criteria for adult and juvenile idiopathic inflammatory myopathies and their major subgroups: A methodology report. *RMD Open* **3**, 1–10 (2017).
9. Zanframundo, G. *et al.* Defining anti-synthetase syndrome: a systematic literature review. *Clin Exp Rheumatol* **40**, 309–319 (2022).
10. Connors, G. R., Christopher-Stine, L., Oddis, C. v. & Danoff, S. K. Interstitial lung disease associated with the idiopathic inflammatory myopathies: What progress has been made in the past 35 years? *Chest* **138**, 1464–1474 (2010).
11. Solomon, J., Swigris, J. J. & Brown, K. K. Myositis-related interstitial lung disease and antisynthetase syndrome. *J Bras Pneumol* **37**, 100–9 (2013).
12. Witt, L. J., Curran, J. J. & Strek, M. E. The diagnosis and treatment of antisynthetase syndrome. *Clin Pulm Med* **23**, 218–226 (2016).
13. Lundberg, I. E. *et al.* Idiopathic inflammatory myopathies. *Nat Rev Dis Primers* **7**, 1–22 (2021).
14. Furst, D. E., Amato, A. A., Iorga, Ş. R., Gajria, K. & Fernandes, A. W. Epidemiology of adult idiopathic inflammatory myopathies in a U.S. managed care plan. *Muscle Nerve* **45**, 676–683 (2012).
15. Iaccarino, L. *et al.* The clinical features, diagnosis and classification of dermatomyositis. *J Autoimmun* **48–49**, 122–127 (2014).
16. Dobloug, G. C., Svensson, J., Lundberg, I. E. & Holmqvist, M. Mortality in idiopathic inflammatory myopathy: Results from a Swedish nationwide population-based cohort study. *Ann Rheum Dis* **77**, 40–47 (2018).

17. Rothwell, S. *et al.* Focused HLA analysis in Caucasians with myositis identifies significant associations with autoantibody subgroups. *Ann Rheum Dis* **78**, 996–1002 (2019).
18. Miller, F. W., Lamb, J. A., Schmidt, J. & Nagaraju, K. Risk factors and disease mechanisms in myositis. *Nat Rev Rheumatol* **14**, 255–268 (2018).
19. Dalakas, M. C. Inflammatory myopathies: Update on diagnosis, pathogenesis and therapies, and COVID-19-related implications. *Acta Myologica* **39**, 289–301 (2020).
20. Mammen, A. L. *et al.* Autoantibodies against 3-hydroxy-3-methylglutaryl-coenzyme a reductase in patients with statin-associated autoimmune myopathy. *Arthritis Rheum* **63**, 713–721 (2011).
21. Allenbach, Y., Benveniste, O., Stenzel, W. & Boyer, O. Immune-mediated necrotizing myopathy: clinical features and pathogenesis. *Nat Rev Rheumatol* **16**, 689–701 (2020).
22. Liu, S. W. *et al.* Dermatomyositis induced by anti-tumor necrosis factor in a patient with juvenile idiopathic arthritis. *JAMA Dermatol* **149**, 1204–1208 (2013).
23. Burd, C. J., Kinyamu, H. K., Miller, F. W. & Archer, T. K. UV radiation regulates Mi-2 through protein translation and stability. *Journal of Biological Chemistry* **283**, 34976–34982 (2008).
24. Loredo Martinez, M. *et al.* Nonimmune mechanisms in idiopathic inflammatory myopathies. *Curr Opin Rheumatol* **32**, 515–522 (2020).
25. Ascherman, D. P. The Role of Jo-1 in the Immunopathogenesis of Polymyositis: Current Hypotheses. *Curr Rheumatol Rep* **5**, 425–430 (2003).
26. Bohan Anthony, Peter James B, Bowman Ralph L & Pearson Carl M. A computer-assisted analysis of 153 patients with polymyositis and dermatomyositis. *Medicine* (1977).
27. Lloyd, T. E. *et al.* Evaluation and construction of diagnostic criteria for inclusion body myositis. *Neurology* **83**, 426–433 (2014).
28. Kissel, J. T. Polymyositis: Not a unicorn or mythological beast...but maybe a duck? *Neurology* **70**, 414–415 (2008).
29. Naddaf, E., Barohn, R. J. & Dimachkie, M. M. Inclusion Body Myositis: Update on Pathogenesis and Treatment. *Neurotherapeutics* **15**, 995–1005 (2018).
30. Greenberg, S. A. Inclusion body myositis: clinical features and pathogenesis. *Nat Rev Rheumatol* **15**, 257–272 (2019).
31. Salajegheh, M. *et al.* Permissive environment for B-cell maturation in myositis muscle in the absence of B-cell follicles. *Muscle Nerve* **42**, 576–583 (2010).
32. Bradshaw, E. M. *et al.* A Local Antigen-Driven Humoral Response Is Present in the Inflammatory Myopathies. *The Journal of Immunology* **178**, 547–556 (2007).
33. Cavagna, L. *et al.* Influence of antisynthetase antibodies specificities on antisynthetase syndrome clinical spectrum time course. *J Clin Med* **8**, (2019).
34. Gasparotto, M. *et al.* Pulmonary involvement in antisynthetase syndrome. *Current Opinion in Rheumatology* vol. 31 603–610 Preprint at https://doi.org/10.1097/BOR.0000000000000663 (2019).

35. Gallay, L., Gayed, C. & Hervier, B. Antisynthetase syndrome pathogenesis: knowledge and uncertainties. *Curr Opin Rheumatol* **30**, 664–673 (2018).

36. Opinc, A. H. & Makowska, J. S. Antisynthetase syndrome – much more than just a myopathy. *Semin Arthritis Rheum* **51**, 72–83 (2021).

37. Adams, R. A. *et al.* Serum-circulating His-tRNA synthetase inhibits organ-targeted immune responses. *Cell Mol Immunol* **18**, 1463–1475 (2021).

38. Pinal-Fernandez, I., Casal-Dominguez, M. & Mammen, A. L. Immune-Mediated Necrotizing Myopathy. *Current Rheumatology Reports* vol. 20 Preprint at https://doi.org/10.1007/s11926-018-0732-6 (2018).

39. Arouche-Delaperche, L. *et al.* Pathogenic role of anti–signal recognition protein and anti–3-Hydroxy-3-methylglutaryl-CoA reductase antibodies in necrotizing myopathies: Myofiber atrophy and impairment of muscle regeneration in necrotizing autoimmune myopathies. *Ann Neurol* **81**, 538–548 (2017).

40. Grable-Esposito, P. *et al.* Immune-mediated necrotizing myopathy associated with statins. *Muscle Nerve* **41**, 185–190 (2010).

41. Trallero-Araguás, E. *et al.* Cancer-associated myositis and anti-p155 autoantibody in a series of 85 patients with idiopathic inflammatory myopathy. *Medicine* **89**, 47–52 (2010).

42. Suber, T. L., Casciola-Rosen, L. & Rosen, A. Mechanisms of disease: Autoantigens as clues to the pathogenesis of myositis. *Nat Clin Pract Rheumatol* **4**, 201–209 (2008).

43. Rasuli, B. & Weerakkody, Y. Usual interstitial pneumonia. in *Radiopaedia.org* (Radiopaedia.org, 2012). doi:10.53347/rID-16895.

44. Euwer, R. L. & Sontheimer, R. D. Dermatologic aspects of myositis. *Curr Opin Rheumatol* **6**, 583–589 (1994).

45. Dalakas, M. C. Inflammatory Muscle Diseases. *New England Journal of Medicine* **372**, 1734–1747 (2015).

46. Fiorentino, D., Chung, L., Zwerner, J., Rosen, A. & Casciola-Rosen, L. The mucocutaneous and systemic phenotype of dermatomyositis patients with antibodies to MDA5 (CADM-140): A retrospective study. *J Am Acad Dermatol* **65**, 25–34 (2011).

47. Fiorentino, D. F. *et al.* Most patients with cancer-associated dermatomyositis have antibodies to nuclear matrix protein NXP-2 or transcription intermediary factor 1γ. *Arthritis Rheum* **65**, 2954–2962 (2013).

48. Ghirardello, A. *et al.* Gli anticorpi miosite specifici e miosite associati nelle miopatie infiammatorie idiopatiche: Studio sierologico di 46 pazienti. *Reumatismo* **57**, 22–28 (2005).

49. Liang, L. *et al.* Anti-Mi-2 antibodies characterize a distinct clinical subset of dermatomyositis with favourable prognosis. *European Journal of Dermatology* **30**, 151–158 (2020).

50. Hengstman, G. J. D. *et al.* Anti-signal recognition particle autoantibodies: Marker of a necrotising myopathy. *Ann Rheum Dis* **65**, 1635–1638 (2006).

51. Greenberg, S. A. Cytoplasmic 5′-nucleotidase autoantibodies in inclusion body myositis: Isotypes and diagnostic utility. *Muscle Nerve* **50**, 488–492 (2014).

52. Jia, E. *et al.* Diffuse pruritic erythema as a clinical manifestation in anti-SAE antibody-associated dermatomyositis: a case report and literature review. *Clinical Rheumatology* vol. 38 2189–2193 Preprint at https://doi.org/10.1007/s10067-019-04562-w (2019).

53. Zhong, L., Yu, Z. & Song, H. Association of anti-nuclear matrix protein 2 antibody with complications in patients with idiopathic inflammatory myopathies: A meta-analysis of 20 cohorts. *Clinical Immunology* **198**, 11–18 (2019).

54. Fredi, M. *et al.* An Italian Multicenter Study on Anti-NXP2 Antibodies: Clinical and Serological Associations. *Clin Rev Allergy Immunol* **63**, 240–250 (2022).

55. Ghirardello, A. *et al.* Myositis autoantibodies and clinical phenotypes. *Autoimmunity Highlights* **5**, 69–75 (2014).

56. Ghirardello, A. *et al.* Autoantibodies in polymyositis and dermatomyositis. *Curr Rheumatol Rep* **15**, (2013).

57. McHugh, N. J. Ro52, Myositis, and Interstitial Lung Disease. *J Rheumatol* (2022) doi:10.3899/jrheum.221067.

58. McHugh, N. J. & Tansley, S. L. Autoantibodies in myositis. *Nature Reviews Rheumatology* vol. 14 290–302 Preprint at https://doi.org/10.1038/nrrheum.2018.56 (2018).

59. Briani, C., Doria, A., Sarzi-Puttini, P. & Dalakas, M. C. Update on idiopathic inflammatory myopathies. *Autoimmunity* vol. 39 161–170 Preprint at https://doi.org/10.1080/08916930600622132 (2006).

60. del Grande, F., Carrino, J. A., del Grande, M., Andrew Mammen, Þ. L. & Christopher Stine, L. *Magnetic Resonance Imaging of Inflammatory Myopathies*. www.topicsinmri.com (2012).

61. Travis, W. D. *et al.* An official American Thoracic Society/European Respiratory Society statement: Update of the international multidisciplinary classification of the idiopathic interstitial pneumonias. *Am J Respir Crit Care Med* **188**, 733–748 (2013).

62. Hervier, B. *et al.* Pulmonary hypertension in antisynthetase syndrome: Prevalence, aetiology and survival. *European Respiratory Journal* **42**, 1271–1282 (2013).

63. Wang, H. *et al.* Pulmonary hypertension in polymyositis. *Clin Rheumatol* **34**, 2105–2112 (2015).

64. Smith, E. S. *et al.* Dermatomyositis: A Clinicopathological Study of 40 Patients. *Am J Dermatopathol* **31**, 61–67 (2009).

65. Pipitone, N. Value of MRI in diagnostics and evaluation of myositis. *Curr Opin Rheumatol* **28**, 625–630 (2016).

66. Selva-O'Callaghan, A., Martinez-Gómez, X., Trallero-Araguás, E. & Pinal-Fernández, I. The diagnostic work-up of cancer-associated myositis. *Current Opinion in Rheumatology* vol. 30 630–636 Preprint at https://doi.org/10.1097/BOR.0000000000000535 (2018).

67. Dalakas, M. C. Immunotherapy of myositis: issues, concerns and future prospects. *Nat Rev Rheumatol* **6**, 129–137 (2010).

68. Munters, L. A. *et al.* Endurance Exercise Improves Molecular Pathways of Aerobic Metabolism in Patients With Myositis. *Arthritis and Rheumatology* **68**, 1738–1750 (2016).

69. Corrado, B., Ciardi, G. & Lucignano, L. Supervised Physical Therapy and Polymyositis/Dermatomyositis—A Systematic Review of the Literature. *Neurol Int* **12**, 77–88 (2020).

70. Lundberg, I., Kratz, A.-K., Alexanderson, H. & Patarroyo, M. Decreased expression of interleukin-1α, interleukin-1β, and cell adhesion molecules in muscle tissue following corticosteroid treatment in patients with polymyositis and dermatomyositis. *Arthritis Rheum* **43**, 336 (2000).

71. Ernste, F. C. & Reed, A. M. Idiopathic Inflammatory Myopathies: Current Trends in Pathogenesis, Clinical Features, and Up-to-Date Treatment Recommendations. *Mayo Clin Proc* **88**, 83–105 (2013).

72. Oddis, C. v. & Aggarwal, R. Treatment in myositis. *Nat Rev Rheumatol* **14**, 279–289 (2018).

73. Ruperto, N. *et al.* Prednisone versus prednisone plus ciclosporin versus prednisone plus methotrexate in new-onset juvenile dermatomyositis: A randomised trial. *The Lancet* **387**, 671–678 (2016).

74. Dawson, J. K. *et al.* Does methotrexate cause progressive fibrotic interstitial lung disease? A systematic review. *Rheumatol Int* **41**, 1055–1064 (2021).

75. Bunch, T. W. Azathioprine with Prednisone for Polymyositis. *Ann Intern Med* **92**, 365 (1980).

76. Bunch, T. W. Prednisone and azathioprine for polymyositis. Long-term followup. *Arthritis Rheum* **24**, 45–48 (1981).

77. Ernste, F. C. & Reed, A. M. Idiopathic inflammatory myopathies: Current trends in pathogenesis, clinical features, and up-to-date treatment recommendations. *Mayo Clinic Proceedings* vol. 88 83–105 Preprint at https://doi.org/10.1016/j.mayocp.2012.10.017 (2013).

78. Wang, D. X. *et al.* Intravenous immunoglobulin therapy in adult patients with polymyositis/dermatomyositis: A systematic literature review. *Clin Rheumatol* **31**, 801–806 (2012).

79. Nagorka, C. Phase 3 Trial Shows Intravenous Immune Globulin Effective for Dermatomyositis. *Dermatology Times* vol. 387 https://www.dermatologytimes.com/view/phase-3-trial-shows-intravenous-immune-globulin-effective-for-dermatomyositis (2022).

80. Nalotto, L. *et al.* Rituximab in refractory idiopathic inflammatory myopathies and antisynthetase syndrome: Personal experience and review of the literature. *Immunol Res* **56**, 362–370 (2013).

81. Oddis, C. v. *et al.* Rituximab in the treatment of refractory adult and juvenile dermatomyositis and adult polymyositis: A randomized, placebo-phase trial. *Arthritis Rheum* **65**, 314–324 (2013).

82. Barsotti, S. *et al.* The use of rituximab in idiopathic inflammatory myopathies: description of a monocentric cohort and review of the literature. *Reumatismo* **70**, 78–84 (2018).

83. Fasano, S., Gordon, P., Hajji, R., Loyo, E. & Isenberg, D. A. Rituximab in the treatment of inflammatory myopathies: a review. *Rheumatology* **56**, 26–36 (2017).

84. Efthimiou, P. Tumor Necrosis Factor-α in Inflammatory Myopathies: Pathophysiology and Therapeutic Implications. *Semin Arthritis Rheum* **36**, 168–172 (2006).

85. Chen, S. E., Jin, B. & Li, Y. P. TNF-α regulates myogenesis and muscle regeneration by activating p38 MAPK. *Am J Physiol Cell Physiol* **292**, (2007).

86. Tjärnlund, A. *et al.* Abatacept in the treatment of adult dermatomyositis and polymyositis: A randomised, phase IIb treatment delayed-start trial. *Ann Rheum Dis* **77**, 55–62 (2018).

87. Tanaka, Y., Luo, Y., O'Shea, J. J. & Nakayamada, S. Janus kinase-targeting therapies in rheumatology: a mechanisms-based approach. *Nat Rev Rheumatol* **18**, 133–145 (2022).

88. Paik, J. J. *et al.* Long-term extension study of tofacitinib in refractory dermatomyositis. *Arthritis & Rheumatology* **74**, 371–372 (2022).

89. Pineton de Chambrun, M. *et al.* Tofacitinib in antisynthetase syndrome-related rapidly progressive interstitial lung disease. *Rheumatology* **59**, e142–e143 (2020).

90. Chiapparoli, I., Galluzzo, C., Salvarani, C. & Pipitone, N. A glance into the future of myositis therapy. *Ther Adv Musculoskelet Dis* **14**, 1759720X2211002 (2022).

91. Smith, L. N. & Paik, J. J. Promising and Upcoming Treatments in Myositis. *Curr Rheumatol Rep* **22**, 65 (2020).

92. Delvino, P. *et al.* Successful treatment with baricitinib in a patient with refractory cutaneous dermatomyositis. *Rheumatology* **59**, e125–e127 (2020).

93. Zhang, H. *et al.* Plasma exchange therapy in refractory inflammatory myopathy with anti-signal recognition particle antibody: A case series. *Rheumatology (United Kingdom)* **61**, 2625–2630 (2022).

94. Chérin, P. & Herson, S. [Immunoglobulins or plasma exchange? New treatment methods in polymyositis and dermatomyositis: plasma exchange and intravenous immunoglobulins]. *Ann Med Interne (Paris)* **144**, 521–5 (1993).

95. Bazzan, E. *et al.* Critical review of the evolution of extracellular vesicles' knowledge: From 1946 to today. *International Journal of Molecular Sciences* vol. 22 Preprint at https://doi.org/10.3390/ijms22126417 (2021).

96. Veerman, R. E. *et al.* Molecular evaluation of five different isolation methods for extracellular vesicles reveals different clinical applicability and subcellular origin. *J Extracell Vesicles* **10**, (2021).

97. Allelein, S. *et al.* Potential and challenges of specifically isolating extracellular vesicles from heterogeneous populations. *Sci Rep* **11**, 1–12 (2021).

98. Tian, J., Casella, G., Zhang, Y., Rostami, A. & Li, X. Potential roles of extracellular vesicles in the pathophysiology, diagnosis, and treatment of autoimmune diseases. *Int J Biol Sci* **16**, 620–632 (2020).

99. Colombo, M., Raposo, G. & Théry, C. Biogenesis, secretion, and intercellular interactions of exosomes and other extracellular vesicles. *Annu Rev Cell Dev Biol* **30**, 255–289 (2014).

100. Yáñez-Mó, M. *et al.* Biological properties of extracellular vesicles and their physiological functions. *J Extracell Vesicles* **4**, 27066 (2015).

101. Wolf, P. *et al.* Distribution and manifestations of inflammatory bowel disease in asians, hispanics, and african americans: A systematic review. *Journal of Biological Chemistry* **142**, 46-54.e42 (1967).

102. Zhang, Y. *et al.* Exosome: A review of its classification, isolation techniques, storage, diagnostic and targeted therapy applications. *Int J Nanomedicine* **15**, 6917–6934 (2020).

103. Johnstone, R. M., Adam, M., Hammond, J. R., Orr, L. & Turbide, C. Vesicle formation during reticulocyte maturation. Association of plasma membrane activities with released vesicles (exosomes). *Journal of Biological Chemistry* **262**, 9412–9420 (1987).

104. Johnstone, R. M. Revisiting the road to the discovery of exosomes. *Blood Cells Mol Dis* **34**, 214–219 (2005).

105. Molodecky, N. A. *et al.* Increasing Incidence and Prevalence of the Inflammatory Bowel Diseases With Time, Based on Systematic Review. *Gastroenterology* **142**, 46-54.e42 (2012).

106. Hou, J. K., El-Serag, H. & Thirumurthi, S. Distribution and Manifestations of Inflammatory Bowel Disease in Asians, Hispanics and African Americans: A Systematic Review. *Am J Gastroenterol* **104**, 2100–2109 (2009).

107. Théry, C. *et al.* Minimal information for studies of extracellular vesicles 2018 (MISEV2018): a position statement of the International Society for Extracellular Vesicles and update of the MISEV2014 guidelines. *J Extracell Vesicles* **7**, 1535750 (2018).

108. Zhang, Y., Liu, Y., Liu, H. & Tang, W. H. Exosomes: Biogenesis, biologic function and clinical potential. *Cell Biosci* **9**, 1–18 (2019).

109. Henne, W. M., Stenmark, H. & Emr, S. D. Sculpting ESCRT Pathway. *Cold Spring Harbour Perpectives in Biology* **5**, a016766 (2013).

110. Colombo, M. *et al.* Analysis of ESCRT functions in exosome biogenesis, composition and secretion highlights the heterogeneity of extracellular vesicles. *J Cell Sci* **126**, 5553–5565 (2013).

111. Raposo, G. & Stoorvogel, W. Extracellular vesicles: Exosomes, microvesicles, and friends. *Journal of Cell Biology* **200**, 373–383 (2013).

112. Jurj, A. *et al.* A Comprehensive Picture of Extracellular Vesicles and Their Contents. Molecular Transfer to Cancer Cells. *Cancers (Basel)* **12**, 298 (2020).

113. Teng, F. & Fussenegger, M. Shedding Light on Extracellular Vesicle Biogenesis and Bioengineering. *Advanced Science* **8**, 1–17 (2021).

114. McKelvey, K. J., Powell, K. L., Ashton, A. W., Morris, J. M. & McCracken, S. A. Exosomes: Mechanisms of Uptake. *J Circ Biomark* **4**, 1–9 (2015).

115. van Niel, G., D'Angelo, G. & Raposo, G. Shedding light on the cell biology of extracellular vesicles. *Nat Rev Mol Cell Biol* **19**, 213–228 (2018).

116. Liu, M.-L., Williams, K. J. & Werth, V. P. Microvesicles in Autoimmune Diseases. in *Advances in Clinical Chemistry* vol. 77 125–175 (Elsevier Inc., 2016).

117. Andreu, Z. & Yáñez-Mó, M. Tetraspanins in extracellular vesicle formation and function. *Front Immunol* **5**, 1–12 (2014).

118. Stahl, P. D. & Raposo, G. Extracellular Vesicles: Exosomes and Microvesicles, Integrators of Homeostasis. *Physiology* **34**, 169–177 (2019).

119. Nicolas, R. H. & Goodwin, G. H. Isolation and Analysis. in *The Chromosomal Proteins* 41–68 (Elsevier, 1982). doi:10.1016/B978-0-12-386050-7.50008-3.

120. Phuyal, S., Hessvik, N. P., Skotland, T., Sandvig, K. & Llorente, A. Regulation of exosome release by glycosphingolipids and flotillins. *FEBS Journal* **281**, 2214–2227 (2014).

121. Kooijman, E. E., Chupin, V., de Kruijff, B. & Burger, K. N. J. Modulation of Membrane Curvature by Phosphatidic Acid and Lysophosphatidic Acid. *Traffic* **4**, 162–174 (2003).

122. Egea-Jimenez, A. L. & Zimmermann, P. Phospholipase D and phosphatidic acid in the biogenesis and cargo loading of extracellular vesicles. *J Lipid Res* **59**, 1554–1560 (2018).

123. Hessvik, N. P. & Llorente, A. Current knowledge on exosome biogenesis and release. *Cellular and Molecular Life Sciences* **75**, 193–208 (2018).

124. Jarsch, I. K., Daste, F. & Gallop, J. L. Membrane curvature in cell biology: An integration of molecular mechanisms. *Journal of Cell Biology* **214**, 375–387 (2016).

125. Ghanam, J. *et al.* Extracellular vesicle-based nucleic acid delivery: Current advances and future perspectives in cancer therapeutic strategies. *Cell Biosci* **12**, 1–19 (2020).

126. Massaro, C. *et al.* Extracellular Vesicle-Based Nucleic Acid Delivery: Current Advances and Future Perspectives in Cancer Therapeutic Strategies. *Pharmaceutics* **12**, 980 (2020).

127. van Niel, G., D'Angelo, G. & Raposo, G. Shedding light on the cell biology of extracellular vesicles. *Nat Rev Mol Cell Biol* **19**, 213–228 (2018).

128. Bobrie, A., Colombo, M., Raposo, G. & Théry, C. Exosome Secretion: Molecular Mechanisms and Roles in Immune Responses. *Traffic* **12**, 1659–1668 (2011).

129. Sun, H., Burrola, S., Wu, J. & Ding, W. Q. Extracellular vesicles in the development of cancer therapeutics. *International Journal of Molecular Sciences* vol. 21 1–22 Preprint at https://doi.org/10.3390/ijms21176097 (2020).

130. Raposo, G. *et al.* B Lymphocytes Secrete Antigen-presenting Vesicles. *J. Exp. Med.* **183**, 1161–1172 (1996).

131. Buzas, E. I., György, B., Nagy, G., Falus, A. & Gay, S. Emerging role of extracellular vesicles in inflammatory diseases. *Nat Rev Rheumatol* **10**, 356–364 (2014).

132. Harding, C., Heuser, J. & Stahl, P. Receptor-mediated Endocytosis of Transferrin and of the Transferrin Receptor in Rat Reticulocytes Recycling. *J Cell Biol* **97**, 329–339 (1983).

133. Atay, S., Gercel-Taylor, C., Kesimer, M. & Taylor, D. D. Morphologic and proteomic characterization of exosomes released by cultured extravillous trophoblast cells. *Exp Cell Res* **317**, 1192–1202 (2011).

134. Zhao, Y. *et al.* Trends in the biological functions and medical applications of extracellular vesicles and analogues. *Acta Pharm Sin B* **11**, 2114–2135 (2021).

135. Robbins, P. D., Dorronsoro, A. & Booker, C. N. Regulation of chronic inflammatory and immune processes by extracellular vesicles. *Journal of Clinical Investigation* vol. 126 1173–1180 Preprint at https://doi.org/10.1172/JCI81131 (2016).

136. Tung, S. L. *et al.* Regulatory T cell-derived extracellular vesicles modify dendritic cell function. *Sci Rep* **8**, 6065 (2018).

137. Marar, C., Starich, B. & Wirtz, D. Extracellular vesicles in immunomodulation and tumor progression. *Nat Immunol* **22**, 560–570 (2021).

138. Becker, A. *et al.* Extracellular Vesicles in Cancer: Cell-to-Cell Mediators of Metastasis. *Cancer Cell* **30**, 836–848 (2016).

139. Zhang, L. *et al.* Microenvironment-induced PTEN loss by exosomal microRNA primes brain metastasis outgrowth. *Nature* **527**, 100–104 (2015).

140. Abusamra, A. J. *et al.* Tumor exosomes expressing Fas ligand mediate CD8+ T-cell apoptosis. *Blood Cells Mol Dis* **35**, 169–173 (2005).

141. Tauro, B. J. *et al.* Oncogenic H-Ras reprograms madin-darby canine kidney (MDCK) cell-derived exosomal proteins following epithelial-mesenchymal transition. *Molecular and Cellular Proteomics* **12**, 2148–2159 (2013).

142. Kong, J. *et al.* Extracellular vesicles of carcinoma-associated fibroblasts creates a pre-metastatic niche in the lung through activating fibroblasts. *Mol Cancer* **18**, 175 (2019).

143. Peinado, H. *et al.* Melanoma exosomes educate bone marrow progenitor cells toward a pro-metastatic phenotype through MET. *Nat Med* **18**, 883–891 (2012).

144. Zhou, W. *et al.* Cancer-Secreted miR-105 destroys vascular endothelial barriers to promote metastasis. *Cancer Cell* **25**, 501–515 (2014).

145. Lu, M. *et al.* The Role of Extracellular Vesicles in the Pathogenesis and Treatment of Autoimmune Disorders. *Front Immunol* **12**, 1–12 (2021).

146. Perez-Hernandez, J. & Cortes, R. Extracellular Vesicles as Biomarkers of Systemic Lupus Erythematosus. *Dis Markers* **2015**, 1–7 (2015).

147. Colletti *et al.* Exosomes in Systemic Sclerosis: Messengers Between Immune, Vascular and Fibrotic Components? *Int J Mol Sci* **20**, 4337 (2019).

148. Zhu, T., Wang, Y., Jin, H. & Li, L. The role of exosome in autoimmune connective tissue disease. *Ann Med* **51**, 101–108 (2019).

149. López, P., Rodríguez-Carrio, J., Caminal-Montero, L. & Suárez, A. Relationship Between T-Cell Exosomes and Cellular Subsets in SLE According to Type I IFN-Signaling. *Front Med (Lausanne)* **7**, (2020).

150. Zhao, Y., Wei, W. & Liu, M.-L. Extracellular vesicles and lupus nephritis - New insights into pathophysiology and clinical implications. *J Autoimmun* **115**, 102540 (2020).

151. Zhang, B., Zhao, M. & Lu, Q. Extracellular Vesicles in Rheumatoid Arthritis and Systemic Lupus Erythematosus: Functions and Applications. *Front Immunol* **11**, (2021).

152. Maione, F., Cappellano, G., Bellan, M., Raineri, D. & Chiocchetti, A. Chicken-or-egg question: Which came first, extracellular vesicles or autoimmune diseases? *J Leukoc Biol* **108**, 601–616 (2020).

153. Ståhl, A. lie, Johansson, K., Mossberg, M., Kahn, R. & Karpman, D. Exosomes and microvesicles in normal physiology, pathophysiology, and renal diseases. *Pediatric Nephrology* vol. 34 11–30 Preprint at https://doi.org/10.1007/s00467-017-3816-z (2019).

154. Dieker, J. *et al.* Circulating Apoptotic Microparticles in Systemic Lupus Erythematosus Patients Drive the Activation of Dendritic Cell Subsets and Prime Neutrophils for NETosis. *Arthritis and Rheumatology* **68**, 462–472 (2016).

155. Salvi, V. *et al.* Exosome-delivered microRNAs promote IFN-α secretion by human plasmacytoid DCs via TLR7. *JCI Insight* **3**, (2018).

156. Østergaard, O. *et al.* Unique protein signature of circulating microparticles in systemic lupus erythematosus. *Arthritis Rheum* **65**, 2680–2690 (2013).

157. Turpin, D. *et al.* Role of extracellular vesicles in autoimmune diseases. *Autoimmun Rev* **15**, 174–183 (2016).

158. Fu, H., Hu, D., Zhang, L. & Tang, P. Role of extracellular vesicles in rheumatoid arthritis. *Mol Immunol* **93**, 125–132 (2018).

159. Viñuela-Berni, V. *et al.* Proportions of several types of plasma and urine microparticles are increased in patients with rheumatoid arthritis with active disease. *Clin Exp Immunol* **180**, 442–451 (2015).

160. Pásztói, M. *et al.* The recently identified hexosaminidase D enzyme substantially contributes to the elevated hexosaminidase activity in rheumatoid arthritis. *Immunol Lett* **149**, 71–76 (2013).

161. Zhang, H.-G. *et al.* A Membrane Form of TNF-α Presented by Exosomes Delays T Cell Activation-Induced Cell Death. *The Journal of Immunology* **176**, 7385–7393 (2006).

162. Skriner, K., Adolph, K., Jungblut, P. R. & Burmester, G. R. Association of citrullinated proteins with synovial exosomes. *Arthritis Rheum* **54**, 3809–3814 (2006).

163. György, B. *et al.* Improved Flow Cytometric Assessment Reveals Distinct Microvesicle (Cell-Derived Microparticle) Signatures in Joint Diseases. *PLoS One* **7**, e49726 (2012).

164. Cloutier, N. *et al.* The exposure of autoantigens by microparticles underlies the formation of potent inflammatory components: The microparticle-associated immune complexes. *EMBO Mol Med* **5**, 235–249 (2013).

165. Uitto, J. & Kouba, D. Cytokine modulation of extracellular matrix gene expression: relevance to fibrotic skin diseases. *J Dermatol Sci* **24**, S60–S69 (2000).

166. Sgonc, R. *et al.* Endothelial cell apoptosis is a primary pathogenetic event underlying skin lesions in avian and human scleroderma. *Journal of Clinical Investigation* **98**, 785–792 (1996).

167. Deng, L. *et al.* MicroRNA-143 Activation Regulates Smooth Muscle and Endothelial Cell Crosstalk in Pulmonary Arterial Hypertension. *Circ Res* **117**, 870–883 (2015).

168. Wermuth, P. J., Piera-Velazquez, S. & Jimenez, S. A. Exosomes isolated from serum of systemic sclerosis patients display alterations in their content of profibrotic and antifibrotic microRNA and induce a profibrotic phenotype in cultured normal dermal fibroblasts. *Clin Exp Rheumatol* **35 Suppl 106**, 21–30 (2017).

169. Xu, K. *et al.* Extracellular vesicles as potential biomarkers and therapeutic approaches in autoimmune diseases. *Journal of Translational Medicine* vol. 18 Preprint at https://doi.org/10.1186/s12967-020-02609-0 (2020).

170. Gallo, A. *et al.* Targeting the Ca2 + Sensor STIM1 by Exosomal Transfer of Ebv-miR-BART13-3p is Associated with Sjögren's Syndrome. *EBioMedicine* **10**, 216–226 (2016).

171. Kim, S. *et al.* Roles of Exosome-Like Vesicles Released from Inflammatory C2C12 Myotubes: Regulation of Myocyte Differentiation and Myokine Expression. *Cellular Physiology and Biochemistry* **48**, 1829–1842 (2018).

172. Baka, Z. *et al.* Increased serum concentration of immune cell derived microparticles in polymyositis/dermatomyositis. *Immunol Lett* **128**, 124–130 (2010).

173. Shirafuji, T., Hamaguchi, H., Higuchi, M. & Kanda, F. Measurement of platelet-derived microparticle levels using an enzyme-linked immunosorbent assay in polymyositis and dermatomyositis patients. *Muscle Nerve* **39**, 586–590 (2009).

174. Oyabu, C. *et al.* Plasma platelet-derived microparticles in patients with connective tissue diseases. *Journal of Rheumatology* **38**, 680–684 (2011).

175. Jiang, K. *et al.* Plasma exosomes from children with juvenile dermatomyositis are taken up by human aortic endothelial cells and are associated with altered gene expression in those cells. *Pediatric Rheumatology* **17**, (2019).

176. Li, L., Zuo, X., Liu, D., Luo, H. & Zhu, H. The Functional Roles of RNAs Cargoes Released by Neutrophil-Derived Exosomes in Dermatomyositis. *Front Pharmacol* **12**, 1–10 (2021).

177. Zhao, Z., Wijerathne, H., Godwin, A. K. & Soper, S. A. Isolation and analysis methods of extracellular vesicles (EVs). *Extracell Vesicles Circ Nucl Acids* (2021) doi:10.20517/evcna.2021.07.

178. Perocheau, D., Touramanidou, L., Gurung, S., Gissen, P. & Baruteau, J. Clinical applications for exosomes: Are we there yet? *Br J Pharmacol* **178**, 2375–2392 (2021).

179. Xu, K. *et al.* Extracellular vesicles as potential biomarkers and therapeutic approaches in autoimmune diseases. *J Transl Med* **18**, 432 (2020).

180. Lane, R. E., Korbie, D., Hill, M. M. & Trau, M. Extracellular vesicles as circulating cancer biomarkers: opportunities and challenges. *Clin Transl Med* **7**, (2018).

181. Tian, J., Casella, G., Zhang, Y., Rostami, A. & Li, X. Potential roles of extracellular vesicles in the pathophysiology, diagnosis, and treatment of autoimmune diseases. *Int J Biol Sci* **16**, 620–632 (2020).

182. Lu, T. X. & Rothenberg, M. E. MicroRNA. *Journal of Allergy and Clinical Immunology* **141**, 1202–1207 (2018).

183. Tian, T., Wang, J. & Zhou, X. A review: MicroRNA detection methods. *Org Biomol Chem* **13**, 2226–2238 (2015).

184. Mohr, A. & Mott, J. Overview of MicroRNA Biology. *Semin Liver Dis* **35**, 003–011 (2015).

185. Watson, C. N., Belli, A. & di Pietro, V. Small Non-coding RNAs: New Class of Biomarkers and Potential Therapeutic Targets in Neurodegenerative Disease. *Front Genet* **10**, (2019).

186. Yoshida, T., Asano, Y. & Ui-Tei, K. Modulation of MicroRNA Processing by Dicer via Its Associated dsRNA Binding Proteins. *Noncoding RNA* **7**, 57 (2021).

187. Wang, Y. microRNA: Past and present. *Frontiers in Bioscience* **12**, 2316 (2007).

188. Bushati, N. & Cohen, S. M. microRNA Functions. *Annu Rev Cell Dev Biol* **23**, 175–205 (2007).

189. Shang, X., Fang, Y., Xin, W. & You, H. The Application of Extracellular Vesicles Mediated miRNAs in Osteoarthritis: Current Knowledge and Perspective. *J Inflamm Res* **Volume 15**, 2583–2599 (2022).

190. Fernández-Messina, L., Gutiérrez-Vázquez, C., Rivas-García, E., Sánchez-Madrid, F. & de la Fuente, H. Immunomodulatory role of microRNAs transferred by extracellular vesicles. *Biol Cell* **107**, 61–77 (2015).

191. Groot, M. & Lee, H. Sorting Mechanisms for MicroRNAs into Extracellular Vesicles and Their Associated Diseases. *Cells* **9**, 1–16 (2020).

192. Murphy, C. *et al.* Emerging role of extracellular vesicles in musculoskeletal diseases. *Mol Aspects Med* **60**, 123–128 (2018).

193. Raggi, F. *et al.* Extracellular vesicle-derived microRNAs as potential biomarkers in oligoarticular juvenile idiopathic arthritis patients: methodological challenges and new perspectives. *Clin Transl Med* **12**, (2022).

194. Faruq, O. & Vecchione, A. microRNA: Diagnostic Perspective. *Front Med (Lausanne)* **2**, (2015).

195. Gaur, A. *et al.* Characterization of microRNA expression levels and their biological correlates in human cancer cell lines. *Cancer Res* **67**, 2456–2468 (2007).

196. Esquela-Kerscher, A. & Slack, F. J. Oncomirs — microRNAs with a role in cancer. *Nat Rev Cancer* **6**, 259–269 (2006).

197. Johnson, S. M. *et al.* RAS is regulated by the let-7 microRNA family. *Cell* **120**, 635–647 (2005).

198. Sengupta, D. *et al.* Dissecting miRNA facilitated physiology and function in human breast cancer for therapeutic intervention. *Semin Cancer Biol* **72**, 46–64 (2021).

199. Ichii, O. *et al.* Decreased miR-26a Expression Correlates with the Progression of Podocyte Injury in Autoimmune Glomerulonephritis. *PLoS One* **9**, e110383 (2014).

200. Chi, M. *et al.* Immunological Involvement of MicroRNAs in the Key Events of Systemic Lupus Erythematosus. *Front Immunol* **12**, (2021).

201. Chau, B. N. *et al.* MicroRNA-21 Promotes Fibrosis of the Kidney by Silencing Metabolic Pathways. *Sci Transl Med* **4**, (2012).

202. Tan, L. *et al.* Downregulated Serum Exosomal miR-451a Expression Correlates With Renal Damage and Its Intercellular Communication Role in Systemic Lupus Erythematosus. *Front Immunol* **12**, (2021).

203. Alsaleh, G. *et al.* Bruton's Tyrosine Kinase Is Involved in miR-346-Related Regulation of IL-18 Release by Lipopolysaccharide-Activated Rheumatoid Fibroblast-Like Synoviocytes. *The Journal of Immunology* **182**, 5088–5097 (2009).

204. Nakasa, T. *et al.* Expression of MicroRNA-146 in rheumatoid arthritis synovial tissue. *Arthritis Rheum* **58**, 1284–1292 (2008).

205. Pauley, K. M. *et al.* Upregulated miR-146a expression in peripheral blood mononuclear cells from rheumatoid arthritis patients. *Arthritis Res Ther* **10**, R101 (2008).

206. Szabo, I. *et al.* Novel Concepts in Systemic Sclerosis Pathogenesis: Role for miRNAs. *Biomedicines* **9**, 1471 (2021).

207. Peng, L. *et al.* MicroRNA profiling in Chinese patients with primary sjögren syndrome reveals elevated miRNA-181a in peripheral blood mononuclear cells. *Journal of Rheumatology* **41**, 2208–2213 (2014).

208. Wang-Renault, S. F. *et al.* Deregulation of microRNA expression in purified T and B lymphocytes from patients with primary Sjögren's syndrome. *Ann Rheum Dis* **77**, 133–140 (2018).

209. Yin, Y. *et al.* MIR-146a Regulates Inflammatory Infiltration by Macrophages in Polymyositis/Dermatomyositis by Targeting TRAF6 and Affecting IL-17/ICAM-1 Pathway. *Cellular Physiology and Biochemistry* **40**, 486–498 (2016).

210. Ye, Q. & Chen, Z. MicroRNA-409-3p regulates macrophage migration in polymyositis through targeting CXCR4. *Autoimmunity* **54**, 353–361 (2021).

211. Yutao, L. *et al.* MicroRNA-381 reduces inflammation and infiltration of macrophages in polymyositis via downregulating HMGB1. *Int J Oncol* **53**, 1332–1342 (2018).

212. Georgantas, R. W. *et al.* Inhibition of myogenic microRNAs 1, 133, and 206 by inflammatory cytokines links inflammation and muscle degeneration in adult inflammatory myopathies. *Arthritis and Rheumatology* **66**, 1022–1033 (2014).

213. Parkes, J. E. *et al.* MicroRNA and mRNA profiling in the idiopathic inflammatory myopathies. *BMC Rheumatol* **4**, 25 (2020).

214. Oshikawa, Y. *et al.* Decreased miR-7 expression in the skin and sera of patients with dermatomyositis. *Acta Derm Venereol* **93**, 273–276 (2013).

215. Yu, L. *et al.* hsa-miR-7 Is a Potential Biomarker for Idiopathic Inflammatory Myopathies with Interstitial Lung Disease in Humans. *Ann Clin Lab Sci* **48**, 764–769 (2018).

216. Hirai, T. *et al.* Circulating plasma microRNA profiling in patients with polymyositis/dermatomyositis before and after treatment: miRNA may be associated with polymyositis/dermatomyositis. *Inflamm Regen* **38**, 1 (2018).

217. Bozzini, S. *et al.* A Proof-of-Concept Analysis of Plasma-Derived Exosomal microRNAs in Interstitial Pulmonary Fibrosis Secondary to Antisynthetase Syndrome. *Int J Mol Sci* **23**, 14579 (2022).

218. Paterson, E., Blenkiron, C., Danielson, K. & Henry, C. Recommendations for extracellular vesicle miRNA biomarker research in the endometrial cancer context. *Transl Oncol* **23**, 101478 (2022).

219. He, X., Park, S., Chen, Y. & Lee, H. Extracellular Vesicle-Associated miRNAs as a Biomarker for Lung Cancer in Liquid Biopsy. *Front Mol Biosci* **8**, (2021).

220. de Miguel Pérez, D. *et al.* Extracellular vesicle-miRNAs as liquid biopsy biomarkers for disease identification and prognosis in metastatic colorectal cancer patients. *Sci Rep* **10**, 3974 (2020).

221. Wang, W. *et al.* Promising Roles of Exosomal microRNAs in Systemic Lupus Erythematosus. *Front Immunol* **12**, (2021).

222. Li, W. *et al.* Circulating exosomal micrornas as biomarkers of systemic lupus erythematosus. *Clinics* **75**, 1–6 (2020).

223. Wielińska, J. *et al.* Exploring the Extracellular Vesicle MicroRNA Expression Repertoire in Patients with Rheumatoid Arthritis and Ankylosing Spondylitis Treated with TNF Inhibitors. *Dis Markers* **2021**, 1–15 (2021).

224. Yamashiro, K. *et al.* Exosome-Derived microRNAs from Mouthrinse Have the Potential to Be Novel Biomarkers for Sjögren Syndrome. *J Pers Med* **12**, 1483 (2022).

225. Simeone, P. *et al.* Extracellular vesicles as signaling mediators and disease biomarkers across biological barriers. *Int J Mol Sci* **21**, 1–27 (2020).

226. Veziroglu, E. M. & Mias, G. I. Characterizing Extracellular Vesicles and Their Diverse RNA Contents. *Front Genet* **11**, 1–30 (2020).

227. Benedikter, B. J. *et al.* Redox-dependent thiol modifications: implications for the release of extracellular vesicles. *Cellular and Molecular Life Sciences* **75**, 2321–2337 (2018).

228. Royo, F., Théry, C., Falcón-Pérez, J. M., Nieuwland, R. & Witwer, K. W. Methods for Separation and Characterization of Extracellular Vesicles: Results of a Worldwide Survey Performed by the ISEV Rigor and Standardization Subcommittee. *Cells* **9**, 1955 (2020).

229. Liangsupree, T., Multia, E. & Riekkola, M. L. Modern isolation and separation techniques for extracellular vesicles. *J Chromatogr A* **1636**, 461773 (2021).

230. Franco, C. *et al.* Size-Exclusion Chromatography Combined with Ultrafiltration Efficiently Isolates Extracellular Vesicles from Human Blood Samples in Health and Disease. *Int J Mol Sci* **24**, 3663 (2023).

231. Berckmans, R. J., Lacroix, R., Hau, C. M., Sturk, A. & Nieuwland, R. Extracellular vesicles and coagulation in blood from healthy humans revisited. *J Extracell Vesicles* **8**, 1688936 (2019).

232. Palviainen, M. *et al.* Extracellular vesicles from human plasma and serum are carriers of extravesicular cargo—Implications for biomarker discovery. *PLoS One* **15**, 1–19 (2020).

233. Gomes, J. *et al.* Analytical Considerations in Nanoscale Flow Cytometry of Extracellular Vesicles to Achieve Data Linearity. *Thromb Haemost* **118**, 1612–1624 (2018).

234. Johnsen, K. B., Gudbergsson, J. M., Andresen, T. L. & Simonsen, J. B. What is the blood concentration of extracellular vesicles? Implications for the use of extracellular vesicles as blood-borne biomarkers of cancer. *Biochim Biophys Acta Rev Cancer* **1871**, 109–116 (2019).

235. Rikkert, L. G., Nieuwland, R., Terstappen, L. W. M. M. & Coumans, F. A. W. Quality of extracellular vesicle images by transmission electron microscopy is operator and protocol dependent. *J Extracell Vesicles* **8**, 1555419 (2019).

236. de Rond, L. *et al.* Comparison of generic fluorescent markers for detection of extracellular vesicles by flow cytometry. *Clin Chem* **64**, 680–689 (2018).

237. Vogel, R. *et al.* A standardized method to determine the concentration of extracellular vesicles using tunable resistive pulse sensing. *J Extracell Vesicles* **5**, 31242 (2016).

238. Görgens, A. *et al.* Optimisation of imaging flow cytometry for the analysis of single extracellular vesicles by using fluorescence-tagged vesicles as biological reference material. *J Extracell Vesicles* **8**, 1587567 (2019).

239. Botha, J., Pugsley, H. R. & Handberg, A. Conventional, high-resolution and imaging flow cytometry: Benchmarking performance in characterisation of extracellular vesicles. *Biomedicines* **9**, 1–24 (2021).

240. Lannigan, J. & Erdbruegger, U. Imaging flow cytometry for the characterization of extracellular vesicles. *Methods* **112**, 55–67 (2017).

241. Buzas, E. I. The roles of extracellular vesicles in the immune system. *Nat Rev Immunol* (2022) doi:10.1038/s41577-022-00763-8.

242. Franco, C., Gatto, M., Iaccarino, L., Ghirardello, A. & Doria, A. Lymphocyte immunophenotyping in inflammatory myositis: a review. *Curr Opin Rheumatol* **33**, 522–528 (2021).

243. Lindenbergh, M. F. S. & Stoorvogel, W. Antigen Presentation by Extracellular Vesicles from Professional Antigen-Presenting Cells. *Annu Rev Immunol* **36**, 435–459 (2018).

244. Kato, T., Fahrmann, J. F., Hanash, S. M. & Vykoukal, J. Extracellular Vesicles Mediate B Cell Immune Response and Are a Potential Target for Cancer Therapy. *Cells* **9**, 1518 (2020).

245. Burbano, C. *et al.* Potential Involvement of Platelet-Derived Microparticles and Microparticles Forming Immune Complexes during Monocyte Activation in Patients with Systemic Lupus Erythematosus. *Front Immunol* **9**, (2018).

246. Li Yubin *et al.* Plasma-derived DNA containing-extracellular vesicles induce STING-mediated proinflammatory responses in dermatomyositis. *Theranostics* **11**, 7308–7321 (2021).

247. Brennan, K. *et al.* A comparison of methods for the isolation and separation of extracellular vesicles from protein and lipid particles in human serum. *Sci Rep* **10**, 1–13 (2020).

248. Ibrahim, A., Ibrahim, A. & Parimon, T. Diagnostic and Therapeutic Applications of Extracellular Vesicles in Interstitial Lung Diseases. *Diagnostics* **11**, 87 (2021).

249. Sellam, J. *et al.* Increased levels of circulating microparticles in primary Sjögren's syndrome, systemic lupus erythematosus and rheumatoid arthritis and relation with disease activity. *Arthritis Res Ther* **11**, 1–11 (2009).

250. Parker, B. *et al.* Suppression of inflammation reduces endothelial microparticles in active systemic lupus erythematosus. *Ann Rheum Dis* **73**, 1144–1150 (2014).

251. Raposo, G. *et al.* B Lymphocytes Secrete Antigen-presenting Vesicles. *J. Exp. Med.* **183**, 1161–1172 (1996).

252. Grada, A. & Weinbrecht, K. Next-Generation Sequencing: Methodology and Application. *Journal of Investigative Dermatology* **133**, 1–4 (2013).

253. Behjati, S. & Tarpey, P. S. What is next generation sequencing? *Arch Dis Child Educ Pract Ed* **98**, 236–238 (2013).

254. Lu, Y., Shen, Y., Warren, W. & Walter, R. Next Generation Sequencing in Aquatic Models. in *Next Generation Sequencing - Advances, Applications and Challenges* (InTech, 2016). doi:10.5772/61657.

255. Luo, S. MicroRNA expression analysis using the illumina MicroRNA-Seq platform. *Methods in Molecular Biology* **822**, 183–188 (2012).

256. Prajzlerová, K. *et al.* High miR-451 expression in peripheral blood mononuclear cells from subjects at risk of developing rheumatoid arthritis. *Sci Rep* **11**, 4719 (2021).

257. Foers, A. D. *et al.* Extracellular Vesicles in Synovial Fluid from Rheumatoid Arthritis Patients Contain miRNAs with Capacity to Modulate Inflammation. *Int J Mol Sci* **22**, 4910 (2021).

258. Nejad, C., Stunden, H. J. & Gantier, M. P. A guide to miRNAs in inflammation and innate immune responses. *FEBS J* **285**, 3695–3716 (2018).

259. Ying, X. *et al.* Epithelial ovarian cancer-secreted exosomal miR-222-3p induces polarization of tumor-associated macrophages. *Oncotarget* **7**, 43076–43087 (2016).

260. Matsuda, S. *et al.* Exploration of pathomechanism using comprehensive analysis of serum cytokines in polymyositis/dermatomyositis-interstitial lung disease. *Rheumatology (United Kingdom)* **59**, 310–318 (2020).

261. Xia, F., Bo, W., Ding, J., Yu, Y. & Wang, J. MiR-222-3p Aggravates the Inflammatory Response by Targeting SOCS1 to Activate STAT3 Signaling in Ulcerative Colitis. *The Turkish Journal of Gastroenterology* **33**, 934–944 (2022).

262. Casal-Dominguez, M., Pinal-Fernandez, I. & Mammen, A. L. Inhibiting Interferon Pathways in Dermatomyositis: Rationale and Preliminary Evidence. *Curr Treatm Opt Rheumatol* **7**, 258–271 (2021).

263. Fu, X. *et al.* Exosomal microRNA-32-5p induces multidrug resistance in hepatocellular carcinoma via the PI3K/Akt pathway. *Journal of Experimental and Clinical Cancer Research* **37**, (2018).

264. Yan, T. *et al.* miR-32-5p-mediated Dusp5 downregulation contributes to neuropathic pain. *Biochem Biophys Res Commun* **495**, 506–511 (2018).

265. Ni, Y. *et al.* miR-15a-5p inhibits metastasis and lipid metabolism by suppressing histone acetylation in lung cancer. *Free Radic Biol Med* **161**, 150–162 (2020).

266. Ma, X. *et al.* miR-185-5p Regulates Inflammation and Phagocytosis through CDC42/JNK Pathway in Macrophages. *Genes (Basel)* **13**, 468 (2022).

267. Shen, Y., Cui, J. Y., Yuan, J. & Wang X. *Role of miR-451a in non-small cell lung cancer*. www.targetscan.org (2018) doi:10.26355/eurrev_201809_15818.

268. Du, B., Tan, X. H., Cheng, L., Wang, F. & Zhang, H. F. MiR-451a ameliorates alcoholic hepatitis via repressing HDAC8-mediated proinflammatory response. *Kaohsiung Journal of Medical Sciences* **36**, 904–910 (2020).

269. Roush, S. & Slack, F. J. The let-7 family of microRNAs. *Trends Cell Biol* **18**, 505–516 (2008).

270. Chen, W., Liu, D., Li, Q.-Z. & Zhu, H. The function of ncRNAs in rheumatic diseases. *Epigenomics* **11**, 821–833 (2019).

271. Salvi, V., Gianello, V., Tiberio, L., Sozzani, S. & Bosisio, D. Cytokine Targeting by miRNAs in Autoimmune Diseases. *Front Immunol* **10**, (2019).

272. Grossi, I., Salvi, A., Baiocchi, G., Portolani, N. & de Petro, G. Functional Role of microRNA-23b-3p in Cancer Biology. *MicroRNA* **7**, 156–166 (2018).

273. Ye, L. *et al.* Specific Autoantibodies and Clinical Phenotypes Correlate with the Aberrant Expression of Immune-Related MicroRNAs in Dermatomyositis. *J Immunol Res* **2019**, 1–12 (2019).

274. Perez-Sanchez, C. *et al.* miR-374a-5p regulates inflammatory genes and monocyte function in patients with inflammatory bowel disease. *Journal of Experimental Medicine* **219**, (2022).

275. Shen, J. & Ma, X. miR-374a-5p alleviates sepsis-induced acute lung injury by targeting ZEB1 via the p38 MAPK pathway. *Exp Ther Med* **24**, 564 (2022).

276. Chen, X. *et al.* Fucosylated exosomal miRNAs as promising biomarkers for the diagnosis of early lung adenocarcinoma. *Front Oncol* **12**, (2022).

277. Cai, T. *et al.* EVI5 is an oncogene that regulates the proliferation and metastasis of NSCLC cells. *Journal of Experimental & Clinical Cancer Research* **39**, 84 (2020).

278. ElKhouly, A. M., Youness, R. A. & Gad, M. Z. MicroRNA-486-5p and microRNA-486-3p: Multifaceted pleiotropic mediators in oncological and non-oncological conditions. *Noncoding RNA Res* **5**, 11–21 (2020).

279. Ninawe, A. *et al.* MiR-486-5p: A Prognostic Biomarker for Chronic Myeloid Leukemia. *ACS Omega* **6**, 7711–7718 (2021).

280. Xu, L., Yao, Y., Lu, T. & Jiang, L. miR-451a targeting IL-6R activates JAK2/STAT3 pathway, thus regulates proliferation and apoptosis of multiple myeloma cells. *J Musculoskelet Neuronal Interact* **22**, 251–260 (2022).

281. Yin, C. *et al.* miR-185-5p inhibits F-actin polymerization and reverses epithelial mesenchymal transition of human breast cancer cells by modulating RAGE. *Mol Med Rep* **18**, 2621–2630 (2018).

282. Ma, Y., Shen, N., Wicha, M. S. & Luo, M. The Roles of the Let-7 Family of MicroRNAs in the Regulation of Cancer Stemness. *Cells* **10**, 2415 (2021).

283. Bayat, Z., Ghaemi, Z., Behmanesh, M. & Soltani, B. M. Hsa-miR-186-5p regulates TGFβ signaling pathway through expression suppression of SMAD6 and SMAD7 genes in colorectal cancer. *Biol Chem* **402**, 469–480 (2021).

284. Singh, R. P., Hahn, B. H. & Bischoff, D. S. Identification and Contribution of Inflammation-Induced Novel MicroRNA in the Pathogenesis of Systemic Lupus Erythematosus. *Front Immunol* **13**, (2022).

285. Xiang, Y., Tian, Q., Guan, L. & Niu, S. The Dual Role of miR-186 in Cancers: Oncomir Battling With Tumor Suppressor miRNA. *Front Oncol* **10**, (2020).

286. Ceolotto, G. *et al.* MiR-30c-5p regulates macrophage-mediated inflammation and pro-atherosclerosis pathways. *Cardiovasc Res* **113**, 1627–1638 (2017).

287. Schneider, L., Hax, V., Marcondes, N., Xavier, R. & Chakr, R. AB0174 Lymphocyte subsets t, b and nk cels in systemic sclerosis. in *Abstracts Accepted for Publication* 1107.3-1108 (BMJ Publishing Group Ltd and European League Against Rheumatism, 2017). doi:10.1136/annrheumdis-2017-eular.7028.

288. Wienke, J. *et al.* Endothelial and Inflammation Biomarker Profiles at Diagnosis Reflecting Clinical Heterogeneity and Serving as a Prognostic Tool for Treatment Response in Two

Independent Cohorts of Patients With Juvenile Dermatomyositis. *Arthritis and Rheumatology* **72**, 1214–1226 (2020).

289. Ye, W. *et al.* LncRNA MALAT1 Regulates miR-144-3p to Facilitate Epithelial-Mesenchymal Transition of Lens Epithelial Cells via the ROS/NRF2/Notch1/Snail Pathway. *Oxid Med Cell Longev* **2020**, 1–23 (2020).
290. Zheng, Y., Cai, B., Li, X., Li, D. & Yin, G. MiR-125b-5p and miR-181b-5p inhibit keratinocyte proliferation in skin by targeting Akt3. *Eur J Pharmacol* **862**, 172659 (2019).
291. Zhou, S., Liang, P., Zhang, P., Zhang, M. & Huang, X. The long noncoding RNA PDK1-AS/miR-125b-5p/VEGFA axis modulates human dermal microvascular endothelial cell and human umbilical vein endothelial cell angiogenesis after thermal injury. *J Cell Physiol* **236**, 3129–3142 (2021).
292. Inoue, K. *et al.* Down-regulation of miR-223 contributes to the formation of Gottron's papules in dermatomyositis via the induction of PKCε. *European Journal of Dermatology* **23**, 160–167 (2013).
293. Zhang, J., Zhu, L., Shi, H. & Zheng, H. Protective effects of miR-155-5p silencing on IFN-γ-induced apoptosis and inflammation in salivary gland epithelial cells. *Exp Ther Med* **22**, 882 (2021).
294. Wang, Y. Z. *et al.* Delivery of an miR155 inhibitor by anti-CD20 single-chain antibody into B cells reduces the acetylcholine receptor-specific autoantibodies and ameliorates experimental autoimmune myasthenia gravis. *Clin Exp Immunol* **176**, 207–221 (2014).
295. Singh, A., Patro, P. S. & Aggarwal, A. MicroRNA-132, miR-146a, and miR-155 as potential biomarkers of methotrexate response in patients with rheumatoid arthritis. *Clin Rheumatol* **38**, 877–884 (2019).
296. Matsuzaka, Y. & Yashiro, R. Immune Modulation Using Extracellular Vesicles Encapsulated with MicroRNAs as Novel Drug Delivery Systems. *Int J Mol Sci* **23**, 5658 (2022).
297. Jin, F. *et al.* Serum microRNA Profiles Serve as Novel Biomarkers for Autoimmune Diseases. *Front Immunol* **9**, 2381 (2018).